PROTEIN TRANSLOCATION ON THE DELTA pH-DEPENDENT PATHWAY OF CHLOROPLASTS

By

VIVIAN FINCHER

A DISSERTATION PRESENTED TO THE GRADUATE SCHOOL
OF THE UNIVERSITY OF FLORIDA IN PARTIAL FULFILLMENT
OF THE REQUIREMENTS FOR THE DEGREE OF
DOCTOR OF PHILOSOPHY

UNIVERSITY OF FLORIDA

2001

This dissertation is dedicated to those few men and women who strive to exercise genuine integrity in the pursuit of science and to those less perfect humans who must admire and endure them. While genuine integrity is the underpinning of all science, the burden it imposes on the scientists is a heavy one. By its very definition, integrity makes no exceptions, is indifferent in the face of desire and unrelenting in the wake of fatigue.

ACKNOWLEDGMENTS

The author wishes to thank her advisor, Dr. Kenneth C. Cline, for his exceptional accessibility and guidance throughout her research project. Dr. Cline has provided a consistent model of integrity and a display of work ethic that have been invaluable. She also expresses gratitude to her other committee members, Dr. Robert J. Ferl, Dr. Alice C. Harmon, Dr. Paul C. Sehnke and Dr. John P. Aris, for their patience and scientific support. An additional acknowledgement goes to Dr. Ralph Henry who spent many hours instructing her in laboratory techniques. This work would not have been possible without the technical advice and assistance of Mike McCaffery and Dr. Hiroki Mori.

TABLE OF CONTENTS

page

Abstract of Dissertation Presented to the Graduate School
of the University of Florida in Partial Fulfillment of the
Requirements for the Degree of Doctor of Philosophy

PROTEIN TRANSLOCATION ON THE DELTA pH-DEPENDENT PATHWAY OF CHLOROPLASTS

By

Vivian Fincher

May 2001

Chairman: Kenneth C. Cline
Major Program: Plant Molecular and Cellular Biology

Plastids are evolutionarily derived from an endosymbiotic relationship with an ancient relative of cyanobacteria. The legacy of that endosymbiosis includes nuclear genes whose protein products must be imported into chloroplasts and routed to the thylakoid membranes or the lumenal space enclosed by those membranes. The Delta pH-dependent pathway is one of four chloroplast export pathways having prokaryotic ancestry. The Delta pH-dependent pathway is unique in its exclusive dependence on the trans-thylakoid pH gradient for energy, its use of transit peptides with a recognizable motif, and its ability to translocate folded proteins.

I hypothesize that the Delta pH-dependent pathway has evolved from the most ancient means of protein translocation, spontaneous insertion. Early investigation of protein transport revealed initial interaction of amino acids with lipids and formation of a loop structure within the lipid bilayer. Subsequent research documented export initiation via loop formation in the Sec pathway of *Escherichia coli* and the endoplasmic reticulum.

I have demonstrated that initiation of export of a fusion protein on the Delta pH-dependent pathway also occurs via loop formation.

Evolutionary advances in control of protein translocation have resulted in machinery that can monitor substrates for appropriate characteristics such as targeting sequences, folding, and cofactor insertion. When a substrate does not meet criteria for continued translocation, transport-arrest results. I have captured a membrane-spanning translocation intermediate resulting from transport-arrest on the Delta pH-dependent pathway. I characterized the interaction by mutation of the substrate-protein and by chemical treatments of the recovered membranes. Manipulation of the intermediate may allow investigation of the transport process and of translocation machinery.

The known components of the Delta pH-dependent pathway machinery comprise three membrane-associated proteins. I have demonstrated incorporation of *in vitro*-translated components into complexes formed by endogenous components visualized by blue native polyacrylamide gel electrophoresis and fluorography. Incorporation of *in vitro*-translated and radiolabeled components allows tracking of substrate and component interactions. I have documented that the change of a single amino acid in one component can abolish the incorporation of that component into endogenous complexes. The methodology developed in this project will be used in subsequent research on component and substrate interactions.

CHAPTER 1
LITERATURE REVIEW

Modern Chloroplasts Are Descended from Photosynthetic Prokaryotes.

While the precise nature of the endosymbiotic events leading to the formulation of modern eukaryotic cells is a subject of intense debate, the derivation of modern chloroplasts from an ancient relative of cyanobacteria is well accepted. The prokaryotic ancestry of chloroplasts is evidenced genetically, topologically and biochemically. Chloroplasts and, more generally speaking, all plastid types found in various developmental and functional forms of plant cells have retained portions of the bacterial chromosome. Genes encoded in the plastid genome are transcribed and translated within the plastid using machinery that is formulated from a mix of nuclear and plastid-encoded proteins and RNA. However, the majority of formerly bacterial genes has been transferred to the plant nucleus. The integration of plastid-gene and nuclear gene products into a multi-compartmented functional organelle is dependent on the plastid envelope import machinery and the thylakoid membrane export machinery.

The topological relationships of the compartments of the chloroplast reflect its prokaryotic heritage. The organelle is delimitated by a double membrane comprising the outer envelope, inter-envelope space, and inner envelope. Within the organelle, the fluid compartment called the stroma is analogous to the bacterial cytoplasm. The chloroplast has an extensive intra-organellar membrane system termed the thylakoid membranes. Within the thylakoid membranes and the lumen they enclose resides the chloroplast

photosynthetic machinery. The thylakoids are derived from the bacterial inner membrane and thus their enclosed space, the thylakoid lumen, is topologically equivalent to the bacterial periplasmic space. Therefore, export processes from the stroma to the thylakoid membrane or lumen accomplish translocation of the proteinaceous components of the photosynthetic machinery (Schatz and Dobberstein, 1996).

Targeting of cytoplasmically translated proteins to the chloroplast stroma or the thylakoid compartments is controlled by cleavable N-terminal transit peptides (Keegstra and Cline, 1999). For proteins destined to the stroma and for many thylakoid membrane proteins, the transit peptides consist of a single domain, which is both necessary and sufficient for transport of the precursors across the chloroplast envelope. Integral membrane proteins contain additional targeting information, typically coded in their membrane-spanning domains. Those transit peptides of precursors destined for the thylakoid lumen, as well as some membrane-targeted proteins, have a lumenal targeting domain following the cleavage site of the stromal-targeting domain. The sequence and structure of the lumenal targeting domain determines the export pathway utilized by the protein. Following translocation of the stromal intermediate, the lumenal targeting domain is cleaved by the lumenal protease resulting in the mature sized protein. Investigation of energetic and stromal component requirements for protein export has led to the defining of four translocation pathways. One group of integral thylakoid membrane proteins may be inserted spontaneously without the aid of proteinaceous components. Three other groups are dependent on complex membranal, and in some cases stromal, machinery.

A subset of thylakoid lumenal proteins is translocated by the chloroplast Sec (cpSec) pathway (Keegstra and Cline, 1999). The lumenal targeting domains of Sec pathway precursors are characterized by a tripartite signal peptide structurally similar to prokaryotic Sec system signal peptides. The two components of the pathway that have been identified genetically, cpSecY, and cpSecA, are homologous to bacterial Sec system proteins. Purified cpSecA has been shown to promote ATP dependent and azide sensitive translocation of the 33-kDa subunit of photosystem II oxygen evolving complex (OE33) and plastocyanin (PC). cpSec pathway directed proteins interact with cpSecA on the thylakoid membrane forming a stable complex in the absence of ATP. Following addition of ATP, a portion of the complex bound precursor can be exported to the lumen. The degree to which export is stimulated by the trans-thylakoid pH gradient (ΔpH) is substrate dependent. Translocation can be blocked by antibody bound to cpSecY (Mori et al., 1999) and can be competitively inhibited only by other cpSec pathway precursors.

Export of a family of nuclear encoded integral thylakoid proteins, the light harvesting chlorophyll-binding proteins (LHCP), is dependent on the chloroplast signal recognition particle-like pathway (Keegstra and Cline, 1999). Following cleavage of its stromal targeting domain, LHCP interacts with the chloroplast homologue of the mammalian SRP54 subunit (also homologous to *Escherichia coli* Ffh) and a novel 43-kD protein, cpSRP43, to form a 120-kD soluble transit complex. Additionally, GTP and the stromal protein cpFtsY, chloroplast homologue of mammalian SRP receptor α-subunit (and *E. coli* FtsY), have been demonstrated to be essential for LHCP integration (Kogata et al., 1999). The trans-thylakoid pH gradient is stimulatory, but not essential for LHCP integration. Integration of LHCP into the thylakoid membrane is dependent on Oxa1p,

the chloroplast homologue of mitochondrial Oxa1p (and *E. coli* YidC), and independent of cpSecY (Moore et al., 2000). Integration can be competitively inhibited by LHCP, but not by cpSec pathway or ΔpH-dependent pathway directed precursors.

Export of proteins to the thylakoid lumen via the ΔpH-dependent pathway is energetically unique in its sole dependence on the trans-thylakoid pH gradient (Keegstra and Cline, 1999). Proteins targeted to this pathway are synthesized with a signal peptide structurally similar to bacterial Sec transit sequences, but characterized by a twin arginine motif immediately preceding their hydrophobic domain. Membrane localized components of the ΔpH-dependent pathway were first characterized genetically in plants and later in prokaryotes where the system is designated the Tat (for twin-arginine translocation) pathway. As the focus of this dissertation, the ΔpH-dependent pathway will be discussed in considerable detail.

The Bacterial Tat System Is Evolutionarily Related to the Chloroplast ΔpH-dependent Pathway.

The primary export system in prokaryotes is the general secretory (Sec) pathway. Translocation via the Sec pathway is mediated by the peripheral ATPase SecA and membrane components including the SecYEG complex (Manting and Driessen, 2000). Among the auxiliary proteins of the Sec system are SecD and SecF, which are essential to maintenance of the proton motive force (Arkowitz and Wickner, 1994) and regulate SecA activity (Economou et al., 1995). It has been observed that fully sequenced archaeal genomes encode either homologues of SecD and SecF or homologues to Tat pathway proteins TatC and Hcf106, but not both (Eichler, 2000). Since homologues for SecA

were not found among archaeal primary sequences, the role of SecD and SecF in archaea is unknown.

Transport by the bacterial Sec pathway is initiated by insertion of the preprotein into the membrane as a loop (Kuhn et al., 1994) and then progresses by linear translocation of the extended protein chain through the membrane from its amino end to carboxyl end. Because the bacterial Sec machinery requires its substrate proteins to adopt an extended conformation during translocation (Pugsley, 1993), it is unsuitable for export of proteins or protein complexes that must be assembled and tightly folded in the cytoplasm. Prominent among proteins acquiring tightly folded conformations while still cytoplasmically located are the metallo-enzymes and nucleotide cofactor containing enzymes required for anaerobic respiration (Berks et al., 2000a). A survey of the *E. coli* genome revealed twenty-three open reading frames encoding proteins having signal peptides containing a Tat consensus sequence. Of those twenty-three precursors, sixteen bind or are predicted to bind redox factors (Stanley et al., 2001). Assembly of many apoprotein-cofactor complexes is a cytoplasmic process involving dedicated assembly factors and proteases. Indirect evidence from numerous *in vivo* experiments supports a model in which fully folded complexes or oligomers are translocated via the Tat apparatus (Berks et al., 2000b, for review). When green fluorescent protein (GFP) was fused behind the premaltose-binding protein and expressed in *E. coli*, it was exported via the Sec pathway (Feilmeier et al., 2000). The chimeric construct was fully fluorescent in the cytoplasm, but not in the periplasm. The authors concluded that GFP cannot fold correctly in the periplasm. A similar construct having a Tat system compatible signal

peptide was fluorescent in both compartments, leading to the conclusion that it could be exported in its folded state (Thomas et al., 2001).

Although Tat signal sequences share overall structure with Sec signal sequences, some differences are important. Both sets of peptides can be described as tripartite, having a basic N-region at the amino terminus followed by a hydrophobic H-region and ending in a carboxyl C-region containing the signal peptide cleavage site. The N-region of Tat precursors is on average 14 amino acids longer than the corresponding domain in Sec signal peptides with most of that difference being accounted for by the characteristic twin arginine consensus region (Cristóbal et al., 1999). Berks (1996) defined the bacterial twin arginine consensus as (S/T)-R-R-X-F-L-K immediately preceding the H-region. While the two consecutive arginines are invariant, the other amino acids of the consensus may differ in about half of Tat signal peptides. Multiple experimental studies have confirmed that the of the twin arginine motif is essential for export (Berks et al., 2000b, for review). Positive charges are more common in the C-region of Tat signal peptides than in the corresponding domain of Sec precursors (Cristóbal et al., 1999).

Comparing a series of chimeric constructs between variations on the signal peptide of trimethylamine N-oxide reductase (TorA) and the periplasmic P2 domain of *E. coli* protein leader peptidase (Lep) led Cristóbal et al. (1999) to conclude that the overall lower hydrophobicity of the H-region of Tat peptides is important both in Sec avoidance and in Tat transport. Their conclusion was based on data that demonstrated exclusive transport on the Sec pathway when the TorA signal peptide was mutated to contain a more hydrophobic H-region still flanked by its native N- and C- regions. Transport in *tat* deletion mutants was unaffected, while depletion of SecE completely eliminated

translocation. Izard and Kendall (1994) suggested that the apparent decrease in sensitivity to sodium azide inhibition of transport in Sec precursors with artificially increased hydrophobic domains might reflect more efficient utilization of SecA. If the increase in hydrophobicity of the mutated TorA signal peptide is increasing affinity for SecA, sequestering of the precursor may be responsible for the apparent inability of the Tat system to translocate the protein in the SecE depleted cells. Similar constructs having Sec type hydrophobic domains but carrying twin arginine consensus sequence are capable of utilizing either the cpSec or ΔpH-dependent pathway in chloroplasts (Henry et al., 1997). The increased hydrophobicity of the modified TorA H-domain may be necessary to allow Sec dependent transport, but may not inherently prohibit Tat pathway transport. A similar experiment in SecA depleted cells might determine the answer.

The interaction of Tat machinery and *E. coli* membranes has received recent attention. Mikhaleva et al. (1999) examined the role of phospholipids in the translocation of TorA. They concluded that the Tat pathway is more highly dependent on non-bilayer preferring phospholipids, such as phosphatidylethanolamine, than is the Sec pathway. They suggested, "the slow process of translocating folded protein through the Tat pathway may increase the opportunity for a direct, active interaction between the phospholipids and the passenger proteins" (Mikhaleva et al., 1999 p. 335). Stanley et al. (2001) have observed pleiotropic defects in the cell envelope of several *E. coli* mutant strains blocked in Tat translocation. The bacteria appear to be defective in cell separation, forming chains of up to 10 cells. The cells, which are resistant to infection by P1 phage, are supersensitive to killing by hydrophobic drugs and to lysis by lysozyme in

the absence of EDTA. The phenotype was construed to be due to a defect in the biosynthesis of the outer membrane.

The genetic definition of the Tat pathway began with the isolation of a maize mutant termed *hcf106*. Chloroplasts from *hcf106* plants are selectively deficient in the export of ΔpH-dependent pathway precursors OE17 and OE23 (the 17-kDa and the 23-kDa subunits of the photosystem II oxygen-evolving complex, respectively), but are normal in the targeting of cpSec dependent precursors OE33 and PC (Voelker and Barkan, 1995). Cloning of the *Hcf106* gene and comparison of its sequence to available bacterial genomes led Settles et al. (1997) to conclude that the thylakoid ΔpH-dependent pathway evolved from a bacterial redox protein secretory system. In *E. coli* the primary operon controlling that system had been designated *yigTUW*.

Formerly designated *yigTUW*, the Tat operon located at 86 minutes on the *E. coli* chromosome was analyzed, resequenced, and redefined to contain four genes *TatA*, *TatB*, *TatC*, and *Tat D* (Weiner et al., 1998; Sargent et al., 1998). An independent transcriptional unit, *TatE* is located at 14 minutes (Sargent et al., 1998). The *TatA*, *TatB* and *TatE* genes code for homologues of the maize Hcf106 protein. Each protein comprises an N-terminal transmembrane α-helix followed by an amphipathic α-helix and, in the case of TatB, an extended C-terminal region. Analysis of sequence data from all complete genomes of bacteria has shown that homologues of TatA/B/E and of TatC are present in all organisms that encode proteins with twin-arginine transit peptides (Berks et al., 2000b). Additionally, TatC homologues are found in the mitochondrial genomes of *Arabidopsis thaliana*, *Marchantia polymorpha*, and *Reclinomonas americana* (Bogsch et al., 1998). TatC is predicted to span the membrane six times with amino and

carboxyl termini in the cytoplasm (Sargent et al., 1998). *TatD* related sequences are found in all complete genomes except that of *Archaeoglobus fulgidus* (Wu et al., 2000); however, it is not conserved in linkage to other Tat genes (Settles and Martienssen, 1998).

Manipulation of Tat genes in *E. coli* has allowed the roles of the gene products to be assessed separately and together. It was found that mutation (Weiner et al., 1998) or deletion (Sargent et al., 1999) of the *TatB* gene eliminated transport of Tat pathway dependent precursors. In a pulse-chase experiment, TatC protein was shown to be unstable in the absence of *TatB*, implying an interaction of the gene products (Sargent et al., 1999). Western blots of a *TatA* deletion strain revealed only very low levels of TatB, suggesting that TatB is unstable in the absence of TatA (Bolhuis et al., 2000). While disruption of *TatA* or *TatE* individually impaired but did not eliminate Tat dependent protein export, deletion of both the *TatA* and *TatE* genes completely blocked translocation (Sargent et al., 1998). Co-immunoprecipitation experiments in *E. coli* demonstrated that about 5% of TatA is associated with TatB (Bolhuis et al., 2000). As part of the same study, gel filtration results demonstrated a 600- kDa complex containing both TatA and TatB. Disruption of the *TatC* gene also blocked Tat pathway dependent export (Bogsch et al., 1998). In *E. coli* the cytoplasmic protein, TatD, is not required for translocation of Tat system dependent proteins (Wexler et al., 2000).

Purification of the TatA/TatB/TatC complex revealed a 1:1 stoichiometry of TatB to TatC with TatA present in substoichiometric amounts (Bolhuis et al., 2001). The authors concluded that TatA is more loosely associated to the complex than TatB/TatC.

Co-immununoprecipitation results suggested that TatC is required for the interaction of TatA and TatB.

The independence of the Tat and Sec systems in *E. coli* has been demonstrated in several experiments. Neither disruption of TatB (Weiner et al., 1998), deletion of both TatA and TatE (Sargent et al., 1998) nor deletion of TatC (Bogsch et al., 1998) had discernable effects on export via the Sec pathway. Conversely, Cristóbal et al. (1999) found that SecE depletion had no effect on the translocation kinetics of the Tat pathway directed TorA/P2 fusion protein.

The Chloroplast ΔpH-dependent Pathway Was Explored First Biochemically, Then Genetically.

Definition of the ΔpH-dependent pathway in chloroplasts was achieved first through biochemical experiments. Thylakoids that have been recovered from lysed chloroplasts and subsequently washed and resuspended in buffer are capable of translocating ΔpH-dependent precursors when provided with actinic light at 25° C. Rigorous experimentation has led to the consensus that the pathway requires no nucleotide triphosphates (NTP's) and no soluble stromal components, in contrast to both the cpSec and cpSRP pathways (Mould and Robinson, 1991; Cline et al., 1992; Cline et al., 1993; Hulford et al., 1994). Translocation is energically dependent on the trans-thylakoid pH gradient. Where tested, export of any ΔpH-dependent pathway precursor can be competitively inhibited by any other ΔpH-dependent pathway precursor, but not by cpSec or cpSRP pathway precursors (Cline et al., 1993).

The structure of the signal peptides of ΔpH-dependent precursors is similar to the structure of bacterial Tat precursors, cpSec precursors, and bacterial Sec precursors. All

share the tripartite structure described above. Invariably, ΔpH-dependent precursors bear two arginine residues preceding the H-domain. Domain swapping experiments among precursors of the cpSec and ΔpH-dependent pathways have demonstrated that the two arginines are required for ΔpH-dependent targeting of lumenal proteins (Chaddock et al., 1995; Henry et al., 1997) and that the degree of influence of the H-domain and C-domain amino acids varies among precursors (Bogsch et al., 1997; Henry et al., 1997). Signal peptides that direct a protein to the cpSec pathway are unable to promote export of proteins naturally transported by the ΔpH-dependent pathway (Clausmeyer et al., 1993; Henry et al., 1997). However, signal peptides directing export by the ΔpH-dependent pathway are able to promote transport of plastocyanin (PC), which is naturally exported by the cpSec pathway (Robinson et al., 1994; Henry et al., 1994; Henry et al., 1997). A signal peptide comprising the N-domain of OE23, the H-domain of PC, and the C-domain of PC is able to direct PC and OE33 to both the cpSec and the ΔpH-dependent pathways (termed dual-targeting); the same signal peptide directs OE23 exclusively on the ΔpH-dependent pathway (Henry et al., 1997). Henry et al. (1997) hypothesized that the ΔpH-dependent pathway has evolved to export precursors that the cpSec pathway is unable to translocate.

The identification of the *hcf106* mutant in maize and the demonstration that it is deficient specifically in ΔpH-dependent pathway precursor export (Voelker and Barkan, 1995) lay the foundation for system component identification and study. Subsequently, the *Hcf106* gene was cloned and homologous sequences were found in prokaryotic genomes (Settles et al., 1997). Further analysis in maize revealed *Tha4* and *Tha9* as orthologues of *E. coli TatA*. *Hcf106* and a gene bearing >90% identity to it were

described as orthologues to *E. coli TatB* (Walker et al., 1999). Additional evidence of the common evolutionary origin of the bacterial Tat pathway and the chloroplast ΔpH-dependent pathway came from experiments exploring the compatibility of bacterial signal peptides with thylakoid export machinery. Mori and Cline (1998) fused the signal peptide from *E. coli* hydrogenase 1 small subunit to the mature domain of plastocyanin and demonstrated that isolated thylakoids transport it by the ΔpH-dependent pathway. Glucose-fructose oxidoreductase from *Zymomonas mobilis* is similarly exported by isolated thylakoids (Halbig et al., 1999).

The biochemical independence of the cpSec and ΔpH-dependent pathways has been demonstrated by multiple methods from several research groups. Early evidence of separate translocation systems came from competition studies as mentioned previously. As a bridge between the genetic system of maize and the biochemical system of pea, *Tha4* (Mori et al., 1999), *Hcf106* and *cpTatC* (Mori and Cline, unpublished) were cloned from *Pisum sativum*. Following the cloning of pathway components, antibodies to those components were tested for *in vitro* inhibition of export. When isolated thylakoid membranes are pre-treated with antibodies to Tha4, Hcf106, or cpTatC, only translocation of ΔpH-dependent pathway substrates is inhibited (Mori et al., 1999; Summer et al., 2000). Pretreatment of membranes with antibody to cpSecY inhibits only cpSec dependent precursors (Mori et al., 1999).

Independent evidence that cpSec and ΔpH-dependent pathway precursors use different translocation systems came from Asai et al. (1999). A fusion protein comprising the stromal intermediate of OE23 (iOE23) and *E. coli* biotin carboxyl carrier protein (i23K-BCCP) was expressed in *E. coli*. Purified biotinylated i23K-BCCP is

translocated to the lumen of isolated thylakoids where it is processed to mature size (m23K-BCCP) and protected from externally added thermolysin. Transport is dependent on the ΔpH and is azide insensitive as expected for a ΔpH-dependent pathway precursor. When i23K-BCCP is complexed with avidin prior to incubation with isolated thylakoids, the mature sized product is formed indicating processing by the lumenal protease; however, the m23K-BCCP remains sensitive to thermolysin. These results imply that export has been arrested with the amino end of the substrate protein in the lumen while most of the protein remains on the *cis* side of the membrane. When large amounts of avidin complexed i23K-BCCP are incubated with thylakoids, the transport of ΔpH-dependent pathway stromal intermediate iOE23 is blocked. The membranes are still competent to transport cpSec directed stromal intermediate iOE33. The authors concluded, "this means that the translocation pore for the ΔpH-dependent pathway is not shared by substrates for the Sec-dependent pathway" (Asai et al., 1999, p. 20077). Noteworthy also is the implication that biotinylated iOE23-BCCP bound with avidin is an unacceptable substrate for complete translocation due either to size or some other feature of the complex. When a similar construct, pOE17(C)-BioHis, used by Musser and Theg (2000a) is biotinylated and complexed with avidin, it binds to the membrane and competitively inhibits translocation of unbiotinylated precursor. However, the avidin complexed protein is not processed to mature size. The reason for the difference in behavior of precursors in the two studies remains unexplained.

The most unique feature of the ΔpH-dependent system is its ability to translocate folded proteins. The first intimation of folded protein transport by the pathway came from a 1995 study in which Creighton et al. demonstrated that iOE23 contains a protease

resistant, and by implication tightly folded, 22-kDa core. Because data from other translocation systems indicate that proteins are typically transported in an unfolded state, the authors concluded that OE23 was probably unfolded during export. Subsequently, Clark and Theg (1997) demonstrated that the tightly folded 6.5-kDa bovine pancreatic trypsin inhibitor (BPTI) linked behind the ΔpH-dependent pathway precursor to OE17 (pOE17) could be fully translocated to the thylakoid lumen. Transport proceeds even when the BPTI moiety, estimated to be 2.3 nm in diameter, is internally crosslinked and therefore incapable of unfolding during translocation. The export of proteins is achieved without compromising the ability of the thylakoids to maintain an ion gradient (Teter and Theg, 1998). Evidence of the system's ability to export a somewhat larger folded domain came from a study in which dihydrofolate reductase (DHFR) was linked to pOE23 and shown to enter the lumen even when bound to methotrexate (Hynds et al., 1998). In that series of experiments, it was also demonstrated that a malfolded substrate could still be translocated. The latter result suggests that if proofreading of protein structure is an important facet of ΔpH-dependent pathway export, it is substrate specific.

The versatility of the ΔpH-dependent pathway was further demonstrated during the exploration of translocation of the integral thylakoid membrane protein Pftf (plastid fusion/protein translocation factor). The precursor to Pftf, pPftf, carries an RRXFLK motif typical of bacterial Tat pathway proteins. The integration of Pftf was shown by several criteria to be ΔpH-dependent pathway specific, raising the question of how a translocation mechanism that can export folded proteins can also recognize and integrate a transmembrane domain. More surprising was the discovery that integration is not dependent on the presequence but can be accomplished by N-tail export of the mature

protein. Integration of all forms of Pftf is inhibited by antibodies to Hcf106, Tha4, and TatC, but not by antibodies to cpSecY or cpOxa1p, implying that all known components of the ΔpH-dependent pathway are involved in its translocation (Summer et al., 2000).

Attempts to dissect translocation have led to a model in which at least two steps are required for export. In the first step, which is not dependent on the trans-thylakoid pH gradient, the precursor is bound to the *cis* side of the membrane (Ma and Cline, 2000; Musser and Theg, 2000a). Subsequently upon establishment of the ΔpH, the precursor is moved through the membrane and processed to mature size. Ma and Cline (2000) found that the rate of transport of freshly added precursor is comparable to the rate of transport from the bound state, making it unlikely that binding involves insertion into a putative translocon. Biphasic kinetics of transport implies a slow step such as two-dimensional diffusion within the membrane prior to the energy requiring transport step(s) (Musser and Theg, 2000a). A solvent isotope effect implicates proton transfer as the rate-limiting step in protein translocation (Musser and Theg, 2000b). When thylakoids are pre-incubated with antibodies to either Hcf106 (Ma and Cline, 2000) or cpTatC (Cline and Mori, unpublished) the binding and subsequent transport (chase) of ΔpH-dependent pathway directed precursors is inhibited. Pre-incubation of membranes with antibody to Tha4 does not inhibit binding, but does inhibit chase from the bound state. One interpretation of these data is that precursor binds to a complex of Hcf106 and TatC prior to interaction with Tha4. However, the results are not definitive since binding of antibody to pathway components could have multiple and complex effects.

Given the results from the studies of Musser and Theg (2000a) and Ma and Cline (2000), it is now possible to put a slightly different interpretation on the results of an

earlier set of experiments by Berghöfer and Klösgen (1999). When translocation characteristics of a chimeric protein comprising the presequence of OE16 (also called OE17) and the mature domain of OE23 (16/23) were investigated, two presumed translocation intermediates were distinguished. Whereas the mature form of 16/23 was expected to be a 23-kDa lumenal protein, *in organello* transport resulted primarily in a 27-kDa membrane associated protein. Thermolysin treatment of recovered thylakoids yielded a 26-kDa degradation product. It was concluded that the stromal targeting domain had been removed and export of the remainder of the protein had been incomplete, leaving a few N-terminal amino acids on the *cis* side of the membrane. When 16/23 was incubated on ice with isolated thylakoids, it associated tightly with the membranes. The association also took place in the presence of nigericin. Thermolysin treatment of reisolated membranes yielded a 14-kDa degradation product. The degradation product was assumed to be inside the lumen. However, no controls were reported to substantiate that assumption in spite of the fact that OE23 has been demonstrated to yield a 22-kDa protease resistant fragment (Creighton et al., 1995). The authors concluded that the 14-kDa fragment represented an early step in translocation not dependent on functional translocase. Thus the precursor 16/23 may have associated with the membranes in a pathway specific, but ΔpH independent manner as has since been reported for a variety of constructs by Ma and Cline (2000). Upon establishment of conditions favorable to protein translocation (25°C and actinic light), export occurred. Membranes recovered from a time course and treated with thermolysin yielded progressively less 14-kDa degradation product and more 26-kDa degradation product. Membranes were recovered following incubation of 16/23 with isolated thylakoids and

solubilized with digitonin. Samples prepared from those membranes were analyzed by blue native polyacrylamide gel electrophoresis and visualized by radiography. The radioactivity accumulated at two positions. Comparison of the location of those bands to the location of known chloroplast protein complexes gave estimates of 560-kDa and 620-kDa complexes. The authors assumed that the radioactivity was the result of the partially translocated 16/23 previously demonstrated to give rise to the 26-kDa lumenal fragment. However, the bands may have been the result of externally bound precursor that was associated with ΔpH-dependent pathway components.

Summary and Perspective

Recent biochemical studies of the thylakoid ΔpH-dependent pathway and the genetically related bacterial Tat pathway have emphasized the dichotomic relationship of these translocation systems to previously known export pathways. The ΔpH-dependent pathway, like the Sec system, is able to translocate both soluble and transmembrane proteins, but unlike the Sec system, the ΔpH-dependent pathway and Tat pathways are able to translocate folded proteins. While employing an amino terminal signal sequence reminiscent of the eukaryotic, bacterial, and chloroplast Sec system signal peptides, the ΔpH-dependent pathway requires no soluble accessory proteins and no NTP's. The stimulatory effect of the proton motive force is variable in other export systems, but for the ΔpH-dependent pathway, it is the sole energy source. The unique character of the ΔpH-dependent pathway has led to much speculation about its mechanism of energy utilization, the nature of its channel (if any), and its regulation. By investigating the mode of initiation of export and by achieving a translocation intermediate, I have begun to address the mechanism of substrate movement through the translocon. With the

integration of *in vitro*-translated radiolabeled ΔpH-dependent pathway components into functioning membranes, I have created a tool with which component and substrate interactions may be investigated.

CHAPTER 2
EVIDENCE FOR A LOOP MECHANISM OF PROTEIN TRANSPORT BY THE THYLAKOID ΔpH-DEPENDENT PATHWAY

Introduction

Multiple models have been proposed to account for the apparent ability of the ΔpH-dependent pathway to translocate folded proteins without compromising the trans-thylakoid pH gradient. Upon initial cloning of Hcf106, Settles et al. (1997) suggested that the structure and topology of the protein made it a candidate for a receptor function. Considering the bacterial Tat pathway, Berks et al. (2000b) described what they termed a 'sea anemone' model in which multiple copies of TatA/B/E form the pore with their C-terminal regions gating the cytoplasmic side of the bilayer. An iris mechanism would control the size of pore as individual subunits moved against each other. However, they went on to cast doubt on their own model pointing out that a dynamic seal might be insufficient to maintain the proton motive force. Musser and Theg (2000a) envisioned a gated pore in the thylakoid. In their model the precursor is transferred to the pore cavity and the pore sealed from the stromal side prior to its opening to the lumenal side. Berks et al. (2000a) agreed with the idea of two proton-impermeable gates and proposed a more detailed model for export via the bacterial Tat pathway. They suggested TatC as the site of signal peptide recognition and TatB as "physically connecting, and thus mediating communication between, the TatA and TatC subunits" (Berks et al., 2000a, p. 328). Long-Fei Wu et al. (2000) favored TatA, TatB, or TatE as both receptors and gates with

TatC as the core structure of the channel. They suggested that the integration of the transmembrane segments of the other Tat components might increase the size of the pore in response to the translocating substrate.

Any model of the ΔpH-dependent pathway mechanism must not only explain translocation of folded proteins, it must also explain integration of Pftf (Summer et al., 2000). Clearly, the translocon does more than sense the presence of a precursor and adjust a channel to accommodate it. The apparatus in some way monitors the substrate as it initiates and as it continues translocation. The bacterial Tat pathway is able to distinguish substrates that are properly assembled with cofactors or partner subunits (Berks et al., 2000b). And the mechanism must be able to properly position an early intermediate in export such that its signal peptide cleavage site is in position to be cut by the lumenal (or periplasmic) processing protease.

Export-type systems, i.e. the Sec system and the endoplasmic reticulum (ER) transport system, initiate transport via a transmembrane loop consisting of the signal peptide and carboxyl-flanking region (Kuhn et al., 1994; Shaw et al., 1988). In contrast, current models of protein import into mitochondria and chloroplasts depict insertion and transport as proceeding amino terminus first (see Schatz, 1996 and Kouranov et al., 1996 for review); peroxisomal and endocytic processes are capable of transporting folded proteins and even gold particles (Gietl, 1996). Here I present evidence that during transport on the ΔpH-dependent pathway, the amino terminus of the precursor protein remains on the *cis* side of the membrane. This is consistent only with the loop mechanism used by export-type systems. Thus, my data suggest that the ΔpH-dependent

pathway shares a common evolutionary origin with other export pathways such as the Sec systems and spontaneous insertion mechanisms.

Materials and Methods

Materials

All reagents, enzymes, and standards were from commercial sources. *In vitro* transcription plasmids for precursors to pOE23[1] from pea, pPC from *Arabidopsis,* and pOE17 from maize have been described elsewhere (Cline et al., 1993). *Escherichia coli*-produced iOE23 has been previously described (Cline et al., 1993). pOE23 was produced in *E. coli* (Cline et al., 1993) and then used for antibody preparation in rabbits. Antibody to pOE17, prepared against the fusion protein pOE17-maltose binding protein, was the generous gift of Dr. Alice Barkan (University of Oregon). Primers used in PCR reactions were manufactured by DNAgency (Malvern, PA).

Construction of Chimeric Precursors

Coding sequences for recombinant proteins were constructed by PCR-based methods using the above plasmids as templates. Amplifications were performed with *Pfu* polymerase (Stratagene, La Jolla, CA). Cloned constructs were verified by DNA sequencing. Sequencing was done with ABI Prism Dye Terminator cycle sequencing protocols developed by Applied Biosystems (Perkin-Elmer Corp., Foster City, CA) and an Applied Biosystems model 373 Stretch DNA Sequencer (Perkin-Elmer Corp.). Sequencing of all clones on both strands was performed by the University of Florida

[1] p-, i-, and m- are abbreviated designations for precursor-, intermediate precursor-, and mature forms of the thylakoid proteins described in the text, respectively.

Interdisciplinary Center for Biotechnology Research (ICBR) DNA Sequencing Core Facility.

The chimeric precursor m23p17 is a fusion of coding sequences for amino acids constituting mOE23 (MAYGEAAN...TASSFSVA), a nine amino acid spacer (QKEKNLGAE), and the complete pOE17 sequence. In an effort to eliminate internal initiation in m23p17, the methionines in the presequence of pOE17 were replaced. The natural presequence beginning MAQAMASM.... was changed to LAQALASL.... Two stages of PCR reactions were used in the construction of the clone for m23p17. In the first stage, two PCR reactions produced fragments coding for mOE23 (containing an XbaI site near the 5' end) and for the nine amino acid spacer plus pOE17 (containing a HindIII site near the 3' end). The forward primer for the nine amino acid spacer plus pOE17 contained an overlap corresponding to the last 17 bases of mOE23. The two PCR products were purified and spliced by overlap extension (SOE) in a third PCR reaction (Horton et al., 1989). The SOE product was restricted and ligated in the SP6 direction into pGEM 4Z cut with XbaI and HindIII.

The chimeric protein m23p is a fusion of coding sequences for the amino acids constituting mOE23, the same nine amino acid spacer, and the complete presequence of pOE17 (MAQAMASM...ALSQAARA). m23p was amplified in a single round of PCR using as template a version of m23p17 in which the original methionines were unmodified.

Preparation of Radiolabeled Precursors by *In Vitro* Translation

Capped RNA for the various precursors was produced *in vitro* with SP6 polymerase essentially as described by Cline (1988). Translation in the presence of [^{3}H] leucine was in rabbit reticulocyte (Promega) or a wheat germ system (Cline et al., 1993),

as indicated in the figure legends. Translations were terminated by transfer to ice, dilution threefold, and adjustment to import buffer [50mM HEPES (pH 8), 0.33 M sorbitol] and 30 mM unlabeled leucine.

Preparation of Chloroplasts, Thylakoids, and Lysate

Intact chloroplasts were isolated from 9- to 10-day old pea seedlings (Laxton's Progress 9) as described (Cline et al., 1993) and were resuspended in import buffer (IB). Lysate and washed thylakoids were prepared from isolated chloroplasts (Cline et al., 1993). Chlorophyll concentrations were determined according to Arnon (1949).

Chloroplast Import and Thylakoid Protein Transport Assays

Import of radiolabeled precursors into isolated chloroplasts or transport into washed thylakoids or chloroplast lysate was conducted in microcentrifuge tubes in a 25^{o}C water bath illuminated with 70 μE $m^{-2}s^{-1}$ white light (Cline et al., 1993) for 10 minutes or the time indicated in the figure legend. For assays conducted in the presence of inhibitors, chloroplast lysates were preincubated with azide (8 mM final concentration) or nigericin (0.5 μM final concentration) and valinomycin (1 μM final concentration) on ice for 10 minutes prior to the addition of Mg-ATP (5 mM final concentration) and radiolabeled precursor. For assays conducted in the absence of ATP, lysate (50 μg chlorophyll in 50 μl) and diluted translation product (25 μl) were each preincubated separately for 10 minutes on ice with 1 U apyrase. Competition assays for thylakoid transport were conducted as described previously (Cline et al., 1993). Assays were generally terminated by transfer to 0^{o}C. Where indicated, recovered chloroplasts or thylakoids were protease post-treated with thermolysin. Chloroplasts were repurified on Percoll cushions; thylakoids were recovered by centrifugation.

Immunoprecipitation

Samples for immunoprecipitation were boiled one minute in SDS (final concentration 1%) and then diluted 1:11 with 10 mM Tris/HCl (pH 7.5), 140 mM NaCl, 1 mM EDTA, 1% Triton-X100 and 1 mM PMSF. Rabbit antiserum (5 μl) was added, the samples incubated over-night at 4^0C, and then rotated slowly for two hours at room temperature. Protein A-Sepharose slurry (30 μl) in 10 mM Hepes/KOH (pH 8.0), 10 mM $MgCl_2$ was added and rotation continued at room temperature for one hour. The pellet was recovered and washed four times with 10 mM Tris/HCl (pH 7.5), 150 mM NaCl, 2 mM EDTA and 0.2% Triton-X100 followed by washing twice with 10mM Tris/HCl (pH 7.5). The pellet was dissolved in SDS sample buffer and heated two minutes at 100ºC. The recovered supernatant was analyzed by SDS-PAGE/fluorography.

Analysis of Samples

Samples were subjected to SDS-PAGE and visualized by fluorography (Cline, 1986). Quantification of the radiolabeled protein in a gel band was accomplished by scintillation counting of the excised and extracted gel band (Cline, 1986). In the time course experiment, the relative molar quantity of m23p17 was calculated as the cpm (minus background) in the m23p17 band divided by the number of leucines in m23p17. The relative molar amount of each product was calculated as the number of cpms (minus background) in each product band divided by the number of leucines expected in the protein at that location. The relative molar percent of each protein is the relative molar amount multiplied by 100 and divided by the relative molar amount of m23p17 at time zero.

Results

A Chimeric Precursor Protein for Examination of Transport Topology Was Constructed

To investigate the topology of transport on the ΔpH-dependent pathway, we constructed a protein, m23p17, consisting of the mature domain of OE23 (mOE23) fused to pOE17 (Fig. 2-1). If the thylakoid Delta pH translocation machinery transports proteins via a loop structure, the internally located LTD must engage the translocon while both mOE23 and mOE17 are on the *cis* side of the membrane. Subsequently the amino acids carboxy-proximal to the LTD would enter the lumen. Cleavage by the lumenal processing protease would release mOE17 on the *trans* side of the membrane, leaving the LTD and amino acids amino-proximal to it, m23p, on the *cis* side (Fig. 2-1).

Incubation of m23p17 with isolated thylakoid membranes under transport-permissive conditions produced two polypeptide products (Fig. 2-2A). At time zero only the translation product, m23p17, and a faint band apparently resulting from internal initiation were visible. By 1 minute, polypeptides with the expected molecular weights of m23p and mOE17 began to accumulate. Quantification of radioactivity in the bands demonstrated that the two products accumulated progressively and stoichiometrically throughout the 15-minute experiment (Fig. 2-2B). Furthermore, the relative molar decrease in m23p17 was equal to the relative molar increase in the two products. This processing was very efficient; approximately 70% of the substrate was cleaved to the two products in the 15-minute assay. The identity of the products was confirmed by co-migration with authentic polypeptides and by immunoprecipitation (Fig. 2-2C). The presumptive m23p migrated identically to an authentic m23p translation product prepared by recombinant methods (lanes 3 and 4) and was immunoprecipitated by antibodies to

A loop mechanism for transport.

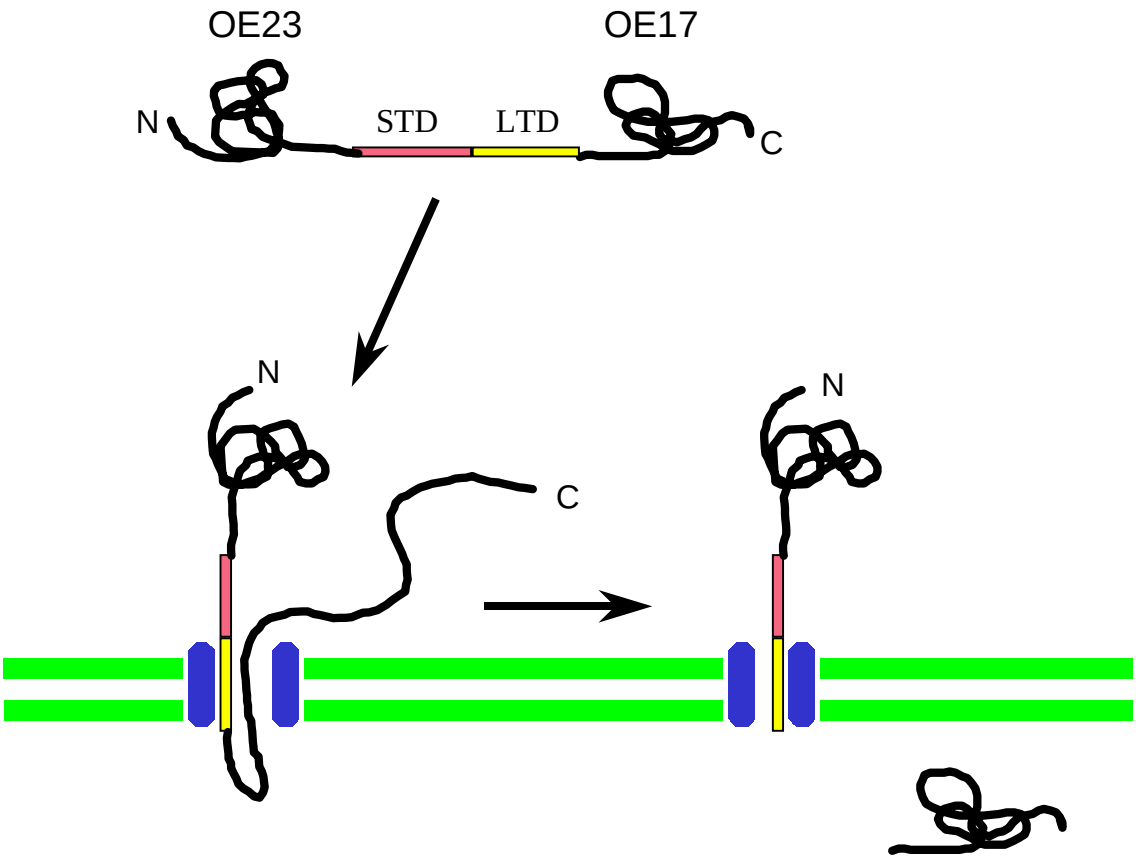

Figure 2-1. Model for translocation of a fusion protein, m23p17, by a loop initiation mechanism. The mature form of OE23 was attached amino terminal to the full sequence of pOE17. The model depicts the substrate and products as well as their relative locations if the ΔpH-dependent pathway initiates transport with a loop.

OE23 (lane 8), but not by preimmune serum (lane 7) or by antibodies to OE17 (lane 9). The mOE17 band migrated identically to authentic mOE17 (see below) and was immunoprecipitated only by antibodies to OE17 (lane 9). The m23p17 present in transport mixtures was immunoprecipitated by both OE23 and OE17 antibodies as expected (lanes 8, 9).

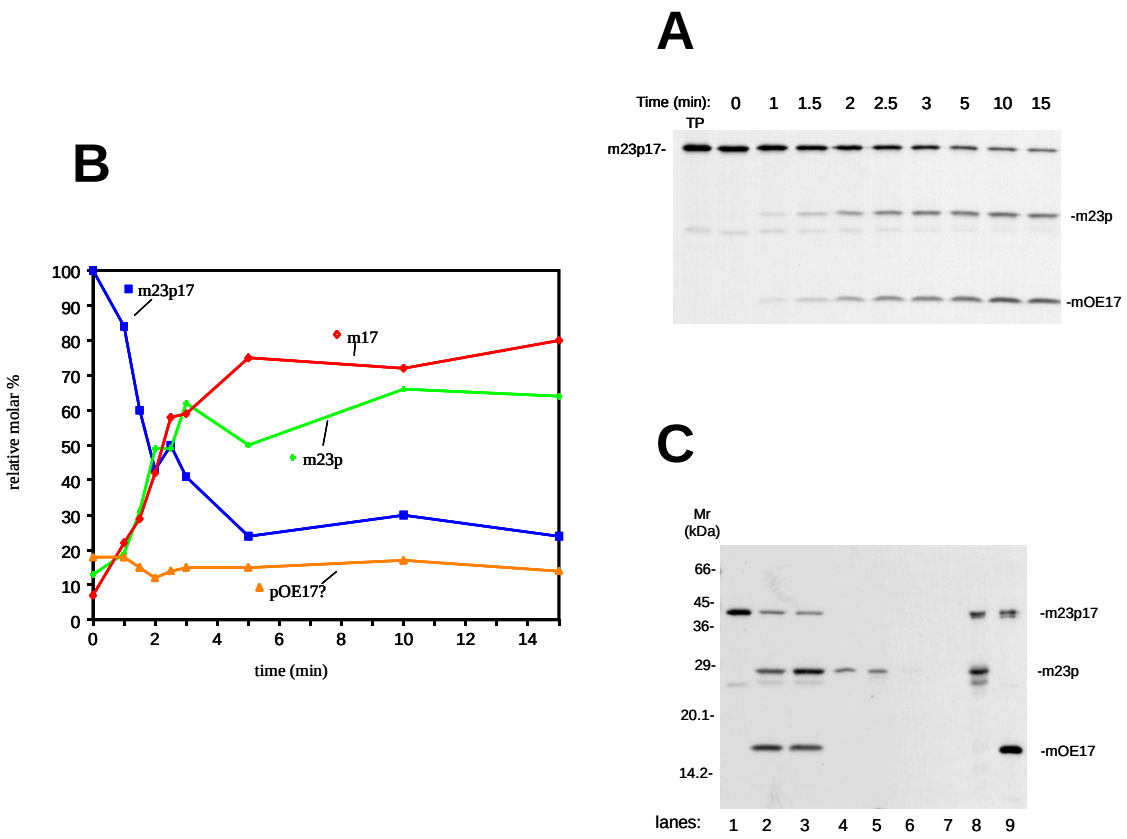

Figure 2-2. Temporal appearance and identities of peptides produced during a transport reaction with m23p17. *(A)* Rabbit reticulocyte-produced m23p17 was incubated with washed thylakoid membranes in an illuminated bath at 25^0C. Samples were taken at the times indicated, boiled in SDS buffer, and analyzed by SDS-PAGE and fluorography. The radiolabeled precursor *(TP)* represents an amount equivalent to that in each assay sample. *(B)* Quantification of bands shown in *(A)*. *(C)* m23p17 and m23p were generated by translation with rabbit reticulocyte and are seen in lanes 1 and 4, respectively. A 10-min transport assay with m23p17 was divided into 5 aliquots. Samples for lanes 2 and 3 were boiled in SDS. The remaining material was processed for immunoprecipitation (see Materials and Methods). Lane 3 contains a mixture of transport products (90% of the amount in lane 2) and translation-generated m23p (equal to the amount in lane 4). Lane 5 and 6 contain m23p subjected to immunoprecipitation with antibodies to OE23 and OE17, respectively. Lanes 7, 8 and 9 contain transport assay samples subjected to immunoprecipitation with preimmune, anti-OE23, and anti-OE17, respectively.

In previous studies with ER membranes, the signal peptide was further cleaved in the hydrophobic core prior to release of the amino terminal portion into the supernatant

(Lyko et al., 1995). No processing of the LTD or degradation of m23p was apparent in our experiments. We estimate that our gel analysis would have detected the loss of as few as six amino acids.

m23p Is Localized to the *Cis* Side of the Membrane, whereas mOE17 Is in the Lumen

To determine the location of the above products, soluble and membrane fractions were obtained from a transport assay. In time course reactions such as the one shown in Fig. 2-2, all of the mOE17 and most of the m23p were recovered with thylakoids (not shown). Accordingly, thylakoids from a 10-minute transport assay were treated with thermolysin to distinguish surface-exposed from lumenal species (Fig. 2-3). The m23p17 and m23p bands were degraded by protease treatment, indicating that they were exposed to the stromal surface of the membranes, whereas the mOE17 band was protease resistant, indicating a lumenal location (lane 5). When the thylakoid lumen was opened by sonication or 1% Triton X-100, the mOE17 was degraded by protease (data not shown). For comparison, *in vitro* translated pOE17 (lane 6) was similarly assayed with thylakoids (lanes 9 and 10). Membrane-associated pOE17 and mOE17 displayed the expected protease sensitivity and insensitivity, respectively.

Also shown in Fig. 2-3, m23p17 was not imported into isolated chloroplasts and even failed to bind significantly to the chloroplast surface (lanes 2 and 3). In chloroplast import experiments with rabbit reticulocyte translated m23p17, a very faint band at the location of mOE17 was produced (data not shown). This apparently resulted from import of a small amount of internally initiated pOE17 that occurs in the reticulocyte system (see Fig. 2-2). These results can be compared to the robust import achieved with the authentic pOE17 precursor (lanes 7 and 8). The lack of import or binding of m23p17 by

chloroplasts is apparently due to their inability to recognize the internally located transit peptide. This agrees with current models of organellar import in which translocation is initiated at the N terminus of the targeting peptide, followed by movement of the precursor linearly through the pore (Kouranov et al., 1996).

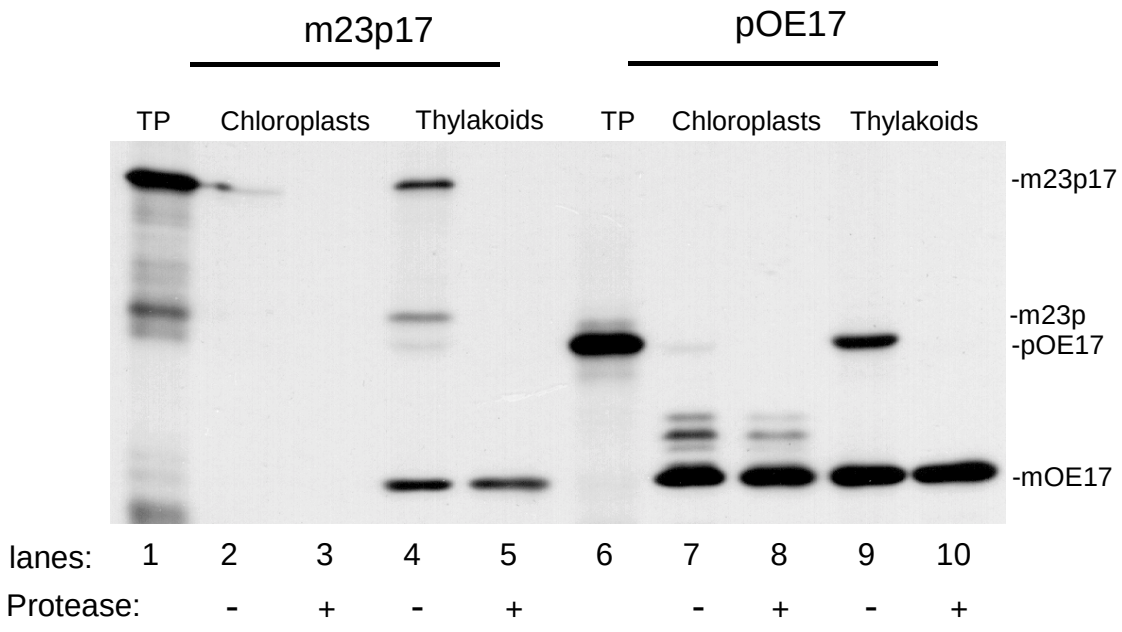

Figure 2-3. Transport of m23p17 delivered mOE17 to the lumen, leaving m23p on the stromal face of the thylakoids. Wheat germ-translated m23p17 and pOE17 were assayed for import into isolated chloroplasts and transport into isolated thylakoids at 25^0C for 10 minutes (see Materials and Methods). Recovered chloroplasts or thylakoids were treated with or without thermolysin as shown below the panel. Lanes 1 and 6 represent 1% of the m23p17 and pOE17, respectively, added to each assay. Lanes 2 through 5 and 7 through 10 contain chloroplasts or membranes equivalent to 6% of that present in each assay.

Production of m23p and mOE17 from m23p17 Results from ΔpH-dependent Pathway Transport.

Because of the alterations necessary to make m23p17, it was important to determine if m23p and mOE17 were produced as a result of transport via the ΔpH-dependent pathway. Assays were conducted under conditions diagnostic for

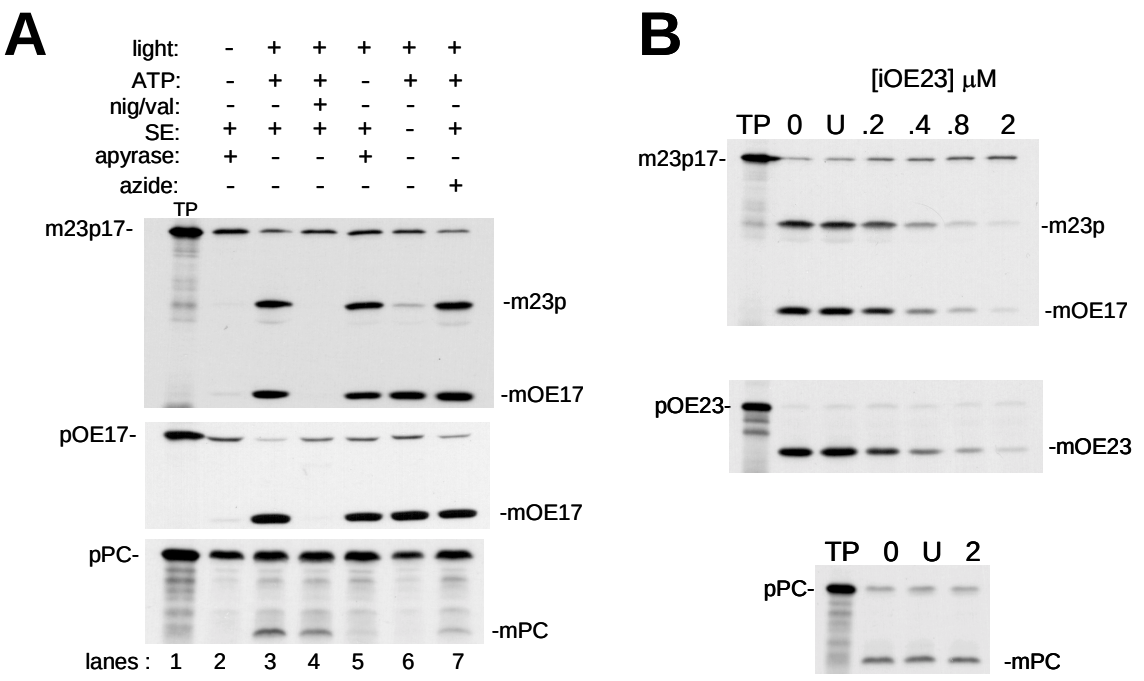

Figure 2-4. m23p17 was transported exclusively on the ΔpH-dependent pathway. *(A)* Transport of wheat germ-produced precursors across thylakoid membranes was conducted for 10 minutes at 25^0C in light or darkness as shown, with lysate to provide stromal extract (*SE*), or with twice-washed thylakoids (see Materials and Methods). Assay conditions were designed to examine the requirement for SE, ATP, a ΔpH, or sensitivity to azide. Apyrase was used to eliminate residual ATP in lysate and translation products. These conditions are designated above the fluorogram panels. Recovered thylakoids were washed and analyzed by SDS-PAGE and fluorography. The radiolabeled precursor *(TP)* represents 1% of the amount in each assay. Lanes were loaded with recovered thylakoids equivalent to 6.7% of each assay. *(B)* Transport competition assays were conducted with chloroplast lysates and 5 mM ATP in the presence of increasing concentrations of unlabeled iOE23 for 10 minutes at 25^0C in the light. Thylakoid membranes were washed and analyzed by SDS-PAGE and fluorography. Lanes were loaded with TP and sample amounts as in *(A)* above. The final concentration of iOE23 competitor is indicated above the fluorograms. The lane designated U represents a control assay containing no iOE23 competitor, but containing urea *(U)* at 167 mM (equal to the concentration of urea in the 2 μM competition assay).

ΔpH- mediated transport (Fig. 2-4). In Fig. 2-4A the energy and stromal requirements for production of m23p and mOE17 are compared to those for transport of ΔpH-dependent pathway-directed pOE17 and cpSec pathway-directed pPC. As with pOE17 transport,

production of m23p and mOE17 was abolished by ionophores that dissipate the trans-thylakoid ΔpH (lane 4) and was unaffected by removal of ATP (lane 5), by the absence of stromal extract (lane 6), or by sodium azide (lane 7), a SecA inhibitor (Oliver et al., 1990). In contrast, cpSec-mediated pPC transport was only slightly diminished by ionophores, but abolished by removal of ATP or stromal extract (the source of approximately 90% of cpSecA) and diminished by addition of sodium azide.

In the experiment shown in Fig. 2-4A, only the recovered membranes were analyzed. An unexpected result was that removal of stromal components and thorough washing of thylakoids used for the assay, while without effect on the amount of mOE17 produced from m23p17 (top panel, lane 6), resulted in much less membrane-associated m23p. In other experiments (not shown), we verified that m23p was indeed produced under these conditions.

As an additional test of pathway utilization by m23p17, precursor competition studies were conducted. Precursor proteins utilizing the ΔpH-dependent pathway are able to compete with one another for transport, but not with cpSecA utilizing precursors. As shown in Fig. 2-4B, the ΔpH-dependent pathway intermediate iOE23 competed for transport of pOE23 and m23p17, but not pPC transport. Taken together, these results demonstrate that transport of the mOE17 moiety of m23p17 occurs via the ΔpH-dependent pathway. Moreover, they substantiate that production of the *cis*-localized m23p is a transport-coupled phenomenon.

Discussion

A hallmark of a loop mechanism of insertion is that the amino-proximal peptide flanking the signal sequence remains on the *cis* side of the membrane, while the carboxyl

flanking polypeptide is transported across the membrane. The loop mechanism was demonstrated for the ER by expression in HeLa cells of a vesicular stomatitis virus glycoprotein (VSV G) with a non-cleavable amino terminal extension (Shaw et al., 1988). The VSV G domain was translocated to the ER lumen, whereas the amino terminal extension remained exposed to the cytoplasmic side of the membrane. The existence of an inserted loop in the ER was further demonstrated by Mothes et al. (1994) who used photo-reactive crosslinkers to show that the polypeptide chain spanned the ER membrane twice prior to, but only once following signal sequence cleavage. Kuhn et al., (1994) demonstrated a loop mechanism for protein translocation by the Sec pathway of *E. coli* with a similar strategy to that employed in our studies; i.e. a chimeric precursor protein having a large amino terminal extension derived from ribulokinase was fused to proOmpA.

Similar to the results obtained with the ER system and the *E. coli* system, the amino terminal domain of m23p17 did not interfere with signal peptide recognition or with translocation by the ΔpH-dependent pathway mechanism of thylakoids. In addition, the m23p domain remained outside of the thylakoids, whereas the OE17 domain was translocated into the lumen (see Fig. 2-1 for model). In studies with ER membranes, the amino terminus remained transiently associated with the membranes prior to release into the supernatant (Lyko et al., 1995). We also observed binding of transport-generated m23p to membranes that varied with the specific conditions of the assay (Fig. 2-4A). Membrane-bound m23p was tightly associated, as much of it remained bound even after washing with high salt or urea. However the physiological relevance of such binding is unclear because m23p produced directly by *in vitro* translation also bound tightly to the

membrane and was resistant to the same salt and urea extractions (Fincher and Cline, unpublished results). Thus, although it is possible that transport-produced m23p remains transiently associated with the translocon as depicted in Fig. 2-1, we cannot currently distinguish this from non-specific association with the membrane surface.

The original loop model as proposed by Inouye and Halegoua (1980) describes a loop formed across the bilayer with the hydrophobic region of the signal peptide extending through the bilayer on one side and the first several amino acids of the mature domain of the substrate protein extending through the bilayer on the opposite side as depicted for m23p17 in Fig. 2-1. In light of evidence that the Tat pathway and ΔpH-dependent pathway are able to translocate folded proteins, the availability of the amino terminus of the mature protein to form the carboxyl side of the loop is open to question. The extent of folding of OE17 in the m23p17 construct is unknown. It has been noted that where crystal structures of bacterial Tat substrates are known, the mature protein lacks a disordered N-terminus that could support loop formation, but that the structure of the precursor might be somewhat different (Berks et al., 2000b). Clearly, the data I have presented indicate that a loop was formed, although the precise amino acids involved in loop formation and the location of the loop (whether in the membrane bilayer, in a receptor site or at a protein-lipid interface) remain undetermined.

The unlooping model was put forward by de Kruijff and coworkers (de Vrije et al., 1990) as an alternative hypothesis for protein translocation through Sec-type systems. In their model, the positively charged N-domain interacts electrostatically with the negatively charged phospholipids. That interaction is followed by insertion of the H-domain as a loop reaching only into the hydrophobic core of the bilayer. The passage of

the peptide through the bilayer locally perturbs lipid organization. The H-domain unloops pulling the mature region of the substrate into the hydrophilic channel (van Voorst and de Kruijff, 2000). Since the alpha carbons of arginine residues are potentially able to reside one or more helical turns within the membrane while the charged group reaches the lipid headgroup region (Monné et al., 1998), the H-domain of m23p17 may be effectively lengthened by several residues. The bending of the H-domain from one α-helix to effectively two (called helix-break-helix) is aided by amino acids common to hydrophobic domains such as glycines and serines (Izard and Kendall, 1994). Data from the experiments I have described with m23p17 as well as data from the *E. coli* Sec system (Kuhn et al., 1994) and the mammalian ER (Shaw et al., 1988; Mothes et al., 1994) are reconcilable with the unlooping mechanism of protein entry. The conclusion that remains is that in all three export pathways and in spontaneous translocation (Thompson et al., 1998), transport is initiated by signal peptide mediated loop formation.

CHAPTER 3
THE CHARACTERIZATION OF A TRANSLOCATION INTERMEDIATE ON THE ΔpH-DEPENDENT PATHWAY

Introduction

The biochemistry of the chloroplast ΔpH-dependent pathway has been studied by defining its signal sequence specificity, energetic requirements, topology of translocation initiation, and its ability to transport folded proteins. While its use of N-terminal targeting sequences and initiation of translocation via a loop mechanism point to an evolutionary relationship with export pathways such as that of the endoplasmic reticulum (ER) and bacterial Sec system, other pathway characteristics set it apart. The ability of the ΔpH-dependent pathway to utilize only the trans-thylakoid pH gradient as an energy source is unique among known protein translocation systems. The recently elucidated capacity to transport folded proteins (Clark and Theg, 1997; Hynds et al., 1998) is rare among protein export systems, but has since been documented in the bacterial twin-arginine translocation pathway to which the thylakoid pathway is evolutionarily related (Berks et al., 2000a for review; Thomas et al., 2001).

The translocation of folded proteins has been clearly demonstrated in peroxisomal import pathways (Gietl, 1996, for review). In spite of the apparent ability of peroxisomes to translocate even large complexes, a translocation intermediate has been characterized in the specialized peroxisomes called glyoxysomes (Pool et al., 1998). Observation of the translocation intermediate was achieved using a fusion protein partially consisting of the immunoglobulin G (IgG) binding domains of *Staphylococcus aureus* protein A. The

authors speculated that the ability to form such an intermediate was not dependent on the tightly folded nature of protein A, but on the unique nature of the protein itself. Protein A had previously been used to form a translocation intermediate and to purify components of the chloroplast protein import machinery (Schnell and Blobel, 1993). Schülke et al. (1997) constructed a chimeric precursor by linking the presequence of a mitochondrial precursor via glutathione S-transferase (GST) to a polypeptide containing multiple IgG binding domains of protein A. Import of the precursor into mitochondria resulted in processing and formation of a translocation intermediate both *in vitro* and *in vivo*. Formation of the translocation intermediate engendered "zippering" of the outer and inner mitochondrial membranes.

Translocation intermediates are an important tool in the elucidation of transport mechanisms and the isolation and identification of machinery components. I have constructed a series of proteins consisting of pOE17 and the IgG binding domains of protein A. The constructs differ in the nature and length of the linker region between the two domains. Using these recombinant proteins, I have demonstrated the formation of translocation intermediates on the ΔpH-dependent pathway.

Materials and Methods

Preparation of Chloroplasts, Thylakoids, and Lysate

Intact chloroplasts were isolated from 9- to 10-day old pea seedlings (Laxton's Progress 9) as described (Cline et al., 1993) and were resuspended in import buffer. Lysate and washed thylakoids were prepared from isolated chloroplasts (Cline et al., 1993). Chlorophyll concentrations were determined according to Arnon (1949).

Construction of Chimeric Precursors

Cloning and analysis of DNA products were by standard molecular biology procedures (Sambrook et al., 1989). Amplifications were performed with *Pfu* polymerase (Stratagene, La Jolla, CA). Cloned constructs were verified by DNA sequencing. Sequencing was done with ABI Prism Dye Terminator cycle sequencing protocols developed by Applied Biosystems (Perkin-Elmer Corp., Foster City, CA) and an Applied Biosystems model 373 Stretch DNA Sequencer (Perkin-Elmer Corp.). Sequencing of all clones on both strands was performed by the University of Florida Interdisciplinary Center for Biotechnology Research (ICBR) DNA Sequencing Core Facility.

The cloning of protein A-containing constructs was a multi-stage process using several templates. In the first step, maize pOE17 (Cline et al., 1993) and mouse dihydrofolate reductase (DHFR) were used as templates in an SOE (Horton et al., 1989) reaction[1]. The final product, p17-DHFR, was ligated in the SP6 direction into pGEM 4Z. The template p17-DHFR was amplified by PCR with a 5' primer having an engineered *EcoRI* restriction site and a 3' primer with coding for Kodak FLAG epitope (amino acid sequence of FLAG epitope: DYKDDDDK). The 3' primer overlapped DHFR so that the final product contained all of pOE17 and 22 amino acids of DHFR followed by the FLAG epitope. The resultant DNA, p17-FLAG, was purified, restricted with *EcoRI* and *HincII*, and ligated in the SP6 direction into pGEM 4Z that had been cut with *EcoRI* and *HincII*.

I made p17Δ-protA by PCR and *SphI*-mediated splicing using maize pOE17 in pGEM 4Z and pS/protA in pET21b (Schnell and Blobel, 1993) as templates. I amplified

[1] p17-DHFR was cloned by Michael McCaffery in 1993.

pOE17 using the same 5' primer as employed in production of p17-FLAG with an engineered *EcoRI* restriction site and a 3' primer having an engineered *SphI* restriction site. The resultant intermediate contained all but the final eight amino acids of pOE17. I amplified pS/protA using a 5' primer having an engineered *SphI* restriction site and a 3' primer having an engineered *BamHI* restriction site. I cut the intermediates with *SphI* and ligated. From the ligation products, I selected the band of appropriate size (1659 base pairs), purified the DNA, restricted it with *EcoRI* and *BamHI*, and ligated it in the SP6 direction into pGEM 4Z that had been cut with *EcoRI* and *BamHI*.

The construct p17-L-protA was cloned in multiple steps including SOE and *SphI*-mediated splicing using a pBluescript SK phagemid (Promega) intermediate. The pBluescript SK phagemid was used as an intermediate cloning vector because of the presence of an *SphI* restriction site in pGEM 4Z that would have complicated cloning. The template p17-FLAG was amplified by PCR using a 5' primer having *EcoRI* and *NdeI* restriction sites and a 3' primer with sequence that amplified coding for all of pOE17 and 19 amino acids from DHFR (but none of FLAG). The 3' primer included an overlap for a portion of the 5' primer for pGEX-2TK (Pharmacia). A portion of the pGEX-2TK template that encodes 25 amino acids including the thrombin site was amplified using a 5' primer with the stated overlap and a 3' primer having an *SphI* restriction site. The two PCR products were purified and spliced by SOE in a third PCR reaction to yield p17-L. The construct described in the previous paragraph, p17Δ-protA, was cut from pGEM 4Z using *EcoRI* and *BamHI*, then ligated into pBluescript SK phagemid that had been cut with *EcoRI* and *BamHI*. The product was restricted with *EcoRI* and *SphI*, resulting in a linear plasmid having an open *SphI* site followed by pS/ProtA. I then cut p17-L with

EcoRI and *SphI* and ligated it into the linear pBluescript SK phagemid. The result was p17-L-protA in pBluescript SK phagemid. I cut p17-L-protA from pBluescript SK phagemid with *EcoRI* and *BamHI* and ligated it in the SP6 direction into pGEM 4Z that had been cut with *EcoRI* and *BamHI*.

The construct p17-LF-protA was cloned similarly to p17-L-protA. The template p17-FLAG was amplified using a 5' primer having *EcoRI* and *NdeI* restriction sites and a 3' primer with sequence that amplified coding for all of p17-FLAG. The 3' primer included an overlap for a portion of the 5' primer for pGEX-2TK. A portion of the pGEX-2TK template that encodes 28 amino acids including the thrombin site was amplified using a 5' primer with the stated overlap and a 3' primer having an *SphI* restriction site. The two PCR products were purified and spliced by SOE in a third PCR reaction to yield p17-LF. The construct p17Δ-protA was cut from pGEM 4Z using *EcoRI* and *BamHI*, and then ligated into pBluescript SK phagemid. The product was cut with *EcoRI* and *SphI*, resulting in a linear plasmid having an open *SphI* restriction site followed by pS/ProtA. I subsequently restricted p17-LF with *EcoRI* and *SphI* and ligated it into the linear pBluescript SK phagemid. The result was p17-LF-protA in pBluescript SK phagemid. Sequencing revealed an error in the clone in the pOE17 portion near the 5' end. I cut the DNA just 3' to the error with *SacII* and at its 3' end with *BamHI* to yield a 1704 base pair product. I restricted p17-L-protA in pGEM 4Z with *SacII* and *BamHI* resulting in a linear plasmid with the 5' end of pOE17 up to the *SacII* restriction site. I ligated the 1704 base pair insert into the pGEM 4Z plasmid to get p17-LF-protA in the SP6 direction in pGEM 4Z.

Truncations of p17-LF-protA termed LF1, LF2, and LF3 were cloned by PCR using p17-LF-protA in pGEM 4Z as the template.[2] The 5' primer was made to the sequence of pGEM 4Z upstream of the clone start site. Because protein A has multiple domains of similar sequence, it was possible to make all three clones using a single 3' primer. Products of the PCR having sizes 1197 base pairs, 1380 base pairs, and 1554 base pairs were purified, restricted with *EcoRI* and *BamHI*, and ligated in the SP6 direction into pGEM 4Z that had been restricted with *EcoRI* and *BamHI* to yield LF1, LF2, and LF3, respectively.

The truncation of p17-LF-protA named LF0 includes the complete linker region of the full construct without any of protein A[3]. It was amplified from LF1 using a 5' primer that initiated in the pGEM-4Z vector and a 3' primer that initiated within the linker region and contained an engineered *BamHI* site. The PCR product was purified, restricted with *EcoRI* and *BamHI*, and ligated in the SP6 direction into pGEM 4Z that had been restricted with *EcoRI* and *BamHI* to yield LF0.

The construct pLF(V/R) was cloned by PCR using SOE[4]. The template was p17-LF-protA; the 5' and 3' primers were to vector regions upstream and downstream, respectively, of the clone. Internal primers were designed to change the single amino acid, valine 229, to arginine and yield products with overlapping sequence in the first set of PCR amplifications. The second round of PCR yielded pLF(V/R). In a similar set of reactions, alanine 290 was mutated to arginine yielding pLF(A/R). The PCR products were purified, restricted with *EcoRI* and *BamHI*, and ligated in the SP6 direction into

---

[2] LF1, LF2, and LF3 were cloned by Justin Delille and Mike McCaffery in 1999.
[3] LF0 was cloned by Mike McCaffery in 1999.
[4] pLF(V/R), pLF(A/R), and pLF(V/R)(A/R) were cloned by Mike McCaffery in 2000.

pGEM 4Z that had been restricted with *EcoRI* and *BamHI*. The dual change pLF(V/R)(A/R) was constructed by *SphI* digestion and splicing of the single change constructs.

Clone pLF(V/R)(A/R) was used as template for the cloning of p17tp-protA by SOE.[5] A 5' primer having an engineered *SstI* site and a 3' primer including an overlap region for the SOE were used to amplify nucleotides encoding the transit peptide of pOE17. A 5' primer with the stated overlap for the SOE was used to amplify the protein A moiety beginning with glutamine 308 from pLF(V/R)(A/R). The 3' primer used for the amplification of the protein A moiety bound in the vector. After the SOE reaction, the product was purified, cut with *SstI* and *XbaI*, and ligated in the SP6 direction into pGEM 4Z that had been cut with *SstI* and *XbaI*.

Preparation of Radiolabeled Precursors

Coupled transcription/translation with wheat germ TnT (Promega) or rabbit reticulocyte TnT (Promega) in the presence of ^{3}H leucine or, where specified, ^{35}S methionine (NEN Life Science Products) was performed following the manufacture's guidelines. *In vitro* transcription with SP6 RNA polymerase (Promega) and translation with wheat germ lysate (Promega) in the presence of ^{3}H leucine was performed following the manufacture's guidelines. Translation products were diluted with one volume 60 mM leucine (or 60 mM methionine for ^{35}S labeled proteins) in 2X import buffer (1X = 50 mM HEPES, KOH, pH 8.0, 0.33 M sorbitol) prior to use.

[5] p17tp-protA was cloned by Mike McCaffery in 2001.

Chloroplast Import and Thylakoid Protein Transport Assays

Import of radiolabeled precursors into isolated chloroplasts or transport into washed thylakoids or chloroplast lysate was conducted in microcentrifuge tubes in a 25^{o}C water bath illuminated with 70 μE $m^{-2}s^{-1}$ white light (Cline et al., 1993) for 10 min or the time indicated in the figure legend. For assays conducted in the presence of inhibitors, chloroplast lysates were preincubated with nigericin (0.5 μM final concentration) and valinomycin (1 μM final concentration) on ice for 10 min prior to the addition of Mg-ATP (5 mM final concentration) and radiolabeled precursor. Competition assays for chloroplast import were conducted as described previously (Cline et al., 1993). Assays were generally terminated by transfer to an ice bath. Termination with $HgCl_2$, where indicated in the figure legend, was used when it was necessary to rapidly halt both transport and all intra-lumenal reactions (Reed et al., 1990). Where indicated, recovered chloroplasts or thylakoids were protease post-treated with thermolysin. Chloroplasts were repurified on Percoll cushions; thylakoids were recovered by centrifugation.

Immunoprecipitation

Samples for immunoprecipitation were heated at 80^{0}C for 5 min in SDS (final concentration 1%) and then diluted 1:11 with 10 mM Tris/HCl (pH 7.5), 140 mM NaCl, 1 mM EDTA, 1% Triton-X100 and 1 mM PMSF. Rabbit antiserum (5 μl) was added and the samples were rotated slowly over-night at 4^{0}C. Protein A-Sepharose slurry (30 μl) in 10 mM Hepes/KOH (pH 8.0), 10 mM $MgCl_2$ was added and rotation continued at 4^{0}C for two hours. The pellet was recovered and washed four times with 10 mM Tris/HCl (pH 7.5), 150 mM NaCl, 2 mM EDTA and 0.2% Triton-X100 followed by washing twice

with 10mM Tris/HCl (pH 7.5). The pellet was dissolved in SDS sample buffer and heated 2 min at 100ºC. The recovered supernatant analyzed by SDS-PAGE and fluorography.

Results

Fusion Proteins Consisting of pOE17 and Protein A Were Constructed Having Varying Linkers.

The seventeen kilodalton component of the oxygen evolving complex, OE17 is encoded in the nucleus, synthesized in the cytoplasm in its precursor form, pOE17, and imported into chloroplasts. Inside the chloroplasts, the ΔpH-dependent pathway exports it to the thylakoid lumen. I created several fusion proteins using maize pOE17 and *S. aureus* protein A. When referred to collectively, these constructs are termed "17-protA"; however, each individual fusion protein is described and given a specific label. The OE17 domain of p17Δ-protA has eight amino acids truncated from its carboxyl end. All other chimeras described include the entire coding sequence of pOE17. The overall design of the constructs is pictured in Fig. 3-1A. Each chimera differs in the length and content of its linker region as described in Fig. 3-1B. The complete amino acid sequence of p17-LF-protA is detailed in Fig. 3-1C with annotations.

S. aureus protein A has five IgG binding domains (Moks et al., 1986). The full-length chimeric constructs described in Fig. 3-1A each comprise four complete binding domains plus a portion of the fifth domain. Each IgG binding domain contains three alpha helices (Stahl and Uhlen, 1997, Alonso and Daggett, 2000) indicated by color in Fig. 3-1C. There is very high amino acid homology among the domains as can be discerned by inspection. Truncated versions of p17-LF-protA were created having no protein A IgG binding domains (LF0), one IgG binding domain (LF1), two IgG binding

A

Overall Design of Constructs

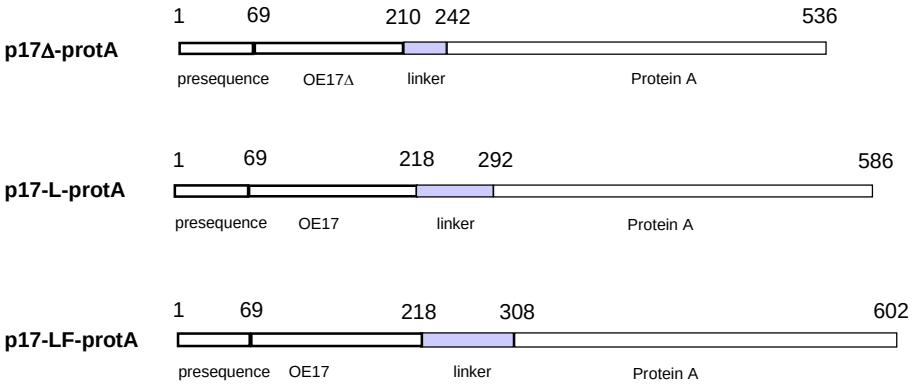

B

Details of Linker Regions

p17Δ-protA

210 - 211 **AC** created by Sph1 splicing
212 - 241 **SQVLKELDEVVAAYPQAFVRIIGFDNVRQV** from small subunit RUBISCO

p17-L-protA

218 - 236 **GMVRPLNCIVAVSQNMGIG** from Dihydrofolate Reductase
237 - 261 **WQATFGGGDHPPKSDLVPRGSRRAC** from pGEX-2TK includes thrombin site **LVPRGS** and modification of kinase site from **RRASV** to **RRAC** by Sph1 splicing
262 - 291 **SQVLKELDEVVAAYPQAFVRIIGFDNVRQV** from small subunit RUBISCO

p17-LF-protA

218 - 239 **GMVR PLNCIVA(V)(R)SQNMGIG KNG** from Dihydrofolate Reductase
240 - 249 **DYKDDDDEED** from Kodak FLAG **DYKDDDDK** with change of **K** to **E** and two additional amino acids added by PCR mutagenesis
250 - 277 **LQGWQATFGGGDHPPKSDLVPRGSRRAC** from pGEX-2TK includes thrombin site **LVPRGS** and modification of kinase site from **RRASV** to **RRAC** by Sph1 splicing
278 - 307 **SQVLKELDE VVA(A)(R)YPQAFVRIIGFDNVRQV** from small subunit RUBISCO

Figure 3-1. Design of fusion proteins. *(A)* The carboxyl end of truncated (OE17Δ) or full length pOE17 followed by a linker region was fused to a portion of the IgG binding segment of *S. aureus* protein A. *(B)* The linkers in each fusion protein differed in length and sequence. The orange amino acids are regions of relatively high hydrophobicity. Within those regions, parenthetical amino acids in orange are those present in p17-LF-protA which were changed to arginines in constructs LF(V/R), LF(A/R), and LF(V/R)(A/R). Lavender amino acids are the site of thrombin cleavage.

C

Sequence of p17-LF-protA

Figure 3-1. Design of fusion proteins (continued). *(C)* The full sequence of p17-LF-protA is detailed. The presequence includes the stromal targeting domain in gray and the tripartite lumenal targeting domain with the N-domain in dark red, the H-domain in dark blue, and the C-domain in brown. The linker region is colored as in (B). The first amino acid from the protein A moiety, glutamine 308, is turquoise. Protein A comprises five IgG binding domains E, D, A, B, and C named in order from amino to carboxyl terminus (Stahl and Uhlen, 1997). Each of these domains contains three alpha helices show in light red, light green and light blue. Only the first two helices of domain C are included in this construct. The carboxyl ends of truncated proteins LF0, LF1, LF2, and LF3 are indicated.

domains (LF2), and three IgG binding domains (LF3). The point of truncation for each of these constructs is indicated in Fig. 3-1C.

Fractionation of Chloroplasts Following Import Demonstrated a Thylakoid Localized Mature Form of 17-protA.

The panels of Fig. 3-2 display the results of assays conducted on three versions of p17-protA. Import of *in vitro*-translated p17-protA into intact chloroplasts or transport

into washed thylakoids resulted in processing of the precursor to mature size. Fractionation of chloroplasts revealed that the mature sized product was primarily associated with the membrane (Fig. 3-2, lane 4), although some remained soluble in the

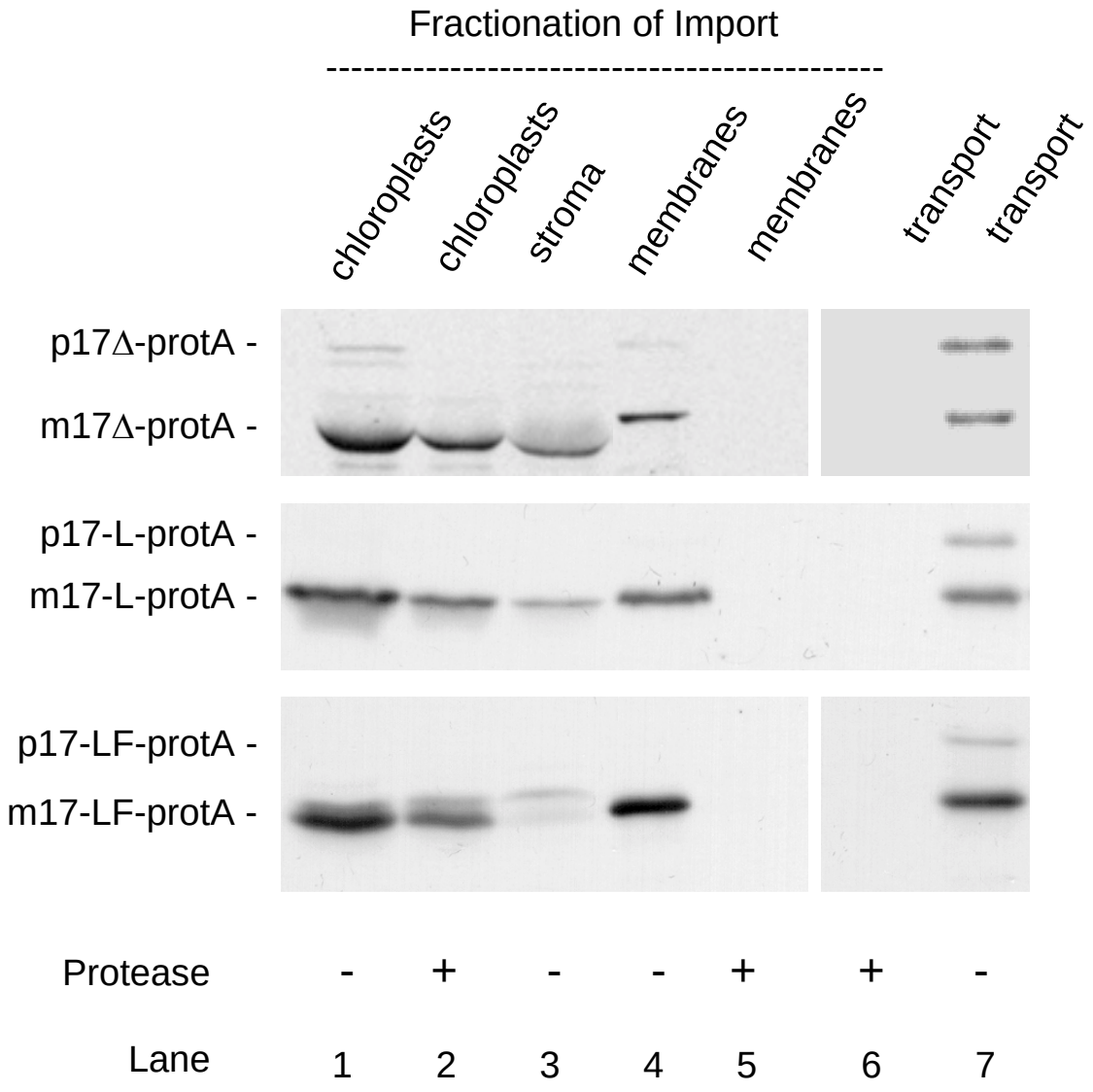

Figure 3-2. Intact chloroplasts and washed thylakoids process p17-protA resulting in a membrane associated mature form. Rabbit reticulocyte TnT generated precursors were incubated with intact chloroplasts (import) or washed thylakoids (transport) for 10 min. Import and transport assays were divided. Chloroplasts were recovered and aliquots were subfractionated by centrifugation to yield stroma and membranes. Membranes were protease treated with thermolysin where indicated below the panels. Samples were analyzed by SDS-PAGE (7.5% acrylamide) and fluorography.

stromal fraction (Fig. 3-2, lane 3). Membrane associated m17-protA was sensitive to treatment with thermolysin (Fig. 3-2, lane 5 and lane 6). When m17Δ-protA (approximately 52 kDa) is associated with intact chloroplasts or with stroma, it runs in a curved band on an SDS-PAGE gel as can be seen in Fig. 3-2, lanes 1-3. The band also runs lower on the gel in the presence of stroma than in washed thylakoids (Fig. 3-2, lanes 1, 2, and 3 versus lane 4 and 7). This phenomenon is probably due to the proximity of other stromal proteins, notably the large subunit of ribulose bisphophate carboxylase/oxygenase (RUBISCO).

Processing of p17-protA to the Mature Size Occurs Only under Transport Permissive Conditions.

For ΔpH-dependent pathway precursors, export to the thylakoid lumen is dependent on the trans-thylakoid pH gradient. Dissipation of that gradient by ionophores such as nigericin results in the accumulation of the stromal intermediate form as demonstrated in lanes 4 and 5 of Fig. 3-3 for ΔpH-dependent pathway precursor pOE23. Import of p17-protA in the presence ionophores resulted in the accumulation of intermediate forms (lanes 4 and 5). (As seen in Fig. 3-2, the *m17Δ-protA runs lower in the presence of stromal proteins.) The accumulation of the intermediate in the stroma implies that processing to the mature size is dependent on access to the thylakoid lumenal processing protease. The inhibition of transport by ionophores was incomplete for OE23 and 17Δ-protA. As a result, some mOE23 can be seen in the lumen in lanes 4 and 6. Because m17Δ-protA is able to back out of the lumen, it is visible along with i17Δ-protA in the chloroplasts and stroma of ionophore treated samples (lanes 4 and 5).

Precursor proteins utilizing the ΔpH-dependent pathway are able to compete with one another for thylakoid transport, but not with cpSecA utilizing precursors. It has been

demonstrated that the import of pOE23 into intact chloroplasts can concentrate the stromal intermediate for thylakoid transport to supersaturating levels (Cline et al., 1993). A model of *in organello* competition is displayed in Fig. 3-4A. In the presence of increasing concentrations of the unlabeled ΔpH-dependent pathway competitor pOE23, the processing of labeled pOE17 and p17-ProtA is progressively inhibited (Fig. 3-4A). When 0.2 to 0.4 μM pOE23 is present (Fig. 3-4A, lanes 4 and 5), the mature sized proteins are replaced by the intermediate forms. This observation implies that the formation of m17-protA is dependent on access to the lumen and processing via the ΔpH-dependent pathway. At 2.0 μM pOE23, import of p17-protA is competitively inhibited, resulting in inhibition of intermediate processing as well (lane 6). Even at 2.0 μM pOE23, all of the imported cpSec pathway precursor, pPC, is processed to mature size.

Following p17-LF-protA import competition with 0.6 μM pOE23, fractionation of chloroplasts was performed to determine the location of products (Fig. 3-4B). All of the i17-LF-protA was located in the soluble fraction as would be expected for a stromal intermediate (lane 5).

Following Processing by the Lumenal Protease, the Mature Substrate Spans the Thylakoid Membrane with Its Amino Terminus on the *Trans* Side of the Membrane and Its Carboxyl Terminus on the *Cis* Side of the Membrane.

As demonstrated in Fig. 3-2, membrane-associated m17-protA was sensitive to thermolysin degradation. Analysis of protease treated membranes on a 12.5% SDS gel revealed protease protected fragments. The size of the fragment generated depended on the length and sequence of the linker region. Protease treatment of membrane-associated m17-LF-protA yielded two distinct fragments, Fragment 1 and Fragment 2 (Fig. 3-5A, lane 9). Fragment 1 is approximately 19-kDa; Fragment 2 is approximately 29-kDa (Fig.

3-5B, lanes 3 and 7). Thus, both lumenal fragments are larger than 17-kDa mOE17. As noted in Fig. 3-2 and Fig. 3-3, much of m17Δ-protA is in the stromal fraction. Since the

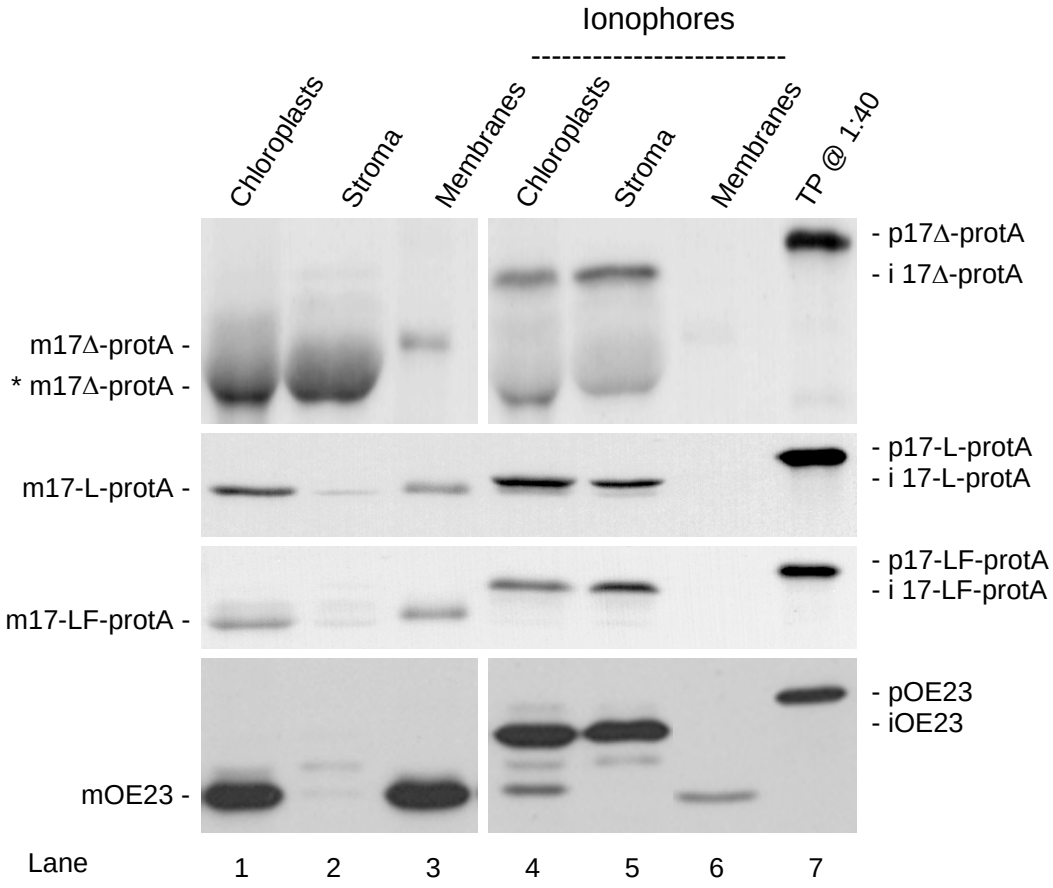

Figure 3-3. Dissipation of the trans-thylakoid pH gradient during import results in the accumulation of stromal intermediate forms of 17-protA. p17Δ-protA was generated from rabbit reticulocyte TnT using ^{35}S labeled methionine. pOE23 was generated from rabbit reticulocyte TnT using ^{3}H labeled leucine. Rabbit reticulocyte generated translation products were desalted. p17-L-protA and p17-LF-protA were generated from wheat germ TnT using ^{3}H labeled leucine. Translation products (TP, lane 7) were incubated with intact chloroplasts, and ATP in the light at 25ºC for 10 min in the absence (lanes 1-3) or presence (lanes 4-6) of nigericin and valinomycin. Chloroplasts recovered from import assays were subfractionated to membranes and stroma and visualized by SDS-PAGE (7.5% acrylamide for 17-protA and 12.5% acrylamide for OE23) and fluorography. In the presence of stromal proteins m17Δ-protA migrates as *m17Δ-protA.

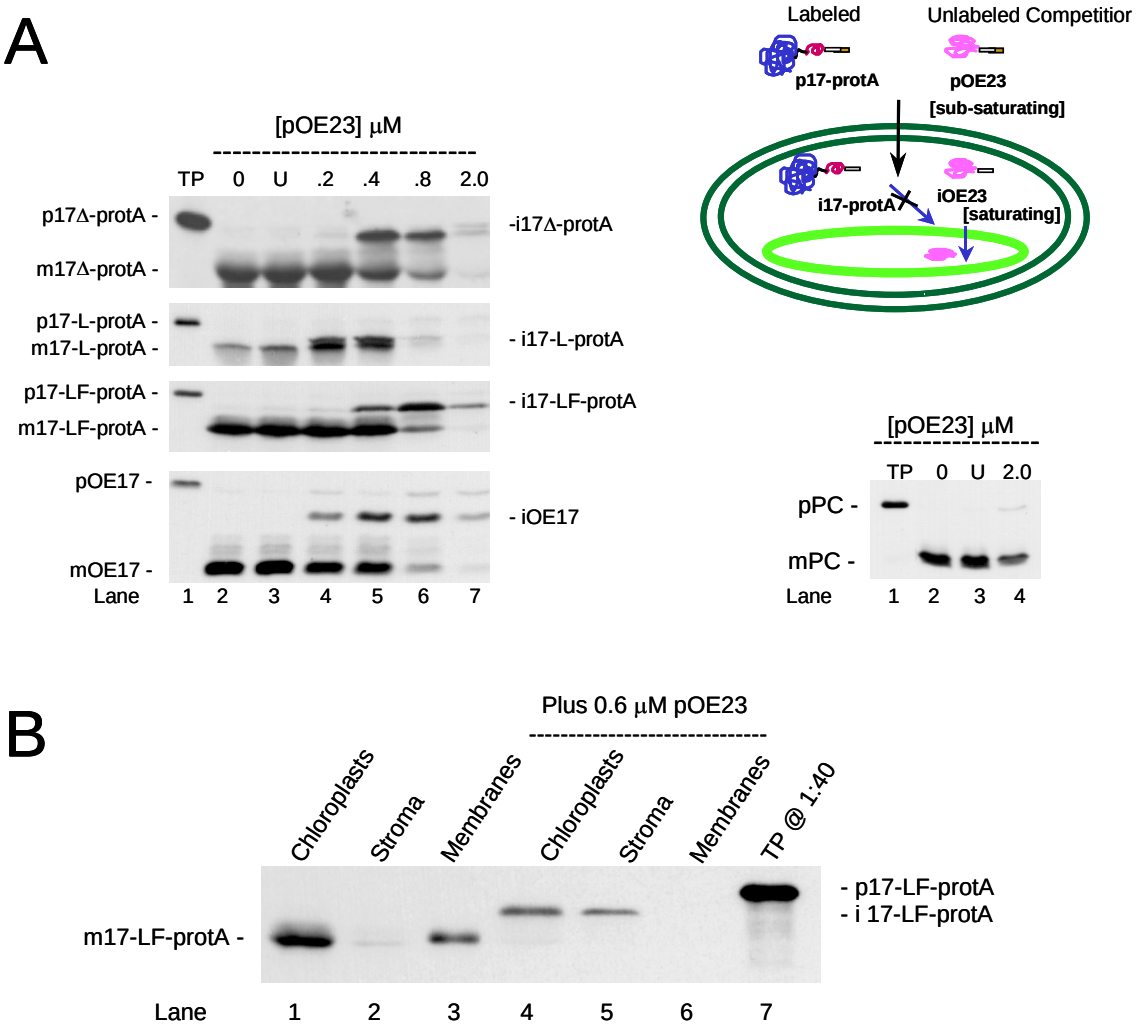

Figure 3-4. Import of p17-protA was competitively inhibited by ΔpH-dependent pathway precursor pOE23. Import substrates p17Δ-protA, p17-L-protA, pOE17, and pPC were generated in rabbit reticulocyte TnT; p17-LF-protA was generated in wheat germ TnT. Chloroplasts were preincubated with indicated concentrations of unlabeled competitor pOE23 and ATP for 7 min in light at 25º C prior to import of labeled precursors. Incubation was continued 10 min following the addition of labeled import substrates. *(A)* Whole chloroplasts were recovered and analyzed by SDS-PAGE (7.5% acrylamide for 17-protA, 12.5% acrylamide for OE17, and 15% acrylamide for PC) and fluorography. The lane designated U represents a control assay containing no pOE23 competitor, but containing urea (U) at 167 mM (equal to the concentration of urea in the 2 μM competition assay). *(B)* Chloroplasts recovered from the import assay were subfractionated by centrifugation to yield stromal and membrane samples. Samples were analyzed by SDS-PAGE (7.5% acrylamide) and fluorography.

linker region is only 32 amino acids and the OE17 moiety of p17Δ-protA is truncated at its carboxyl end, OE17 may not fold properly in the lumen and thus be free to back out of the translocon following processing. Accordingly, protease treated membranes from p17Δ-protA assays yielded little protected peptide (Fig. 3-5A, lane 7). The fragments retained were approximately the same size as Fragment 1 generated by both m17-L-protA (Fig. 3-5A, lane 8) and m17-LF-protA (Fig. 3-5A, lane 9). The generation of fragments was dependent on thermolysin treatment, and fragments were not intrinsically protease resistant. Incubation of membranes without thermolysin, but under otherwise identical conditions (mock) did not lead to generation of lumenal fragments (Fig. 3-5B, lanes 2 and 6). When recovered membranes were solubilized with Triton-X-100 prior to thermolysin treatment, both Fragment 1 and Fragment 2 were digested (Fig. 3-5B, lanes 4 and 8). Therefore, I conclude that the protease resistant fragments are on the *trans* side of the thylakoid membrane. Washing with NaOH, but not Na_2CO_3, disrupts the thylakoid membrane releasing lumenal contents as seen for mOE23 in lanes 10 and 9 of Fig. 3-5C. Both protease generated fragments were released by NaOH wash (Fig. 3-5C, lane 5), indicating that they were soluble inside the lumen.

Fragment 1 and Fragment 2 were derived from OE17 as determined by immunoprecipitation with appropriate antibodies. As would be expected, p17-protA could be immunoprecipitated by irrelevant antibody due to its protein A moiety (Fig. 3-5D, lanes 6 and 13). Neither Fragment 1 nor Fragment 2 could be immunoprecipitated by irrelevant antibody (Fig. 3-5D, lanes 4 and 11), but were specifically precipitated by antibody to OE17 (Fig. 3-5D, lanes 5 and 12). From Fig. 3-5, I conclude that the amino

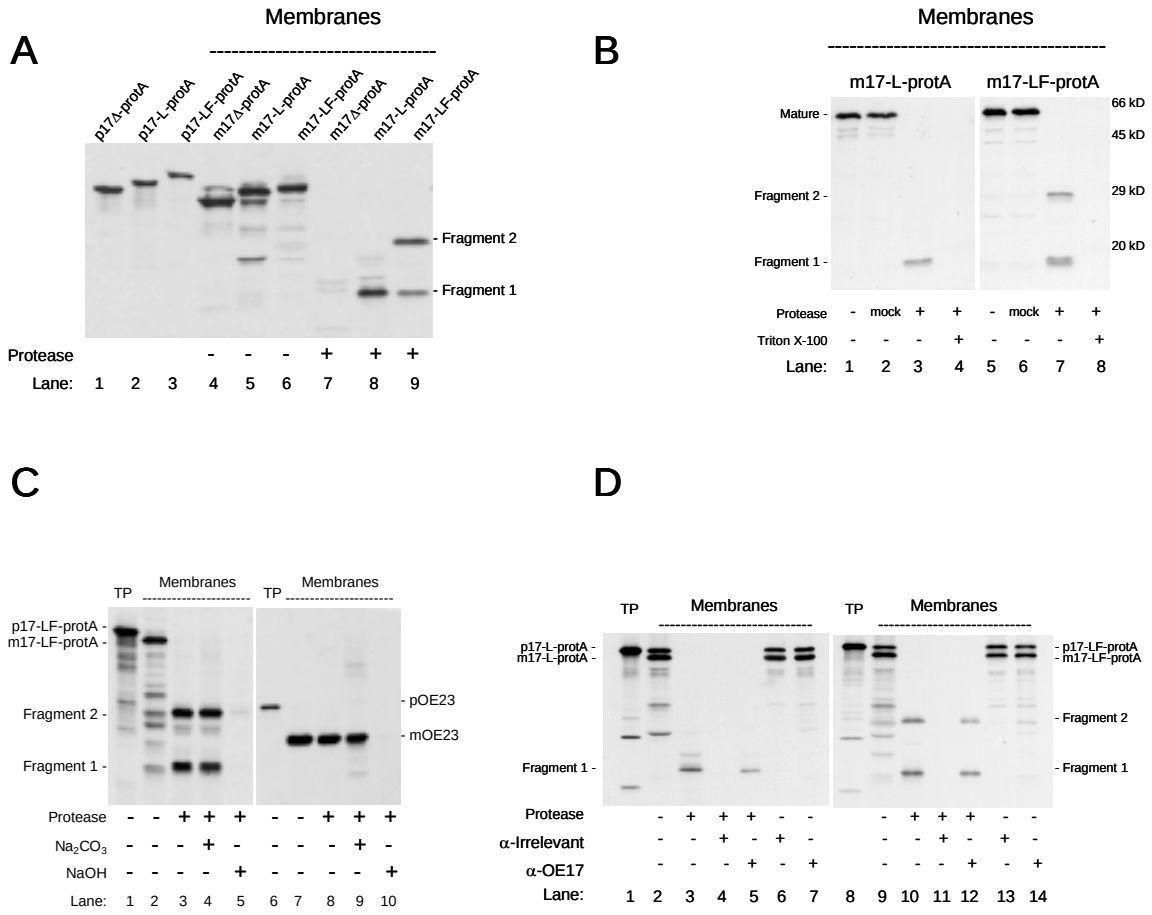

Figure 3-5. m17-protA spans the thylakoid membrane. Analysis of thermolysin (Protease) treated membranes by SDS-PAGE (12.5% acrylamide) and fluorography revealed the location and identity of protease protected fragments. *(A)* p17-protA was generated from wheat germ TnT (lanes 1-3). Translation products were imported into intact chloroplasts. Chloroplasts were recovered and lysed. Recovered membranes were protease treated with thermolysin as indicated below the panel. *(B)* p17-protA was generated from rabbit reticulocyte TnT. Translation products were imported into intact chloroplasts. Chloroplasts were recovered and lysed. Recovered membranes were divided into three aliquots. Membranes were solubilized with 1% Triton X-100 where indicated below the panels. Samples were protease treated with thermolysin or mock treated as indicated below the panels. *(C)* p17-LF-protA and pOE23 were generated from wheat germ TnT (TP, lanes 1 and 6). Translation products were imported into intact chloroplasts. Chloroplasts were recovered and lysed. Recovered membranes were protease treated with thermolysin as indicated below the panel. Protease treated samples were subsequently washed with Na_2CO_3 or NaOH as indicated. *(D)* p17-protA was generated from wheat germ TnT (TP, lanes 1 and 8). Transport assays were conducted on washed thylakoid membranes and divided into six aliquots. Recovered membranes were treated with thermolysin as indicated below the panel. Samples in lanes 4, 6, 11, and 13 were subjected to immunoprecipitation with irrelevant antibody. Samples in lanes 5, 7, 12, and 14 were subjected to immunoprecipitation with anti-OE17.

terminus of p17-protA entered the lumen where it was processed and retained, while the carboxyl end remained on the *cis* side of the membrane.

The Membrane-spanning Intermediate Is Not Integrated into the Lipid Bilayer.

To be of maximum value for investigating ΔpH-dependent pathway translocation, the intermediate must be in contact with translocon components. If the ΔpH-dependent pathway uses a channel, it can be imagined that m17-protA remains in the channel spanning the membrane. Alternatively, the processed protein may have slipped out of the channel and been integrated into the lipid bilayer. The latter possibility was a particular concern given the presence of two mildly hydrophobic stretches of amino acids in the linker detailed in Fig. 3-1B. The size of Fragment 1, approximately 19-kDa, implies that membrane-associated m17-L-protA rests primarily in the region derived from dihydrofolate reductase (DHFR). The appearance of Fragment 2 from m17-LF-protA demonstrates that the change in the linker region allowed additional amino acids to reach the lumen. The linker region of p17-LF-protA includes a highly charged region derived from Kodak FLAG that effectively lowers the hydrophobicity of the DHFR segment. The size of Fragment 2 could reflect either translocation up to the protein A moiety or arrest in the relatively hydrophobic region derived from the small subunit of RUBISCO. Arrest by hydrophobic segments of the linker region may be dictated by association with membrane proteins or with the bilayer. A cartoon illustrating the proposed derivation of Fragments 1 and Fragment 2 from m17-LF-protA is displayed in Fig. 3-6C.

To test for bilayer integration, I imported p17-protA, recovered the membranes, and washed them with IB, NaCl, Na_2CO_3, NaOH, or urea (Fig.3-6A). The membrane-

associated m17-protA was fully resistant to all treatments except NaOH (lane 5). Only about 40% of membrane-associated p17-protA was resistant to NaOH wash (Fig. 3-6D).

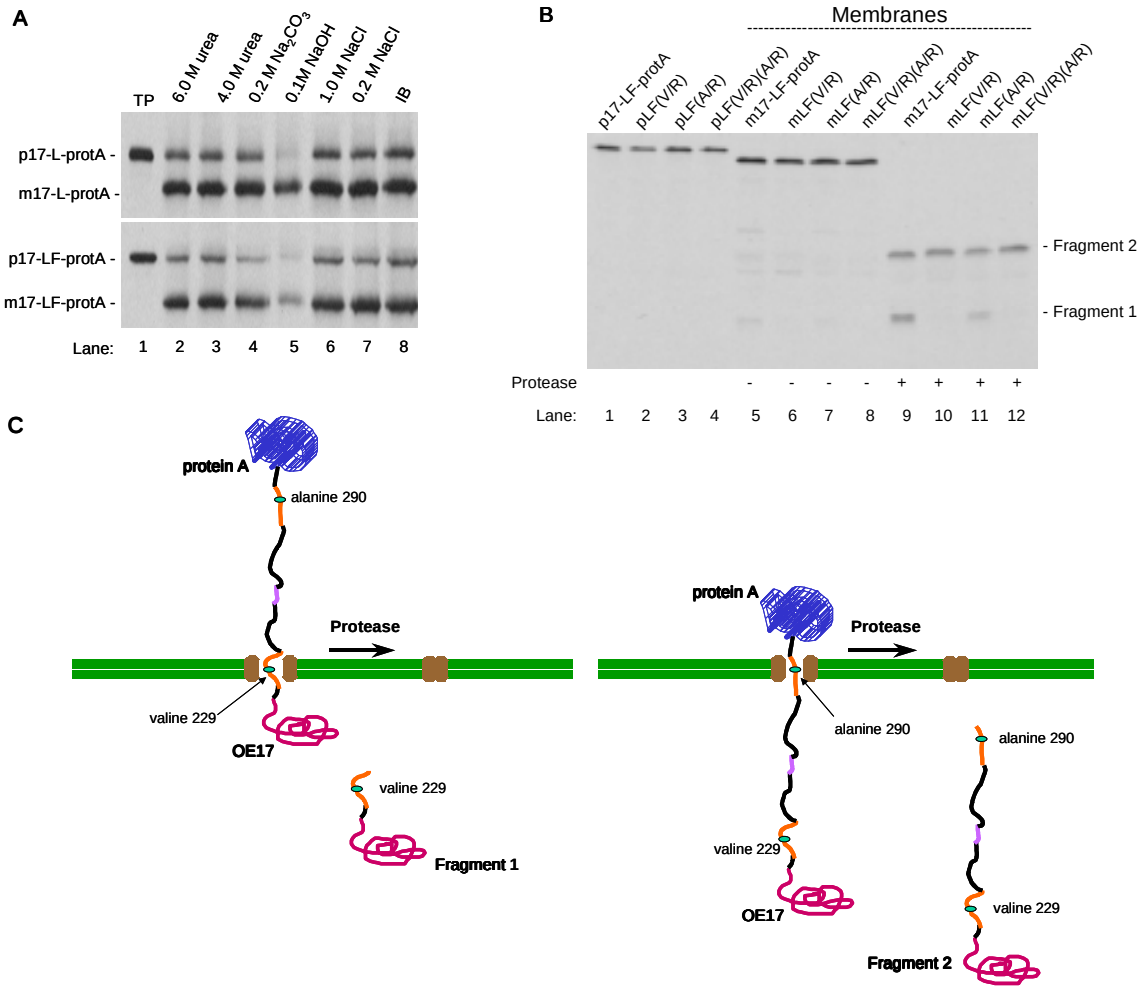

Figure 3-6. The mildly hydrophobic stretches of amino acids in the linker region of p17-protA do not cause the translocation intermediate to move into the lipid bilayer. *(A)* Intact chloroplasts were incubated with p17-protA from rabbit reticulocyte TnT (TP, lane 1) and ATP in light at 25ºC for 15 min. Chloroplasts were recovered and lysed. Recovered membranes were washed as indicated above each lane. Samples were analyzed by SDS-PAGE (7.5% acrylamide) and fluorography. *(B)* p17-LF-protA and three similar precursors having differences in one or two amino acids in the linker region were generated in wheat germ TnT (lanes 1-4). Intact chloroplasts were incubated with precursors and ATP in light at 25ºC for 15 min. Chloroplasts were recovered and lysed. Recovered membranes were protease treated with thermolysin as indicated below the panel. Samples were analyzed by SDS-PAGE (12.5% acrylamide) and fluorography. *(C)* Models of m17-LF-protA membrane-spanning intermediate are displayed. For clarity, the length of the linker region is greatly exaggerated relative to the protein A moiety and OE17. Colors in the linker region correspond to colors in Fig. 3-1 B and C.

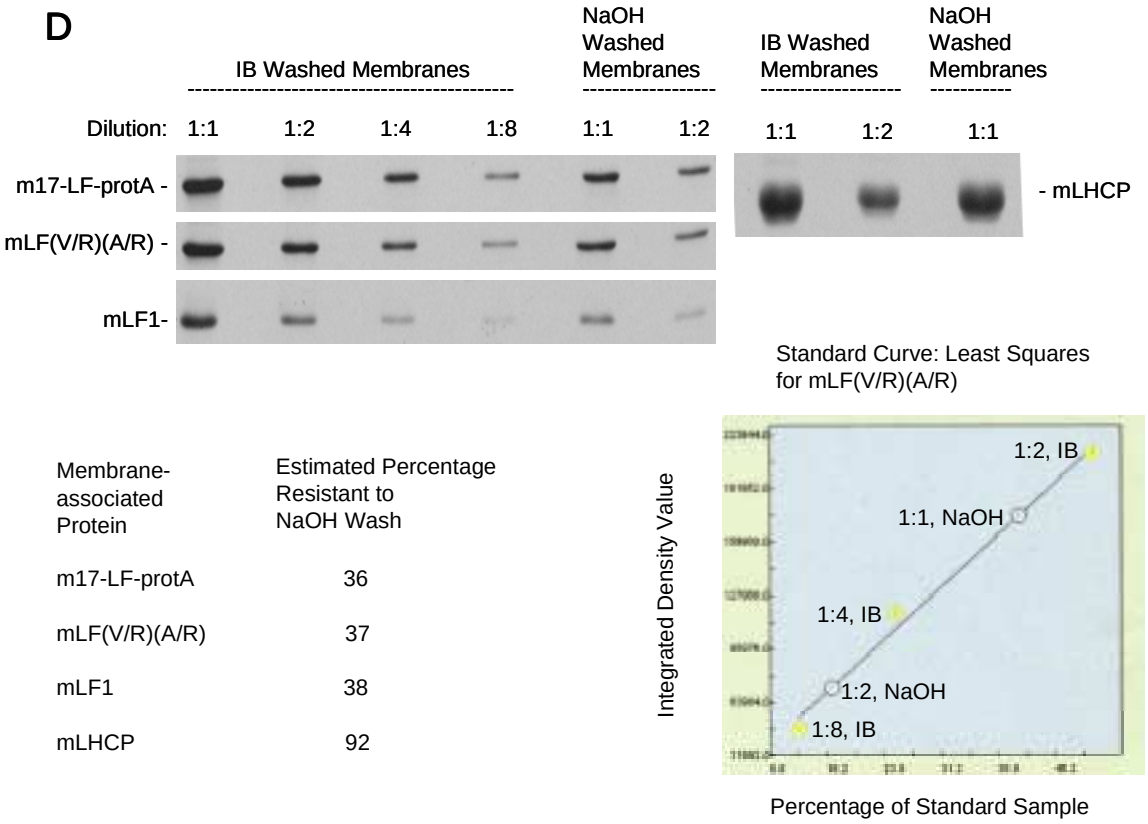

Figure 3-6. The mildly hydrophobic stretches of amino acids in the linker region of p17-protA do not cause the translocation intermediate to move into the lipid bilayer (continued). *(D)* Intact chloroplasts were incubated with pLHCP generated from mRNA and wheat germ or p17-protA from wheat germ TnT and ATP for 30 min in light at 25ºC. Chloroplasts were repurified, lysed, and recovered membranes were washed as indicated above the panels. Membranes were again recovered and samples were adjusted to equal chlorophyll content, diluted as indicated above the panels, and analyzed by SDS-PAGE (12.5% acrylamide). The density of scanned bands from the X-ray film was determined using Alpha Imager software. Relative protein quantities were estimated by averaging values derived from 1:1 and 1:2 dilution points of NaOH washed membranes.

From these data, I conclude that the membrane-spanning intermediate is not integrated in the bilayer.

To further test the influence of the amino acid sequence in the linker region, I protease treated membranes following import of three mutated versions of p17-LF-protA

(diagramed in Fig. 3-1B). Within a stretch of fifteen amino acids derived from DHFR identified as mildly hydrophobic, the eighth amino acid (valine 229) was mutated to arginine. The change of valine 229 to arginine in pLF(V/R) resulted in an increased abundance of Fragment 2 relative to Fragment 1 (Fig. 3-6B, lane 10). Within a stretch of ten amino acids derived from the small subunit of RUBISCO identified as mildly hydrophobic, the fourth amino acid (alanine 290) was mutated to arginine. The change of alanine 290 to arginine in pLF(A/R) had no apparent influence on the relative abundance of Fragment 2 versus Fragment 1 (Fig. 3-6B, lane 11). When both valine 229 and alanine 290 were changed to arginine in pLF(V/R)(A/R) Fragment 2 dominated (lane 12). The variations in size and abundance of the fragments generated means that the nature of the amino acids in the linker region influences the point at which the majority of intermediate rests relative to the *cis* side of the membrane. However, mutating hydrophobic amino acids to positively charged arginine did not prevent arrest. Because changing alanine 290 to arginine did not increase the apparent size of Fragment 2, it is likely that Fragment 2 results from translocation up to the beginning of the Protein A moiety. In other experiments, I imported pLF(V/R)(A/R), recovered the membranes, and washed them with NaOH. As with m17-LF-protA, about 60% of mLF(V/R)(A/R) was released (Fig. 3-6D). Therefore, it does not appear that the hydrophobicity of the amino acids in the linker region determines translocation arrest.

The Membrane-spanning Intermediate is Arrested Due to the Protein A Moiety.

As seen in Fig. 3-6, mLF(V/R)(A/R) is translocated up to the beginning of the protein A segment. The reason for arrest is unclear, given that folded protein transport has been documented on the ΔpH-dependent pathway and the related bacterial Tat

pathway. I therefore investigated the size of protein A segment necessary to arrest translocation by importing three truncated versions of p17-LF-protA: LF1, LF2, and LF3 having one, two, or three IgG binding domains, respectively (Fig. 3-1C). Following import, I recovered the membranes and protease treated with them thermolysin. Each substrate generated Fragment 1 and Fragment 2 as seen for full-length p17-LF-protA (Fig. 3-7A, lanes 9-12).

I demonstrated that arrest is dependent on at least one IgG binding domain by removing the entire protein A moiety enzymatically and by genetic truncation. The genetically truncated precursor, pLF0 is processed and exported to the thylakoid lumen where it is resistant to externally added protease. The mature product is labile to endogenous proteases so that it could only be observed by arresting lumenal protease activity with $HgCl_2$ prior to thermolysin treatment. A time-course revealed accumulation and endogenous degradation of mLF0 (Fig. 3-7B).

The linker region of p17-L-protA includes an engineered thrombin cleavage site (See Fig. 3-1B for amino acids and Fig. 3-6C, lavender segment, for illustration). Partial digestion of the precursor with thrombin prior to import assays yielded three products: undigested p17-L-protA, the amino segment up to the thrombin site (p17-T), and the carboxyl segment beyond the thrombin site (T-protA) (Fig. 3-7C lane 4). Because T-protA has no stromal targeting domain, it did not enter the chloroplasts during the subsequent import assay. The amino end of the precursor, p17-LT, was imported, processed to m17-LT, and fully transported to the lumen (Fig. 3-7C, lane 5). Treatment of recovered membranes with thermolysin demonstrated that m17-LT is on the *trans* side of the membrane (Fig. 3-7C, lane 6).

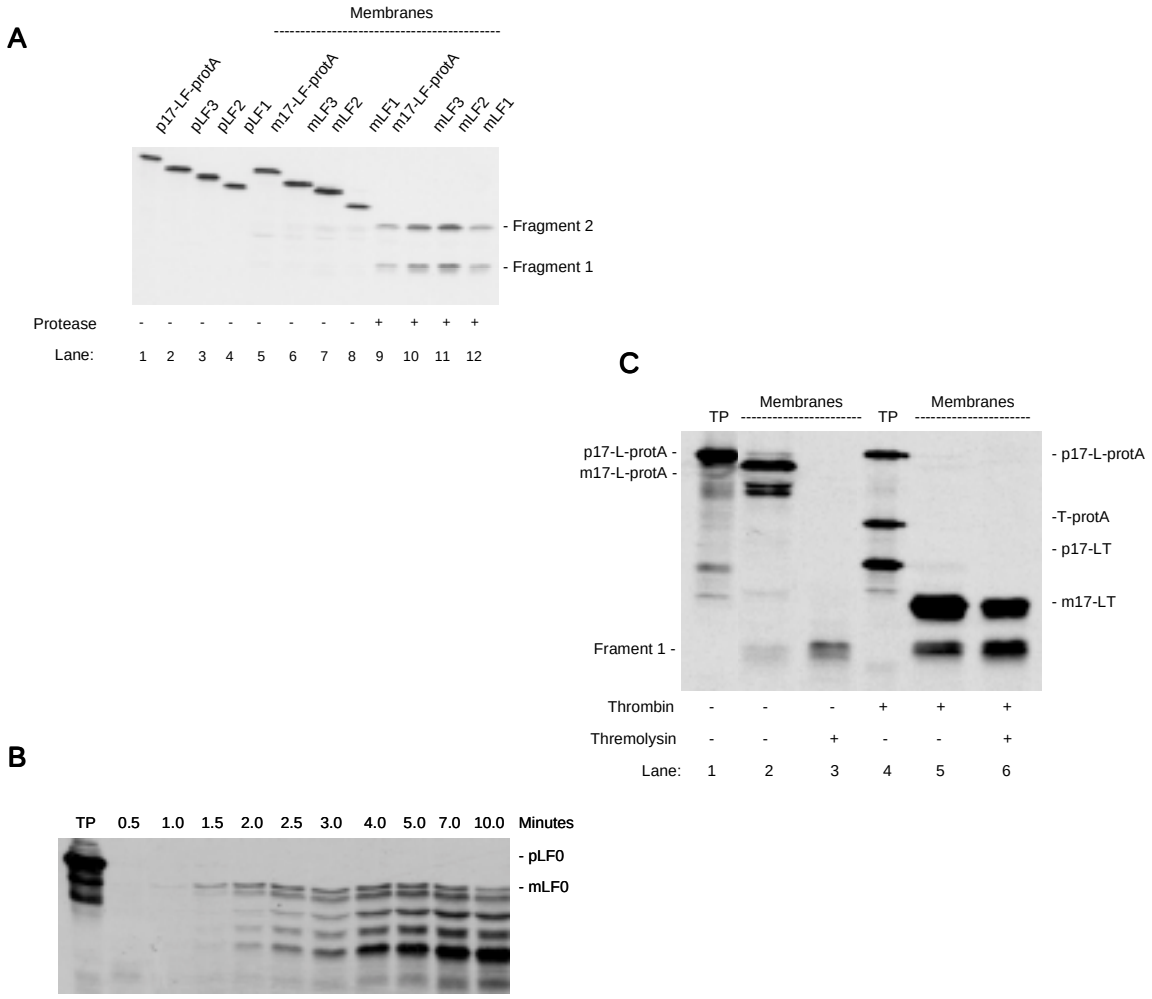

Figure 3-7. Translocation arrest is dependent on the Protein A segment of p17-protA. All samples were analyzed by SDS-PAGE (12.5% acrylamide) and fluorography. *(A)* Precursor proteins generated from wheat germ TnT (lanes 1-4) were incubated with intact chloroplasts and ATP for 15 min in light at 25ºC. Chloroplasts were recovered and lysed. Recovered membranes were protease treated with thermolysin where indicated below the panel. *(B)* Washed thylakoid membranes were incubated with precursor protein generated from wheat germ TnT in light at 25ºC. Samples were taken at the times indicated above the panel and added to tubes containing $HgCl_2$ (final concentration 1.6 mM). Membranes were recovered, $HgCl_2$ was removed by washing with IB containing EDTA, and samples were protease treated with thermolysin. *(C)* p17-L-protA (TP, lane 1) was generated in wheat germ TnT; an aliquot was partially digested with thrombin (TP, lane 4). Intact chloroplasts were incubated with ATP and translation product (native, lane 2 or thrombin treated, lane 5) and ATP for 15 min in light at 25ºC. Chloroplasts were recovered and lysed. Recovered membranes were protease treated with thermolysin where indicated below the panel.

The Protein A Moiety Alone Is Insufficient to Arrest Transport.

The data exhibited in Fig. 3-6 demonstrated that arrest was not due to bilayer integration resulting from mildly hydrophobic stretches in the linker. The data exhibited in Fig. 3-7 demonstrated that arrest was dependent of the presence of a least one IgG binding domain carboxy to the linker. Thus, the question arises: Is arrest dependent on some inherent property of the IgG binding domains, or is it the result of the position of those domains? In pursuit of an answer to that question, the full protein A derived moiety was linked carboxy to the complete transit peptide from pOE17 without an intervening mOE17 protein or linker, yielding p17tp-protA.

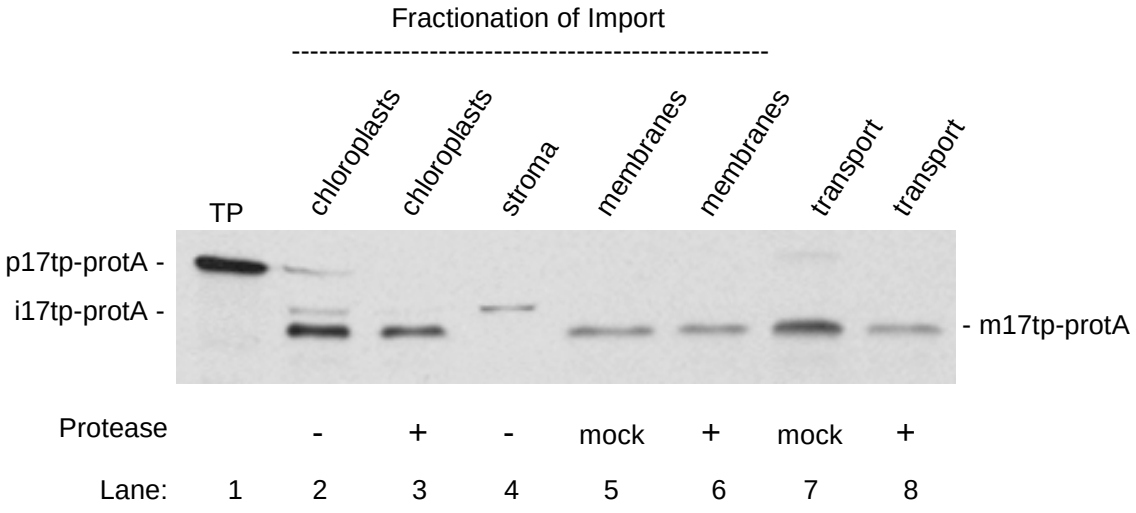

Figure 3-8. The ΔpH-dependent pathway is able to transport protein A. p17tp-protA generated from wheat germ TnT was incubated with intact chloroplasts (Import) or lysate (transport) and ATP for 15 min in light at 25ºC. Chloroplasts were recovered from the import assay and subfractionated to yield stromal and membrane samples. Recovered membranes were protease treated with thermolysin or mock treated as indicated beneath the panel. Samples were analyzed by SDS-PAGE (12.5% acrylamide).

The construct, p17tp-protA, was translated *in vitro* and incubated with chloroplasts under import permissive conditions. As exhibited in Fig. 3-8, p17tp-protA was imported and processed to an intermediate and to a mature form. A small amount of intermediate remained in the stroma (lane 4); however, most of the translation product was processed to mature size and localized to the thylakoid lumen where it was resistant to externally applied protease (lane 6). A transport assay using lysed chloroplasts resulted in processing to mature size (lane 7) with most of the processed substrate resistant to externally applied protease (lane 8). Thus, it is not an inherent property of the protein A derived moiety of p17-protA that arrests transport on the ΔpH-dependent pathway.

Discussion

The ΔpH-dependent pathway and the related bacterial Tat pathway are unique among export systems in being able to translocate folded proteins. The mechanism of protein transport and energy utilization is unknown for either system. Numerous laboratories have attempted to create a membrane-spanning translocation intermediate in the thylakoid system. Attempts have resulted in two published accounts of folded protein translocation. Clark and Theg (1997) demonstrated that the tightly folded 6.5-kDa bovine pancreatic trypsin inhibitor (BPTI) linked behind the ΔpH-dependent pathway precursor to OE17 (pOE17) could be fully translocated to the thylakoid lumen. Transport proceeds even when the BPTI moiety, estimated to be 2.3 nm in diameter, is internally crosslinked and therefore incapable of unfolding during translocation. Evidence of the system's ability to export a somewhat larger folded domain came from a study in which

dihydrofolate reductase (DHFR) was linked to pOE23 and shown to enter the lumen even when bound to methotrexate (Hynds et al., 1998).

Two laboratories have achieved translocation arrest. A biotinylated protein, i23K-BCCP, complexed to avidin was processed, but the bulk of the protein apparently remained on the *cis* side of the membrane, since no lumenal fragment was recovered (Asai et al., 1999). When i23K-BCCP is complexed with avidin prior to incubation with isolated thylakoids, the mature-sized product is formed indicating processing by the lumenal protease; however, the m23K-BCCP remains sensitive to thermolysin. These results imply that export has been arrested with the amino end of the substrate protein in the lumen while most of the protein remains on the *cis* side of the membrane. Additional data from the laboratory that achieved the arrest has not been forthcoming. A fusion protein having the lumenal targeting domain of OE17 and the mature domain of OE23 was partially translocated after being abnormally processed, but the amino end, not the carboxyl end, was apparently retained in the membrane (Berghöfer and Klösgen, 1999). The nature of its association with the membrane was unknown.

I have generated a membrane-spanning translocation intermediate, confirmed its transport via the ΔpH-dependent pathway by energetic and competition studies, and investigated the nature of its membrane association. I have confirmed that the protein A derived domain of the m17-protA is responsible for translocation arrest; however, the reason for that arrest is unclear, as the ΔpH-dependent pathway is able to transport the protein A moiety. A possible cause for arrest m17-protA versus complete transport of m17tp-protA is the presence of the linker region (seventy amino acids) between the mature OE17 precursor and the protein A derived domain.

Evidence has mounted for initial interaction of precursor with an Hcf106/cpTatC complex and subsequent interaction with Tha4 (Ma and Cline, 2000; Cline and Mori, unpublished; Mori et al., submitted). The isolation of a membrane-spanning translocation intermediate supports the idea of channel utilization by the ΔpH-dependent pathway. It is possible that channel formation is a dynamic process with pore size being determined early. If so, then translocation of folded mature OE17 followed by an unfolded linker might allow adjustment of the channel, since the ion impermeable state of the membrane must be maintained. In the absence of the transit peptide, it may not be possible for the channel size to be re-adjusted to accommodate the folded protein A moiety following the linker. Future research may take advantage of this tool to elucidate the mechanism of translocation and the participation of pathway components.

CHAPTER 4
MEMBRANE INTEGRATION OF *IN VITRO*-TRANSLATED ΔpH-DEPENDENT PATHWAY COMPONENTS

Introduction

The Tat operon of *E. coli* encodes three proteins known to function in Tat dependent protein translocation: TatA, TatB and TatC (Weiner et al., 1998; Sargent et al., 1998). A fourth gene encodes a protein, TatE, similar in sequence and under some conditions functionally interchangeable with TatA (Sargent et al., 1998). An orthologue to TatB was first discovered in maize and designated Hcf106 (Voelker and Barkan, 1995). An orthologue of TatA/E was discovered in pea and termed Tha4 (Mori et al., 1999). Subsequently, two orthologues of TatA/E were discovered in maize and termed Tha4 and Tha9 (Walker et al., 1999). The cDNAs for maize Hcf106 (Settles et al., 1997) and Tha4 (Walker et al., 1999) have been cloned, as have been cDNAs for Hcf106 (Mori et al., submitted), Tha4 (Mori et al., 1999), and cpTatC (Mori et al., submitted) from pea.

The precursor to Tha4 (pTha4), transcribed and translated *in vitro* from pea cDNA, was imported into chloroplasts where it was processed to mature size (mTha4) and localized to the thylakoid membrane (Mori et al., 1999). The thylakoid-associated mTha4 was resistant to Na_2CO_3 wash, but protease sensitive. In submitted work, Mori et al. performed similar experiments on precursors for cpTatC (pcpTatC from pea) and Hcf106 (pHcf106 from both maize and pea). Import of the 36-kDa pcpTatC resulted in a 34-kDa mature membrane-associated form (mcpTatC). mcpTatC was resistant to

washing with Na_2CO_3, but partially degraded by thermolysin yielding fragments of 26-kDa and 23-kDa.

Blue native polyacrylamide gel electrophoresis (BN PAGE) and immunoblotting with antibodies to cpTatC and to Hcf106 demonstrated association of those two endogenous components in a 700-kDa complex (Mori et al., submitted). Smaller species of Hcf106 were observed from a diffuse band just below 700 kDa to an approximately 80-kDa band depending on detergent/protein ratio. Tha4 was detected in bands from about 400 kDa to about 70 kDa, also depending on detergent/protein ratio. However, no conditions were found under which Tha4 appeared at the same position as Hcf106 or cpTatC.

The putative transmembrane domains of Tha4 and Hcf106 include a conserved glutamate. Because there is an energetic cost to maintaining a negatively charged amino acid in a transmembrane domain, the conservation of glutamates in these two components is likely to be of functional significance. The nature of the association between endogenous cpTatC and Hcf106 is unknown. One possible interaction may take place between the conserved glutamate in the transmembrane domain of Hcf106 and a conserved arginine in a transmembrane domain of cpTatC.

Biochemical analysis of protein translocation has been most effectively pursued using isolated chloroplasts from peas with *in vitro*-translated translocation substrates. The cloning of pathway components Hcf106, Tha4, and cpTatC has made their gene products available for *in vitro* mutation, antibody production and for *in vitro* translation. I have investigated the integration of *in vitro*-translated components as translocation substrates in thylakoid membranes of pea and maize. Integration of radiolabeled

components allows the visualization of complex formation by fluorography. The effects of changes in amino acids within components on complex formation can thus be monitored. The position of complexes can be visualized, allowing a shift in the complex size due to translocation substrate binding to be investigated. One long-term goal is the reconstitution of mutant maize thylakoid membranes to wild type using *in vitro*-translated components. Reconstitution would be a step in the definition of component roles.

Materials and Methods

Preparation of Precursor Proteins

Cloning and analysis of DNA products were by standard molecular biology procedures (Sambrook et al., 1989). Amplifications were performed with *Pfu* polymerase (Stratagene, La Jolla, CA). Cloned constructs were verified by DNA sequencing. Sequencing was done with ABI Prism Dye Terminator cycle sequencing protocols developed by Applied Biosystems (Perkin-Elmer Corp., Foster City, CA) and an Applied Biosystems model 373 Stretch DNA Sequencer (Perkin-Elmer Corp.). Sequencing of all clones on both strands was performed by the University of Florida Interdisciplinary Center for Biotechnology Research (ICBR) DNA Sequencing Core Facility.

The mature form of zm Hcf106 (zm mHcf106) was cloned by PCR amplification from zm pHcf106 (Settles et al., 1997) based on the transit peptide cleavage site predicted by ChloroP (Emanuelsson et al., 1999)[1]. The 5' primer (including an engineered *EcoRI* site) was used to mutate the nucleotides encoding cysteine 67 to encode methionine; the 3' primer bound in the pGEM 4Z vector. The resulting product was ligated into pGEM 4Z at the *EcoRI* and *BamHI* sites in the SP6 direction. The mature form of ps Hcf106

[1] zm mHcf106 was cloned by Hiroki Mori in 1998.

(ps mHcf106) was cloned by PCR amplification from ps pHcf106 (Mori et al. submitted) based on the transit peptide cleavage site predicted by ChloroP (Emanuelsson et al., 1999)[2]. The 5' primer (including an engineered *EcoRI* site) was used to mutate the nucleotides encoding tyrosine 86 to encode methionine; the 3' primer bound in the pGEM 4Z vector. The resulting product was ligated into pGEM 4Z at the *EcoRI* and *SstI* sites in the SP6 direction. An altered from of ps mHcf106, ps mHcf106 E/Q, was derived by PCR amplification using a 5' primer (including an engineered *KpnI* site) that mutated nucleotides encoding glutamate 11 to glutamine and a 3' primer that bound within pGEM 4Z[3]. The resulting product was ligated into pGEM 4Z at the *KpnI* site in the SP6 direction.

The mature form of ps Tha4 was cloned by PCR amplification from ps pTha4 (Mori et al., 1999) based on the transit peptide cleavage site predicted by ChloroP (Emanuelsson et al., 1999)[4]. The 5' primer (including an engineered *KpnI* site) was used to mutate the nucleotides encoding aspargine 56 to encode methionine; the 3' primer bound in the pGEM 4Z vector. The resulting product was ligated into pGEM 4Z at the *KpnI* site in the SP6 direction. An altered form of ps mTha4, ps mTha4 E/Q, was derived by PCR amplification using a 5' primer (including an engineered *KpnI* site) that mutated nucleotides encoding glutamate 10 to glutamine and a 3' primer that bound within pGEM 4Z[5]. The resulting product was ligated into pGEM 4Z at the *KpnI* site in the SP6 direction.

---

[2] ps mHcf106 was cloned by Hiroki Mori in 1998.
[3] ps mHcf106 E/Q was cloned by Mike McCaffery in 1999.
[4] ps mTha4 was cloned by Hiroki Mori in 2000.
[5] ps mTha4 E/Q was cloned by Hiroki Mori in 2000.

The mature form of ps TatC was cloned by PCR amplification from ps pTatC (Mori et al., submitted) based on the transit peptide cleavage site predicted by ChloroP (Emanuelsson et al., 1999)[6]. The 5' primer (including an engineered *EcoRI* site) was used to mutate the nucleotides encoding leucine 39 to encode methionine; the 3' primer bound in the pGEM 4Z vector. The resulting product was ligated into pGEM 4Z at the *EcoRI* and *BamHI* sites in the SP6 direction.

Preparation of Radiolabeled Precursors

In vitro transcription with SP6 RNA polymerase (Promega) and translation with wheat germ lysate (Promega) or coupled transcription/translation with wheat germ TnT (Promega) in the presence of ^{3}H leucine (NEN Life Science Products) was performed following the manufacture's guidelines. Translation products were diluted with one volume 60 mM leucine in 2X import buffer (1X = 50 mM HEPES, KOH, pH 8.0, 0.33 M sorbitol) prior to use unless otherwise indicated in the figure legend.

Preparation of Chloroplasts, Thylakoids, and Lysate

Intact chloroplasts were isolated from 9- to 10-day old pea seedlings (*Pisum sativum* cv. Laxton's Progress 9) as described (Cline et al., 1993) and were resuspended in import buffer (IB). Maize plants were grown at 26º C in a 16 h light/8h dark cycle for 7-10 days. Experiments on exclusively wild-type maize were conducted on cv. Trucker's Favorite. Mutant *hcf106 mum3* maize seedlings were selected by their pale green phenotype and confirmed by high chlorophyll fluorescence with a hand-held UV lamp. Experiments using *hcf106 mum3* chloroplasts were controlled by wild-type chloroplasts isolated from the same cv. Maize chloroplasts were isolated by essentially the same procedure as pea chloroplasts except that intact chloroplasts were purified on a step

[6] ps mTatC was cloned by Hiroki Mori in 2000.

density gradient consisting of 10 ml of 75% Percoll and 25 ml of 35% Percoll in GR buffer lacking both magnesium and manganese ions. The gradients were centrifuged at 3200 X g for 15 min, and intact chloroplasts were collected at the 35%/75% interface. Lysate and washed thylakoids were prepared from isolated chloroplasts (Cline et al., 1993). Chlorophyll concentrations were determined according to Arnon (1949).

Chloroplast Import and Thylakoid Protein Integration Assays

Import of radiolabeled precursors into isolated chloroplasts or integration into washed thylakoids or chloroplast lysate was conducted in microcentrifuge tubes in a 25^{o}C water bath illuminated with 70 μE $m^{-2}s^{-1}$ white light (Cline et al., 1993) for 10 min or the time indicated in the figure legend. Assays were generally terminated by transfer to 0^{o}C. Where indicated, recovered chloroplasts or thylakoids were protease post-treated with thermolysin. Chloroplasts were repurified on Percoll cushions; thylakoids were recovered by centrifugation.

Quantitative Immunoblots

Immunoblots were developed by ECL procedure (Pierce). For quantitation of translation products, translation products were run on SDS-PAGE in parallel with dilution series of Hcf106 stromal domain or Tha4 stromal domain standards. The content of standard solutions was determined by amino acid analysis conducted by the University of Florida Interdisciplinary Center for Biotechnology Research protein core facility. Proteins were electroblotted to nitrocellulose membranes and then immunodecorated with the appropriate antibodies. The density of scanned bands on X-ray film was determined using Alpha Imager software and protein quantities were estimated by comparison to standards in the linear region of the film.

Blue Native Polyacrylamide Gel Electrophoresis

Blue native polyacrylamide gel electrophoresis (BN PAGE) was carried out as described by Schagger and von Jagow (1991) with the following modifications. Washed thylakoids were suspended in resuspension buffer (20% glycerol, 25mM BisTris-HCl, pH 7.0) at 2.0 mg chlorophyll/ml. An equal volume of resuspension buffer containing twice the final digitonin concentration was added while gently vortexing. After incubation at 4ºC for 30 min with end over end mixing, insoluble material was removed by centrifugation at 200,000 x g_{ave} for 20 min. The resulting supernatant was combined with 1/10 volume of 5% Serva Blue G, 100 mM BisTris-HCl, pH 7.0, 0.5 M 6-amino-n-caproic acid, 30% sucrose and subjected to electrophoresis through 8.4 cm x 5 cm x 0.75 mm mini gels in a Hoefer Mighty Small vertical electrophoresis unit connected to a cooling circulator. The separating gel consisted of a linear 5%-13.5% acrylamide gradient and 5-15% glycerol gradient. The stacking gel was 4% acrylamide. Blue native gels were run at 100-200 V for 3-4 hrs at 2-4ºC. The cathode buffer was exchanged with cathode buffer lacking dye after the top of 1/2-1/3 of the gel was covered with dye and electrophoresis was continued until free dye cleared the bottom of the gel. Gels to be analyzed for fluorography were then treated with DMSO and PPO as described. Molecular markers used for blue native gels are ferritin (880 kDa and 440 kDa) and bovine serum albumin (132 kDa and 66 kDa).

Results

***In Vitro*-translated ΔpH-dependent Pathway Components Associated with Thylakoid Membranes.**

As has been previously reported, *in vitro*-translated components were imported into intact chloroplasts and processed to mature size. Fig. 4-1A exhibits the relative sizes

of precursors and integrated components. The figure is taken from a single gel divided into panels for clarity, but with the relative location of bands maintained to reflect apparent sizes. Also displayed in Fig. 4-1A and Fig. 4-1B are assays performed with mHcf106, mcpTatC, and mTha4 generated from transcription plasmids lacking the coding regions for the transit peptides. Association of translated mcpTatC with membranes from lysate was inefficient as compared to association following import and *in organello* processing (Fig. 4-1A, lane 6 versus lane 7). Translated mHcf106 exhibited very efficient membrane association in lysate as compared to imported and processed mHcf106 (Fig. 4-1A, lane 4 versus lane 2).

It has been previously determined that following import assays of precursor components, processed-cpTatC and Hcf106 are resistant to Na_2CO_3 wash, indicating tight membrane association (Mori et al., submitted). I tested for membrane integration using the more stringent criterion of resistance to NaOH wash. Integration of membrane protein cpSecY was used as a control. Some mature sized cpTatC was recovered in the stromal fraction (Fig. 4-1B, top left panel, lane 3). The membrane-associated mcpTatC is resistant to NaOH wash (Fig.4-1B, top left panel, lane 6) and (as previously reported) yields two protease-protected fragments (Fig. 4-1B, top panel, lane 7). *In vitro*-translated mHcf106 integrated into isolated thylakoids as demonstrated by resistance to NaOH wash (Fig. 4-1B, upper right panel, lane 3). Mutation of a glutamate to glutamine in the putative transmembrane domain of Hcf106 did not abrogate integration as measured by resistance to NaOH wash (Fig. 4-1B, upper right panel, lane 6). Mori et al. (1999) reported that following import, the membrane-associated mTha4 is resistant to Na_2CO_3 wash. In unpublished work, Summer and Cline observed that endogenous Tha4 is

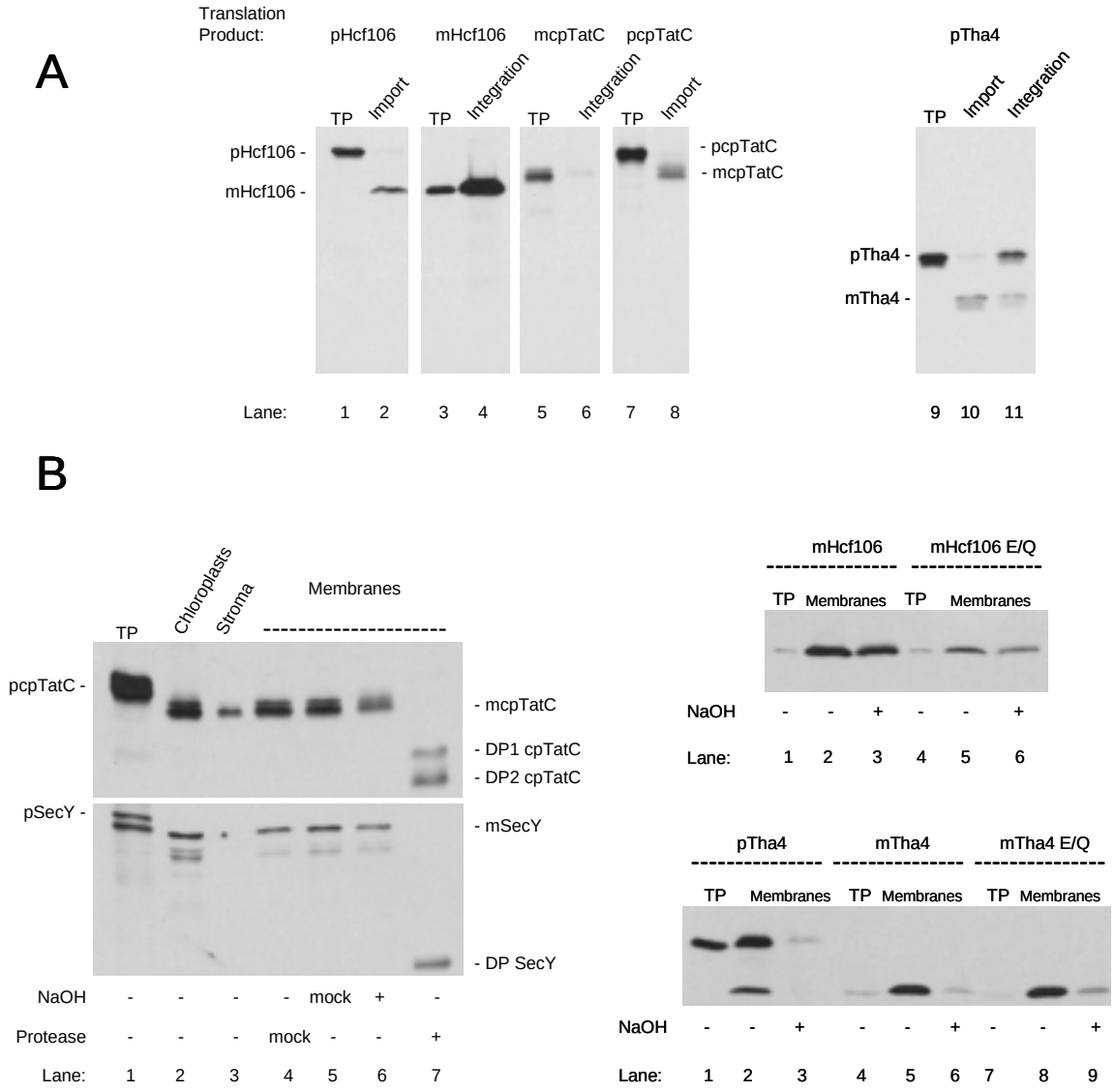

Figure 4-1. *In vitro*-translated ΔpH-dependent pathway components associated with thylakoid membranes. All substrates were generated from wheat germ TnT. *(A)* Translated component-substrates were incubated with intact pea chloroplasts (Import) or lysate (Integration) and ATP for 15 min in the light at 25ºC. Chloroplasts were lysed; membranes were recovered and washed with IB. Samples were analyzed by SDS-PAGE (12.5 % acrylamide) and fluorography. *(B)* Left panels: Intact chloroplasts were incubated with pcpTatC or pSecY and ATP for 30 min in the light at 25ºC. Chloroplasts were recovered; aliquots were lysed and subfractionated by centrifugation to yield stroma and membranes. Membrane fractions were washed with NaOH, treated with thermolysin (protease), or mock treated with IB as indicated. Samples were analyzed by SDS-PAGE (11 % acrylamide) and fluorography. Right panels: Component-substrates were incubated with lysate and ATP at 25ºC for 15 min in the light. Membranes were recovered. Samples were divided and washed with NaOH or with IB as indicated. Samples were analyzed by SDS-PAGE (12.5 % acrylamide) and fluorography.

sensitive to NaOH wash as measured by subsequent immunoblotting of membranes with antibody to Tha4. Incubation of *in vitro*-translated pTha4 with lysate at 25 º C, 5mM ATP, and actinic light for 15 min resulted in processing to mature size and membrane association (Fig. 4-1B, lower right panel, lane 2). The membrane-associated mTha4 was released by NaOH wash (lane 3). The same assay and wash when performed on *in vitro*-translated mTha4 and mTha4 E/Q (glutamate in putative transmembrane domain mutated to glutamine) also resulted in release of membrane-associated label (lanes 5, 6, 8, and 9). Therefore, while the possibility of the hydrophobic domain of Tha4 integrating into the thylakoid membrane cannot be excluded, the association is not as strong as can be demonstrated for Hcf106 and cpTatC.

Quantitative immunoblotting was used to estimate the amount of translation product added to assays (Fig. 4-2A). Comparison of density scans of radiolabeled translation product with integrated radiolabeled translation product allowed me to make an estimate of the amount of translated mHcf106 integrated in membranes (Fig. 4-2B and 4-2C). Approximately 2.0×10^{-13} moles mHcf106 translation product were integrated per μg chlorophyll. A previous analysis of endogenous Hcf106 (Mori et al., submitted) by quantitative immunoblotting estimated 1.6×10^{-13} moles per μg of chlorophyll.

Quantitation of membrane-associated mTha4 was accomplished as described for mHcf106. About 8.5×10^{-13} moles of translation product per μg of chlorophyll were membrane-associated (Fig. 4-3). A previous estimate of endogenous Tha4 found about 2.3×10^{-13} moles per μg chlorophyll (Mori et al., submitted).

The integration *of in vitro*-translated components into the thylakoid membrane in quantities comparable to endogenously present components means that it may be feasible

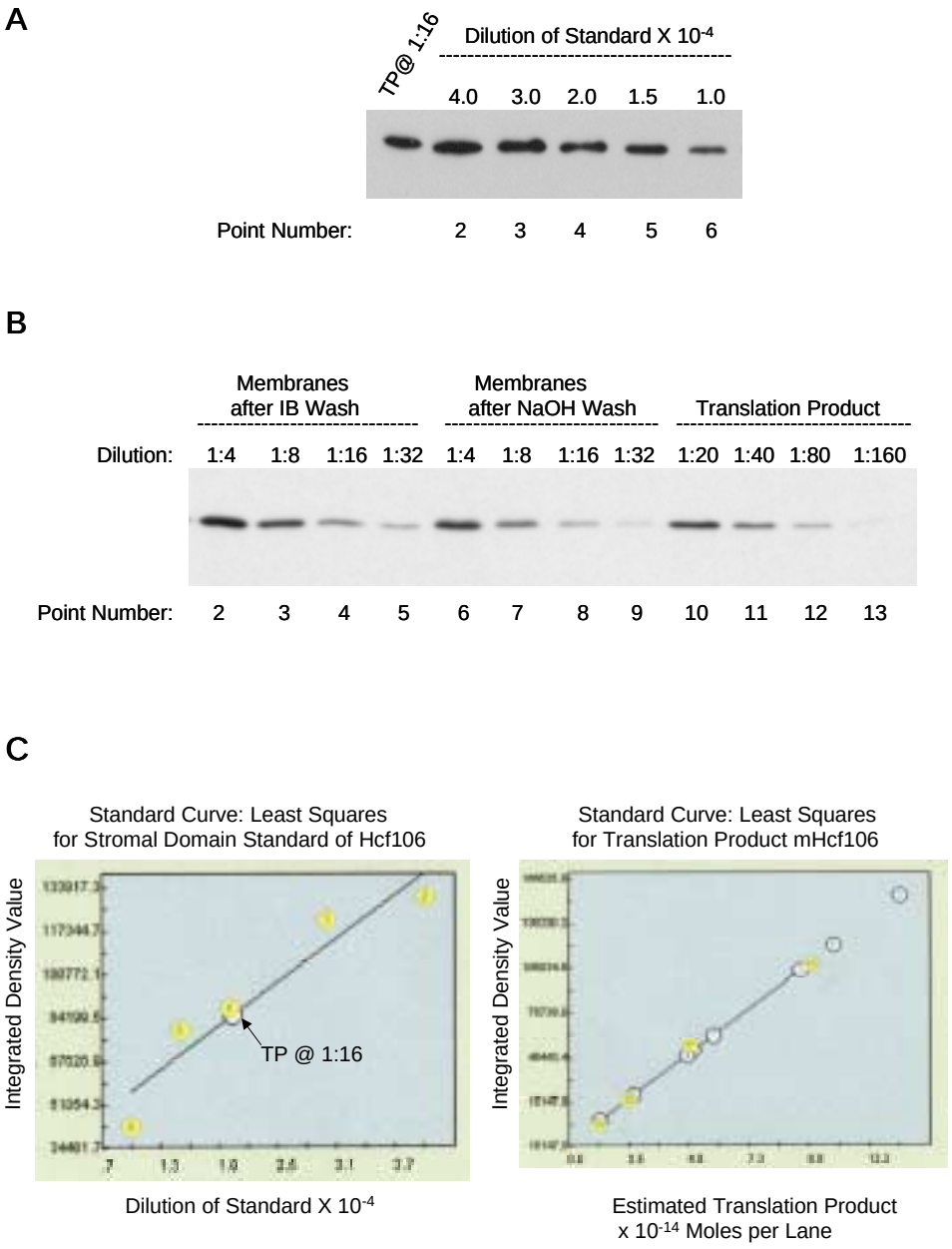

Figure 4-2. Quantitation of *in vitro*-translated mHcf106 integrated into thylakoid membranes. Substrate mHcf106 was generated from mRNA and wheat germ extract. *(A)* A quantitative immunoblot of translation product was developed using expressed stromal domain of Hcf106 as a protein standard. *(B) In vitro*-translated mHcf106 was incubated with lysate and ATP under actinic light for 10 min at 25ºC. Membranes were recovered and washed as indicated. Samples were analyzed by SDS-PAGE (12.5% acrylamide) and fluorography. *(C)* The density of scanned bands from the X-ray film pictured in A an B was determined using Alpha Imager software. The standard curve was drawn from points in yellow; the values of unknowns in the linear range were read from points in white.

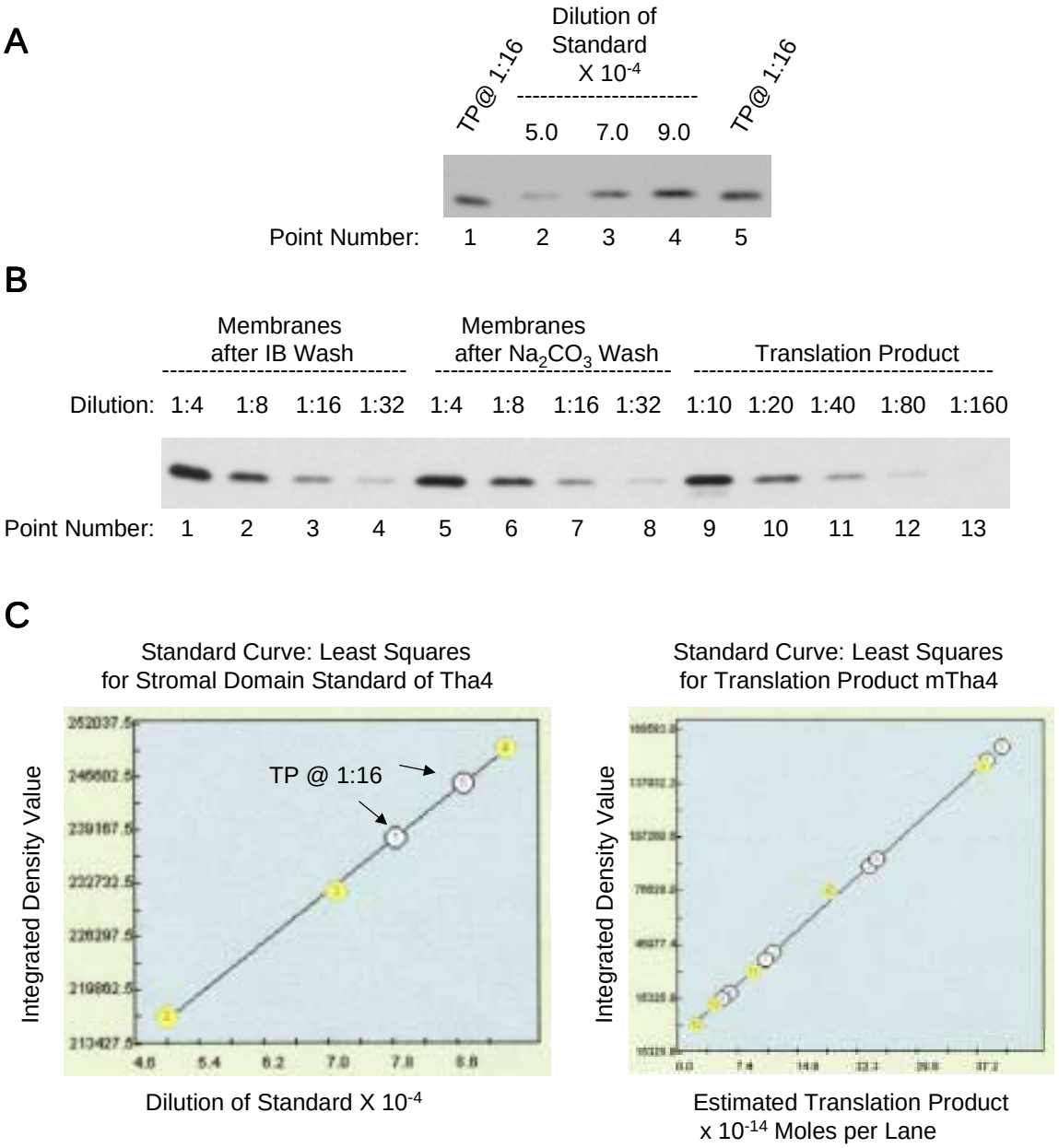

Figure 4-3. Quantitation of *in vitro*-translated mTha4 integrated into thylakoid membranes. Substrate mTha4 was generated from mRNA and wheat germ extract. *(A)* A quantitative immunoblot of translation product was developed using expressed stromal domain of Tha4 as a protein standard. *(B) In vitro*-translated mTha4 was incubated with lysate and ATP under actinic light for 10 min at 25ºC. Membranes were recovered and washed as indicated. Samples were analyzed by SDS-PAGE (12.5% acrylamide) and fluorography. *(C)* The density of scanned bands from the X-ray film pictured in A an B was determined using Alpha Imager software. The standard curve was drawn from points in yellow; the values of unknowns in the linear range were read from points in white.

to evaluate the effects of changes in the amino acid sequence of those components on complex formation. The integration of altered components into endogenous complexes could alter the physiological performance of the complexes. In mutant membranes lacking a given component, it may be possible to integrate sufficient amounts of *in vitro*-translated protein to restore translocation competence.

Association of *In Vitro*-translated Components with Endogenous Complexes.

It was previously determined that endogenous Hcf106 and cpTatC are part of a 700-kDa complex (Mori et al., submitted). Import into intact chloroplasts of *in vitro*-translated pcpTatC resulted in its integration into an approximately 700 kDa complex that was then visualized by BN PAGE and fluorography (Fig. 4-4 A, lane1; 4-4B, lane1; and 4-4C, lane1). Integration of mcpTatC was inefficient, but also resulted in association with the 700-kDa complex (Fig. 4-4A, lane 3).

Import into intact chloroplasts of pHcf106 (Fig. 4-4B, lane 2 and 4-4C, lane 2) or mHcf106 (Fig. 4-4C, lanes 5, 6, and 14) resulted in integration into a 700-kDa complex. In the presence of 1% digitonin, a separate pool of Hcf106 was visualized at lower molecular weights (Fig. 4-4C, lanes 5, 6, and 14). Integrated mHcf106 E/Q did not associate with the 700-kDa complex (Fig. 4-4C lanes 8 and 15), but did generate lower molecular weight species. Similar lower molecular weight species could be generated by combining mHcf106 or mHcf106 E/Q translation product with solubilized membranes (Fig. 4-4C, lanes 12 and 13). The implications from these data are that only the 700-kDa complex may be physiologically relevant and that when the glutamate in the transmembrane domain of mHcf106 is mutated to glutamine, the component is no longer able to associate in the 700-kDa complex.

Import of pTha4 into intact chloroplasts (Fig. 4-4 A, lane 2 and 4-4C, lane 3) or integration of pTha4 or mTha4 into membranes from lysate resulted in species migrating from about 100 kDa (Fig. 4-4A, lane 4) to about 400 kDa (Fig. 4-4B, lane 3 and 4-4C lanes 3, 7, and 20) depending on the amount of digitonin present and on the amount of sample loaded on the gel. Integration of mTha4 E/Q into membranes from lysate yielded

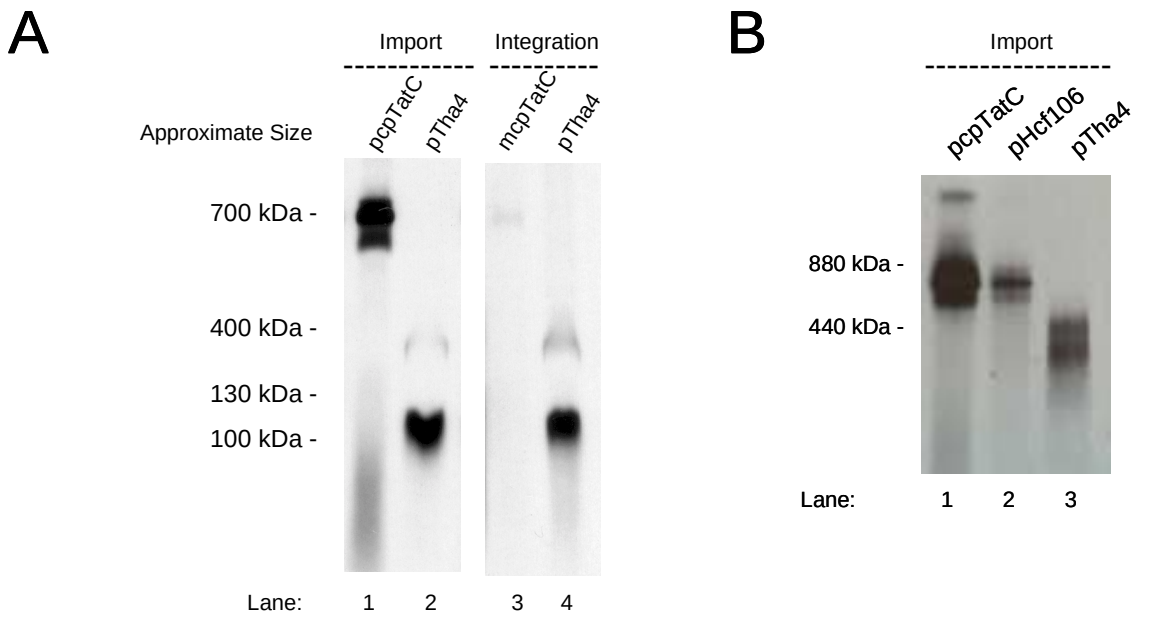

Figure 4-4. Incorporation of *in vitro*-translated components into native complexes. Substrates were generated from wheat germ TnT. Samples were analyzed by BN PAGE and fluorography. *(A)* Chloroplasts (import) or lysate (integration) were incubated with translation product and ATP for 15 min in the light at 25 ºC. Chloroplasts were recovered and lysed. Recovered membranes were washed, solubilized with 1% digitonin, and processed for BN PAGE. The approximate sizes of complexes are given to the left of the fluorograph. The approximations are based on visual inspection of bands on the blue native gel and photosystem complex sizes. *(B)* Chloroplasts were incubated with translation product and ATP for 30 min in the light at 25 ºC. Chloroplasts were recovered and lysed. Recovered membranes were washed, solubilized with 0.5% digitonin, and processed for BN PAGE. Positions of molecular weight markers are indicated to the left of the panel.

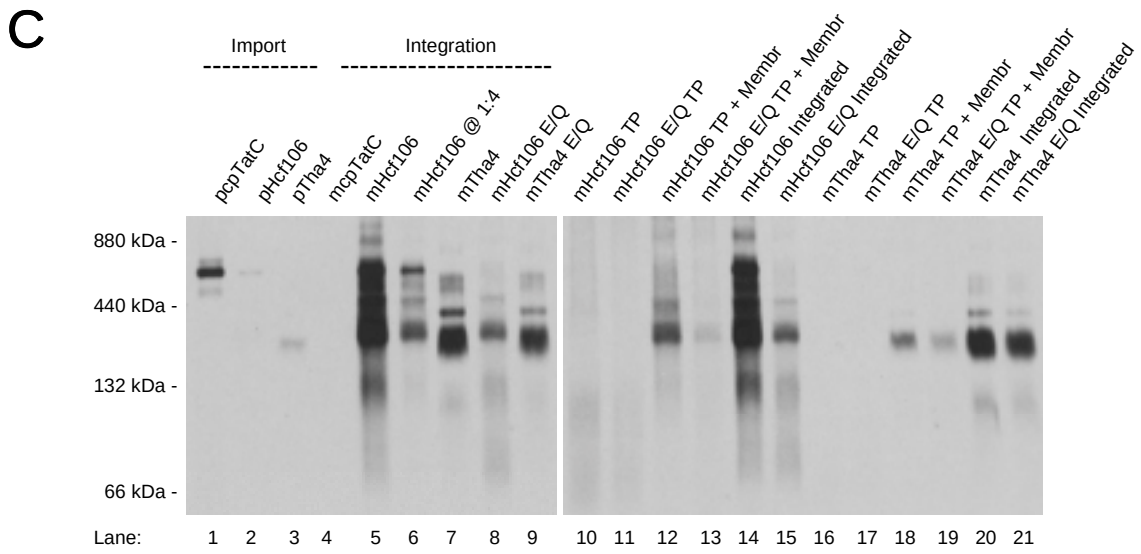

Figure 4-4. Incorporation of *in vitro*-translated components into native complexes. (continued). *(C)* Chloroplasts (Import) were incubated with ATP and translated precursors pcpTatC, pHcf106, and pTha4 for 15 min in the light at 25 ºC. Lysate (Integration) was incubated with ATP and translated mature proteins for 15 min in the light at 25 ºC. Chloroplasts were recovered and lysed. Recovered membranes from import or integration assays were washed, solubilized with 1% digitonin, and processed for BN PAGE. Positions of molecular weight markers are indicated to the left of the panel. A portion of the sample in lane 5 was diluted with three volumes solubilized membranes in BN sample buffer and loaded in lane 6. Lanes labeled *TP* were loaded with translation product in BN sample buffer. Lanes labeled *TP + Membr* were loaded with translation product and solubilized membranes in BN sample buffer. Lanes labeled *Integrated* exhibit samples of solubilized membranes from integration assays with lysate. Lanes 5, 7, 8, and 9 are equivalent to lanes 14, 20, 15, and 21 respectively.

similar results (Fig. 4-4C, lanes 9 and 21). Again, species migrating at the same molecular weights could be generated by adding translation product to solubilized membranes (Fig. 4-4C, lanes 18 and 19). Therefore, the physiological relevance of complexes of Tha4 is questionable.

Integration of *In Vitro*-translated Components Influenced Efficiency of Subsequent ΔpH-dependent Pathway Transport.

Because *in vitro*-translated mHcf106 and mTha4 associated with membranes in amounts comparable to endogenous components, it seemed reasonable that integration of

native or mutated forms of the components might influence translocation of ΔpH-dependent pathway substrates. In the experiment displayed in Fig. 4-5A, mHcf106 or mHcf106 E/Q was integrated into unwashed-membranes. The membranes were recovered and then incubated with iOE23 under transport permissive conditions.

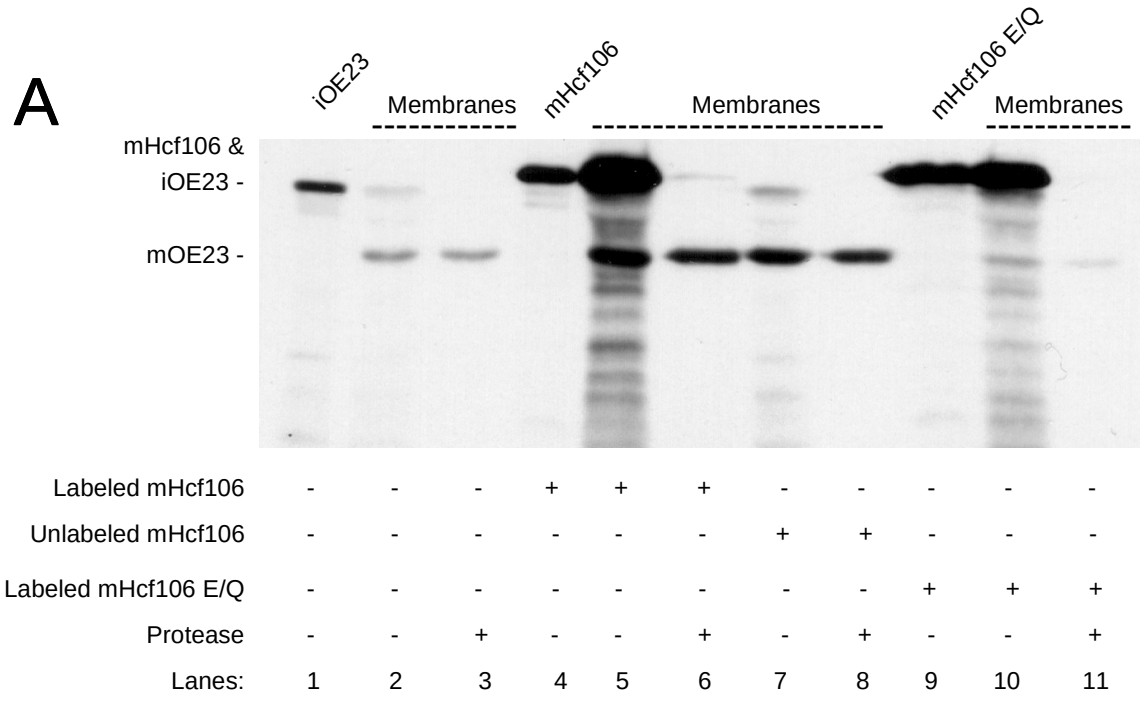

Figure 4-5. Integration of *in vitro*-translated components influenced efficiency of subsequent ΔpH-dependent pathway transport. Substrate iOE23 was generated from mRNA and wheat germ extract, diluted four-fold, and adjusted to IB and 30 mM unlabeled leucine. All component-substrates were generated from wheat germ TnT and diluted as described in Material and Methods. Chloroplasts were lysed and unwashed membranes were adjusted to 2 mg/ml chlorophyll. Assays were conducted by incubating 13 µl of membranes and 31 µl of component-substrate for 10 min in the light at 25ºC. An additional 31 µl of component-substrate was added to the assay and incubation continued 10 min. Control assays (lanes 2 and 3 of both panels) received sequential 31 µl aliquots of equivalently diluted wheat germ TnT. Membranes were recovered by centrifugation and washed with IBM. Membranes were resuspended in 50 µl IBM, 25 µl iOE23 was added, and the assays were returned to 25ºC and light for 10 min. Membranes were recovered, protease treated where indicated, and processed for SDS-PAGE and fluorography. *(A)* Labeled component-substrate mHcf106 was integrated in lanes 5 and 6. Unlabeled component-substrate mHcf106 was integrated in lanes 7 and 8. Labeled component-substrate mHcf106 E/Q was integrated in lanes 10 and 11.

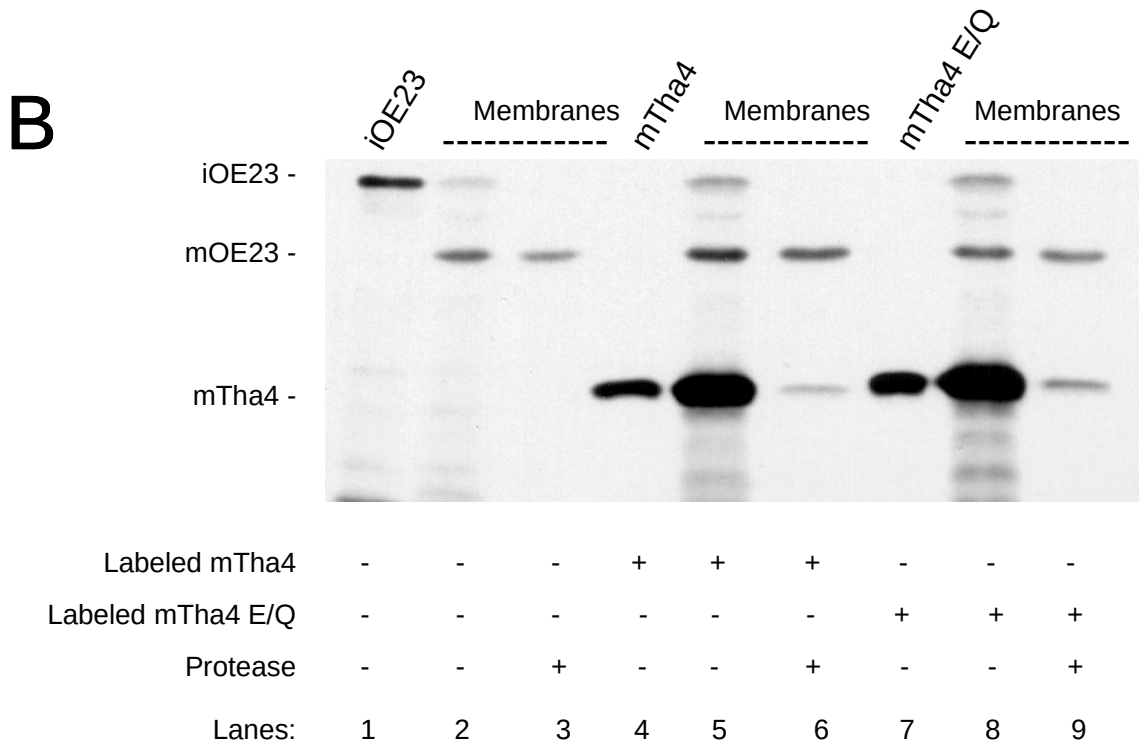

Figure 4-5. Integration of *in vitro*-translated components influenced efficiency of subsequent ΔpH-dependent pathway transport (continued). . *(B)* Labeled component-substrate mTha4 was integrated in lanes 5 and 6. Labeled component-substrate mTha4 E/Q was integrated in lanes 8 and 9.

Thylakoids having previously integrated radiolabeled (lanes 5 and 6) or unlabeled (lanes 7 and 8) mHcf106 accumulated more mature OE23 (mOE23) than control thylakoids (lanes 2 and 3). Thylakoids having previously integrated mHcf106 E/Q accumulated slightly less mOE23 (lanes 10 and 11) than control thylakoids. A similar experiment conducted on the same day comparing thylakoids previously incubated with mTha4 or mTha4 E/Q revealed little difference in mOE23 accumulation among assays (Fig. 4-5B).

The experiments displayed in Fig. 4-5 were repeated numerous times. The results were extremely variable. Stimulation of mOE23 accumulation following mHcf106

integration was frequently, but not always, seen and when seen was less pronounced than exhibited in Fig. 4-5. Likewise, inhibition of accumulation of mOE23 by previously integrated mHcf106 E/Q was rarely seen and never again as evident as in Fig. 4-5. The reason for variability in results is unknown. Because the experiment was well controlled internally and because less pronounced effects (but having the same trends) were occasionally observed, I believe the variability resulted from some uncontrolled physiological factor. The decreased mOE23 accumulation following mHcf106 E/Q integration would be expected if mHcf106 E/Q were displacing endogenous mHcf106 in the 700-kDa complex. However, the results from the experiment in Fig. 4-4C did not demonstrate an association of mHcf106 E/Q in the 700-kDa complex. It is possible that a transient interaction is occurring which is not being captured by the BN PAGE methodology.

Investigation of the Interaction of *In Vitro*-translated Components with Maize Membranes.

The maize mutant *hcf106* results in pale green non-photosynthetic seedlings that die after expansion to three or four leaves (Voelker and Barkan, 1995). Chloroplasts isolated from *hcf106* are devoid of the Hcf106 protein, but do contain wild-type amounts of Tha4 (Walker et al., 1999). Bacterial TatC was demonstrated in a pulse-chase experiment to be unstable in the absence of the Hcf106 orthologue TatB (Sargent et al., 1998). It is not known whether *hcf106* chloroplasts have endogenous cpTatC.

Maize *hcf106* chloroplasts are unable to export ΔpH-dependent pathway precursors to the thylakoid lumen (Settles et al., 1997). A previous attempt to restore transport competence in mutant chloroplasts by introducing Hcf106 protein was unsuccessful (Cline, unpublished). Although Hcf106 was associated with mutant

membranes, the recovered membranes were unable to transport pOE17. One possible reason transport competence was not restored is that the *hcf106* thylakoids lacked endogenous cpTatC. I attempted to restore transport competence by integrating both Hcf106 and cpTatC.

Maize *cpTatC* has not been cloned. Therefore, it was necessary to attempt reconstitution of ΔpH-dependent pathway machinery using cpTatC from pea (ps cpTatC). Hcf106 is available from maize and pea in its precursor (zm pHcf106 and ps pHcf106) and its mature (zm mHcf106 and ps mHcf106) forms. It was unknown how well pea components would integrate into maize membranes and whether pea and maize components would be able to associate in the 700-kDa complex.

Import assays using intact organelles and transport assays using lysate were conducted on chloroplasts isolated from wild-type (cv. Truckers Favorite) maize. Membranes were recovered and prepared for BN PAGE. Aliquots of solubilized membranes were diluted in SDS loading buffer. Fig. 4-6A is a fluorograph displaying the results from SDS-PAGE of those aliquots. Integration of both ps mHcf106 (lane 4) and zm mHcf106 (lane 8) was efficient. However, import of zm pHcf106 was comparatively inefficient (lane 6) and ps pHcf106 was imported minimally (lane 2). Import of ps pcpTatC was efficient (lane10), but there was no apparent integration of ps mcpTatC (lane 12).

Analysis of samples by BN PAGE revealed that integrated pea components were able to interact with endogenous maize components in the 700-kDa complex (Fig. 4-6B). Because of the anticipated efficiency of integration, samples from assays using mHcf106 were diluted 1:6 with solubilized membranes prior to loading them onto the gel. The

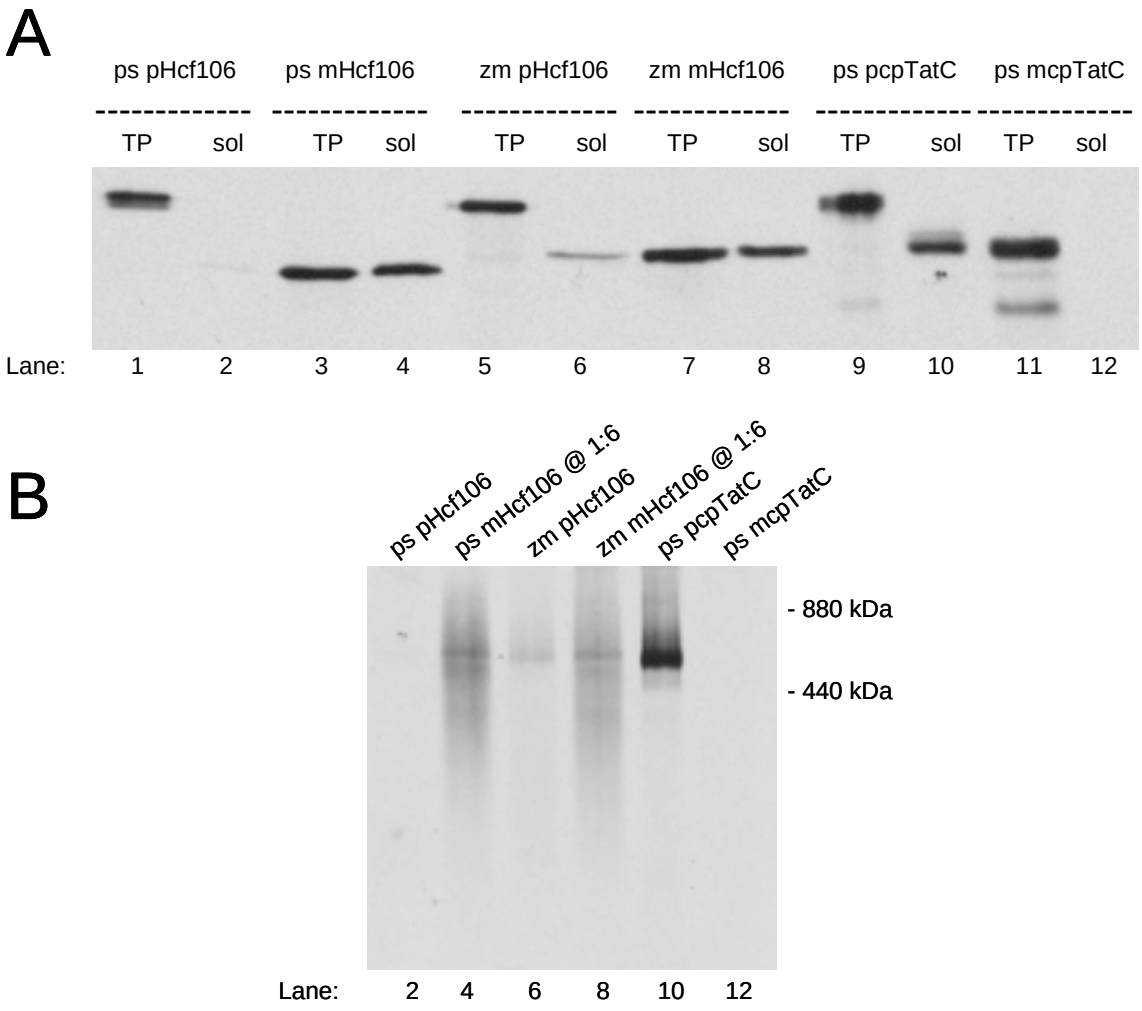

Figure 4-6. *In vitro*-translated ΔpH-dependent pathway components derived from both pea and maize integrated into maize membranes and associated with the endogenous 700-kDa complex. Component-substrates ps pHcf106, ps pcpTatC, and ps mcpTatC were generated from wheat germ TnT. Other component-substrates were generated from mRNA and wheat germ. Intact chloroplasts were incubated with ATP and component-substrates having transit peptides for 30 min in the light at 25ºC. Lysate was incubated with ATP and mature component-substrates for 10 min in the light at 25ºC. Chloroplasts were recovered and lysed. Recovered membranes were solubilized with 0.5% digitonin and processed for analysis by BN PAGE. *(A)* Each pair of lanes is labeled above with the identity of the component-substrate integrated. Aliquots from the solubilized membranes (*sol*) were diluted with SDS loading buffer and analyzed by SDS-PAGE (12.5% acrylamide) and fluorography. *TP* is translation product as indicated above the lanes. *(B)* Samples were analyzed by BN PAGE and fluorography. Lanes are numbered to correspond to samples in (A). Samples in lanes 4 and 8 were diluted with 5 volumes solubilized membranes in BN sample buffer. The identity of the integrated component-substrate is indicated above each lane. Positions of molecular weight markers are indicated to the right of the panel.

interaction of ps cpTatC with endogenous maize Hcf106 implies that imported ps pcpTatC would be capable of interacting with exogenous (*in vitro*-translated and integrated) Hcf106 from either pea or maize.

As a first step in reconstitution of transport competence to maize *hcf106* mutants, I attempted to find conditions under which I could achieve interaction of *in vitro*-translated (exogenous) Hcf106 with cpTatC (either exogenous, or endogenous). If interaction could be achieved, I reasoned that I would be able to visualize it as the 700-kDa complex on a fluorograph following BN PAGE. Because zm pHcf106 had imported significantly better than ps pHcf106 into wild-type maize chloroplasts, I chose zm pHcf106 and zm mHcf106 for these assays. All assays were run in parallel with both wild-type and mutant chloroplasts. Samples from mutant chloroplasts are indicated in Fig. 4-7 by asterisks at the top of the lanes. The integration of components was attempted separately, simultaneously, and sequentially. Samples were recovered and prepared for BN PAGE. Aliquots of solubilized membranes were diluted in SDS loading buffer. Fig. 4-7A is a fluorograph displaying the results from SDS-PAGE of those aliquots. Fig. 4-7B is a fluorograph of samples analyzed by BN PAGE.

Using intact chloroplasts, zm pHcf106 was imported and processed by both wild-type and mutant organelles (Fig. 4-7A, lanes 2 and 3). However, only wild-type chloroplasts were able to integrate Hcf106 into the 700-kDa complex (Fig. 4-7B, lane 2 versus lane 3). Import and processing of ps pcpTatC was inefficient in wild-type chloroplasts (Fig. 4-7A, lane 5) and was not detectable in mutant chloroplasts (Fig. 4-7A, lane 6). Wild-type chloroplasts were able to integrate cpTatC into the 700-kDa complex

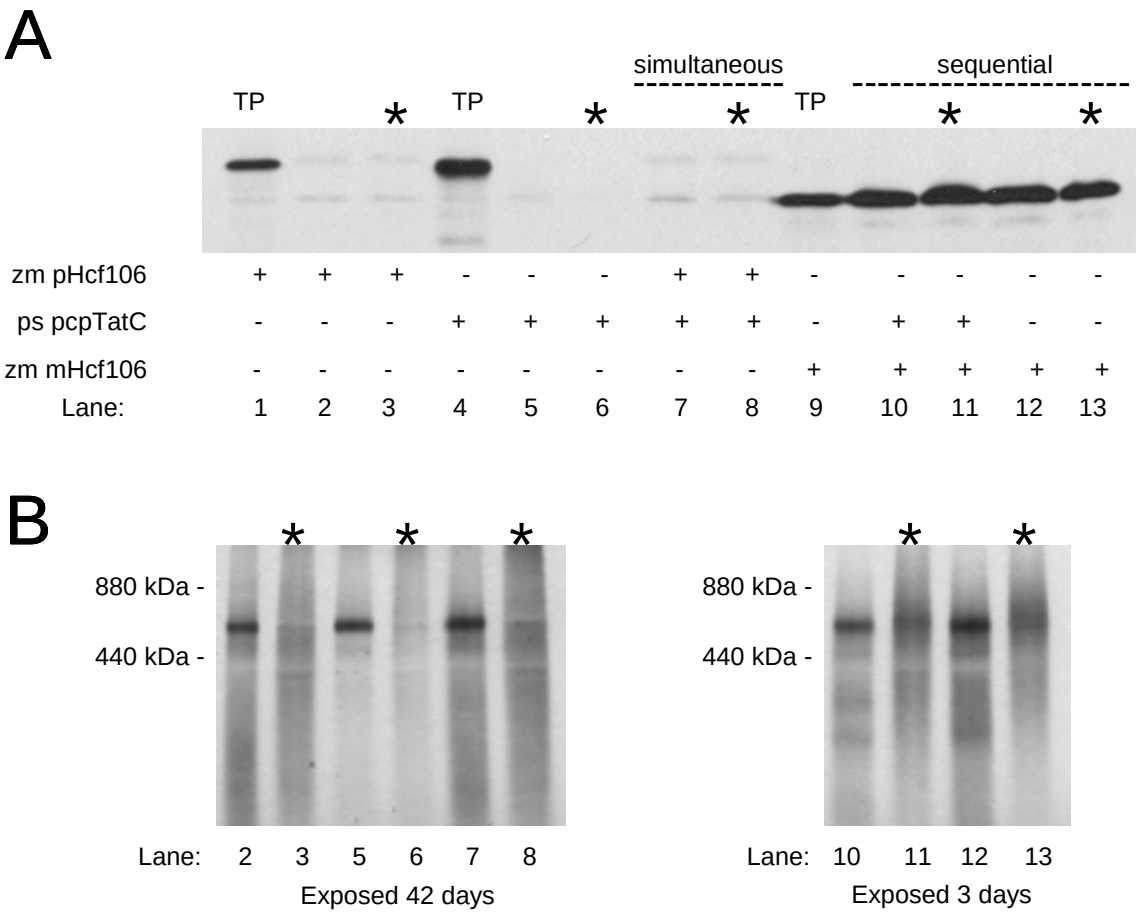

Figure 4-7. Maize mutant *hcf106* chloroplasts did not incorporate *in vitro*-translated component-substrates into a 700-kDa complex. Lanes marked * indicate membranes derived from *hcf106* mutant chloroplasts. Component-substrate ps pcpTatC was generated from wheat germ TnT. Other component-substrates were generated from mRNA and wheat germ. Lanes 1 through 3 and 5 through 8 exhibit samples from assays conducted by incubating intact chloroplasts with ATP and the precursors indicated for 10 min in the light at 25ºC. Lanes 10 through 13 exhibit samples from assays conducted by incubating intact chloroplasts with pcpTatC or buffer for 10 min in the light at 25ºC. Chloroplasts were recovered without repurification and lysed. The lysate from assays exhibited in lanes 10 through 13 was subsequently incubated with zm mHcf106 for 10 min in the light at 25ºC. In all samples, recovered membranes were solubilized with 0.5% digitonin, and processed for BN PAGE. *(A)* Aliquots of samples were diluted with SDS sample buffer and analyzed by SDS-PAGE (12.5% acrylamide) and fluorography. *TP* indicates translation product. *(B)* Lanes are numbered to correspond to assays in (A). Samples were analyzed by BN PAGE and fluorography. Positions of molecular weight markers are indicated to the left of each panel. The time of exposure of film is indicated below each panel.

(Fig. 4-7B, lane 5), but no integration was detectable in mutant chloroplasts (Fig. 4-7B, lane 6).

Incubation of zm mHcf106 with lysate from either wild-type or mutant chloroplasts resulted in membrane association (Fig. 4-7A, lanes 12 and 13). However, only wild-type lysate was able to integrate mHcf106 in the 700-kDa complex (Fig. 4-7B, lane 12 versus lane 13).

Because imported cpTatC may be rapidly degraded in the absence of endogenous Hcf106, I simultaneously imported both components. The sizes of mcpTatC and mHcf106 are too close for bands generated on the fluorograph of a 12.5% SDS gel to be resolved. Membrane association of processed components in wild-type chloroplasts was detected in Fig. 4-7A, lane 7 and in mutant chloroplasts in Fig. 4-7A, lane 8. Only wild-type chloroplasts were able to integrate components in the 700-kDa complex (Fig. 4-7B, lane 7 versus lane 8).

Finally, because mHcf106 is so much more efficiently integrated in lysate than imported Hcf106, I imported ps pcpTatC, lysed the chloroplasts, and then incubated the lysate with zm mHcf106. A band of mature components was visible from both wild-type and mutant membranes (Fig. 4-7A, lanes 10 and 11). However, only wild-type membranes incorporated components in the 700-kDa complex (Fig. 4-7B, lane 10 versus lane 11).

Discussion

I have demonstrated that *in vitro*-translated cpTatC and Hcf106 are integrated into a 700-kDa complex that migrates in BN PAGE identically to the antibody-decorated endogenous complex. When Hcf106 was mutated, changing its conserved glutamate to

glutamine, it failed to integrate in the 700-kDa complex. These data imply that the glutamate in Hcf106 is required for interaction with cpTatC.

I have shown that it is possible to integrate quantities of *in vitro*-translated Hcf106 and Tha4 comparable to the amount of endogenous proteins present in pea membranes. The ability to track the 700-kDa complex with *in vitro*-translated and radiolabeled components will provide a tool for additional biochemical studies such as binding assays. The effects of changing other amino acids in Hcf106 or cpTatC may further inform investigators as to the nature of the complex interaction and translocation mechanism.

In some assays, I saw an influence of exogenously added components on the translocation efficiency of a ΔpH-dependent pathway substrate. The results were highly variable and I was unable to ascertain the reason for the variability. It is likely that some physiological variable such as growth-room temperature was involved. However, the experiments in which I did see the influence were well controlled internally, so that I am convinced the effects were real. The decreased accumulation of OE23 following integration of mHcf106 E/Q implied that Hcf106 E/Q had some limited interaction with other components (presumably cpTatC) disrupting complex formation.

Although my attempt to reconstitute the 700-kDa complex in maize mutant membranes was unsuccessful, additional experiments may reveal conditions under which that reconstitution can be accomplished. In particular, the eventual cloning of maize cpTatC may be key. The variety of maize from which *hcf106* is derived grew more slowly than the Trucker's Favorite variety and generally appeared less robust. Import of ps pcpTatC was minimal in *Hcf106* control plants. Although assays were conducted under conditions that would have allowed integration via any of the known pathways,

integration of mcpTatC in lysate from all chloroplasts, pea or maize, was inefficient. Certainly, lysate does not fully mimic conditions inside the intact chloroplast. One of the most obvious differences between transport in lysate and *in organello* translocation is the concentration of stromal proteins. It is unknown whether any of those proteins or other cofactors may participate in integration of cpTatC. Given the highly efficient integration of mHcf106 in isolated membranes, finding conditions under which mcpTatC could integrate might significantly improve the chances of reconstituting transport of ΔpH-dependent pathway substrates in *hcf106*-derived membranes.

CHAPTER 5
SUMMARY AND CONCLUSIONS

The ΔpH-dependent pathway of chloroplasts is unique among export systems because of its energetic requirements, its use of a recognizable motif in substrate presequences and because of its ability to translocate a spectrum of protein substrates. The exclusive dependence of the pathway on the trans-thylakoid pH gradient has been well established. Multiple studies from several laboratories have attempted to define the presequence requirements of the thylakoid pathway and its bacterial counterpart. The flexibility of the system has been explored, as its ability to translocate folded domains, domains with disrupted folding, and transmembrane domains has been documented. In spite of a decade of investigation, the mechanism by which the system moves proteins across or into the thylakoid membrane remains an enigma.

I have taken a first look at protein translocation initiation. I have shown that the amino-terminal segment of a translocation substrate remains on the *cis* side of the membrane following transport by the ΔpH-dependent pathway, just as it does following transport by other export systems. This phenomenon may reflect an evolutionary relationship among export pathways including spontaneous protein translocation, the prokaryotic Sec pathway, and the endoplasmic reticulum secretion system.

I have arrested the process of translocation across the thylakoid membrane and captured a membrane-spanning intermediate. The existence of an intermediate in the translocation event argues for a dynamic process in which the progress of export is

monitored and nurtured. Manipulation of the intermediate may allow investigation of that process and of the components involved in it.

A model for a possible mechanism of initiation, transport and arrest of transport is displayed in Fig. 5-1. From the unpublished data of Cline and Mori, it is known that ΔpH-dependent pathway precursors can bind to the endogenous 700-kDa complex even in the absence of a delta pH and that binding is dependent on the conserved arginines and hydrophobic domain of the signal sequence. I propose that the perturbation of the bilayer by the hydrophobic domain of the signal peptide in the presence of a trans-thylakoid pH gradient results in localized proton flow. One consequence of that proton flow is a change in the conformation of a component of the 700-kDa complex. I suggest cpTatC as the altered component, because bacterial TatC is in association with the Tha4 orthologue, TatA (Bolhuis et al., 2001). The alteration in the configuration of cpTatC instigates oligomerization of Tha4 forming a channel *de novo* at the site of translocation. The size of the channel is controlled by the three dimensional form of the translocation substrate in contact with the amphipathic helices of multiple Tha4 monomers. The substrate moves through the channel spontaneously with the size of the channel decreasing as the structure passes through. Without the spontaneous insertion of the hydrophobic domain of the signal peptide to promote proton flow and initiate further oligomerization, the channel is unable to adapt to a large folded domain that follows an unfolded domain. Translocation is arrested. The channel collapses, leaving the membrane-spanning intermediate.

By documenting the integration of *in vitro*-translated ΔpH-dependent pathway components in endogenous complexes, I have created a tool for investigating the nature

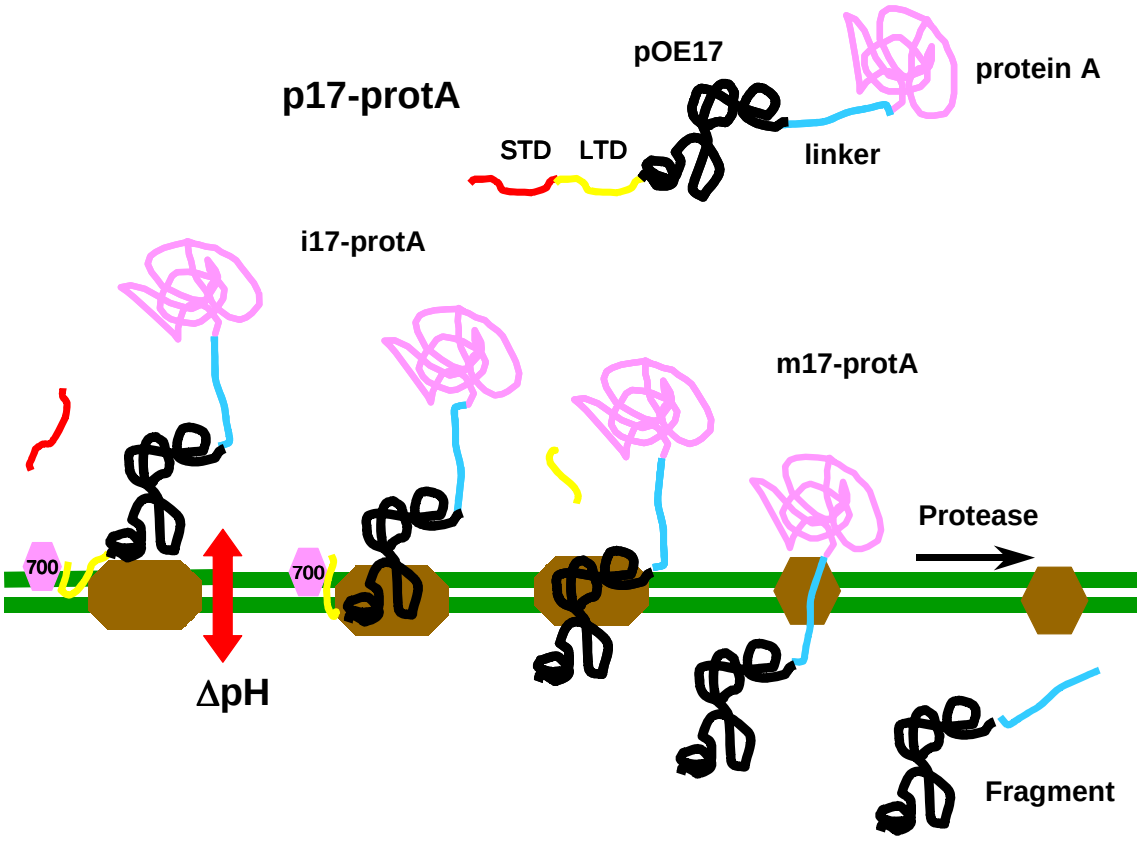

Figure 5-1. Model of protein translocation initiation and arrest on the ΔpH-dependent pathway. Icons representing substrate domains and channel components are not to scale. The stromal targeting domain (STD) is cleaved in the chloroplast stroma. The lumenal targeting domain (LTD) interacts with the endogenous 700-kDa complex (pink hexagon) and the lipid bilayer (green lines). In the presence of a trans-thylakoid pH gradient (ΔpH), the channel (brown hexagon) is formed by the oligomerization of Tha4 monomers. The size of the channel decreases during transport of the linker region. Translocation is arrested when the protein A moiety is unable to enter the channel. Treatment of recovered membranes with protease leads to degradation of the protein A moiety and retention of one or more fragments inside the thylakoid lumen.

of the interaction of those components. I have demonstrated that changing one conserved amino acid in the transmembrane domain of Hcf106 can abrogate that component's ability to participate in endogenous complex formation. A range of *in vitro* mutations and interactions can be envisioned using similar techniques. The incorporation of exogenously derived components may eventually allow restoration of ΔpH-dependent

pathway transport to mutant plants thereby defining component requirements and interactions.

The biochemical investigation of the ΔpH-dependent pathway is beginning to define the roles of machinery components and reveal the translocation mechanism. Research has demonstrated both the unique nature of the pathway and its evolutionary relationship to other export pathways.

LIST OF REFERENCES

Alonso, D.O.V. and V. Daggett. 2000. Staphylococcal protein A: Unflolding pathways, unfolded states, and differences between the B and E domains. *Proc. Natl. Acad. Sci. USA.* 97:133-138.

Arkowitz, R.A. and W. Wickner. 1994. SecD. And SecF are required for the proton electrochemical gradient stimulation of preprotein translocation. *EMBO J.* 13:954-963.

Arnon, D.I. 1949. Copper Enzymes in isolated chloroplasts-polyphenoloxidase in *Beta-vulgaris*. *Plant Physiol.* 24:1-15.

Asai, T., Y. Shinoda, T. Nohara, T. Yoshihisa, and T. Endo.1999. Sec-dependent pathway and ΔpH-dependent pathway do not share a common translocation pore in thylakoidal protein transport. *J. Biol. Chem.* 274:20075-20078.

Berghöfer, J. and R.B. Klösgen. 1999. Two distinct translocation intermediates can be distinguished during protein transport by the TAT (ΔpH) pathway across the thylakoid membrane. *FEBS Lett.* 460:328-332.

Berks, B.C. 1996. A common export pathway for proteins binding complex redox cofactors? *Mol. Microbiol.* 22:393-404.

Berks, B.C., F. Sargent, E. De Leeuw, A. P. Hinsley, N.R. Stanly, R.L. Jack, G. Buchanan, and T. Palmer. 2000(a). A novel protein transport system involved in the biogenesis of bacterial electron transfer chains. *Biochim. Biophys. Acta.* 1459:325-330.

Berks, B.C., F. Sargent, and T. Palmer. 2000(b). The Tat proetin export pathway. *Mol. Microbiol.* 35:260-274.

Bogsch, E., S. Brink, and C. Robinson. 1997. Pathway specificity for the ΔpH-dependent precursor thylakoid lumen protein is governed by a ‘Sec-avoidance’ motif in the transfer peptide and a ‘Sec-incompatible’ mature protein. *EMBO J.* 16:3851-3859.

Bogsch, E.G., F. Sargent, N.R. Stanley, B.C. Berks, C. Robinson, and T. Palmer. 1998. An essential component of a novel bacterial protein export system with homologues in plastids and mitochondria. *J. Biol. Chem.* 273:18003-18006.

Bolhuis, A., E.G. Bogsch, and C. Robinson. 2000. Subunit interactions in the twin-arginine translocase complex of *Escherichia coli*. *FEBS Lett.* 472:88-92.

Bolhuis, A., J.E. Mathers, J.D. Thomas, C.M.L. Barrett, and C. Robinson. 2001.TatB and TatC form a functional and structural unit of the twin-arginine translocase from *Escherichia coli*. *J. Biol. Chem.* In press.

Chaddock, A.M., A. Mant, I. Karnauchov, S. Brink, R.G. Herrmann, R.B. Klösgen, and C. Robinson. 1995. A new type of signal peptide: central role of a twin-arginine motif in

transfer signals for the ΔpH-dependent thylakoidal protein translocase. *EMBO J.* 14:2715-2722.

Chanal, A. C.-L. Santini, and L.-F. Wu. 1998. Potential receptor function of three homologous components, TatA, TatB and TatE, of the twin-arginine signal sequence-dependent metalloenzyme translocation pathway in *Escherichia coli*. *Mol. Microbiol.* 30:673-678.

Clark, S.A. and S.M. Theg. 1997. A folded protein can be transported across the chloroplast envelope and thylakoid membranes. *Mol. Biol. Cell.* 8:923-934.

Clausmeyer, S., R.B. Klosgen and R.G. Herrmann. 1993. Protein import into chloroplasts. The hydrophilic lumenal proteins exhibit unexpected import and sorting specificities in spite of structurally conserved transit peptides. *J. Biol. Chem.* 268:13869-13876.

Cline, K. 1986. Import of proteins into chloroplasts–Membrane integration of a thylakoid precursor protein reconstituted in chloroplast lysates. *J. Biol. Chem.* 261:4804-4810.

Cline, K. 1988. Light-harvesting chloroplyll-A/B protein–Membrane inserstion, proteolytic processing, assembly into LHC-II and localization to appressed membranes occurs in chloroplast lysates. *Plant Physiol*. 86:1120-1126.

Cline, K., W.F. Ettinger, and S.M. Theg. 1992. Protein-specific energy requirements for protein transport across or into thylakoid membranes. *J. Biol. Chem.* 267:2688-2696.

Cline, K., R. Henry, C.J. Li, and J.G. Yuan. 1993. Multiple pathways for protein-transport into or across the thylakoid membrane. *EMBO J.* 12:4105-4114.

Creighton, A.M., A. Hulford, A. Mant, D. Robinson, and C. Robinson. 1995. A monomeric, tightly folded stromal intermediate on the ΔpH-dependent thylakoidal protein transport pathway. *J. Biol. Chem.* 270:1663-1669.

Cristóbal, S., J-W. de Gier, H. Nielsen, and G. von Heijne. 1999. Competition between Sec- and TAT-dependent protein translocation in *Escherichia coli*. *EMBO J.* 18:2982-2990.

de Vrije, G.J., A.M. Batenburg, J.A. Killian, and B. de Kruijff. 1990. Lipid involvement in protein translocation in *Escherichia coli*. *Mol. Microbiol.* 4:143-150.

Economou, A., J.A. Pogliano, J. Beckwith, D.B. Oliver, and W. Wickner. 1995. SecA membrane cycling a SecYEG is driven by distinct ATP binding and hydrolysis events and is regulated by SecD and SecF. *Cell.* 83:1171-1181.

Eichler, J. 2000. Achaeal protein translocation. *Eur. J. Biochem*. 267:3402-3412.

Feilmeier, B.J., G. Iseminger, D. Schroeder, H. Webber, and G.J. Phillips. 2000. Green fluorescent protein functions as a reporter for protein localization in *Escherichia coli*. *J. Bacteriol.* 182:4068-4076.

Gietl, C. 1996. Protein targeting and import into plant peroxisomes. *Physiol. Plant.* 97:599-608.

Halbig, D., B. Hou, R. Freudl, G.A. Sprenger, R.B. Klösgen. 1999. Bacterial proteins carrying twin-R signal peptides are specifically targeted by the ΔpH-dependent transport machinery of the thylakooid membrane system. *FEBS Lett.* 447:95-98.

Henry, R., M. Carrigan, M. McCaffery, X. Ma, and K. Cline. 1997. Targeting determinants and proposed evolutionary basis for the Sec and the Delta pH protein transport systems in chloroplast thylakoid membranes. 1997. *J. Cell Biol.* 136:823-832.

Henry, R., A. Kapazoglou, M. McCaffery, and K. Cline. 1994. Differences between lumen targeting domains of chloroplast transit peptides determine pathway specificity for thylakoid transport. *J. Biol. Chem.* 14:10189-10192.

Horton, R.M., H.D. Hunt, S.N. Ho, J.K. Pullen, and L.R. Pease. 1989. Engineering hybrid genes without the use of restriction enzymes – gene-splicing by overlap extension. *Gene.* 77:61-68.

Hulford, A., L. Hazell, R.M. Mould, and C. Robinson. 1994. Two distinct mechanisms for the translocation of proteins across the thylakoid membrane, one requiring the presence of a stromal protein factor and nucleotide triphosphates. *J. Biol. Chem.* 269:3251-3256.

Hynds, P.J., D. Robinson, and C. Robinson. 1998. The Sec-independent twin-arginine translocation system can transport both tightly folded and malfolded proteins across the thylakoid membrane. *J. Biol. Chem.* 273:34868-34874.

Inouye, M. and S. Halegoua. 1980. Secretion and membrane localization of proteins in *Escherichia coli*. *CRC Crit. Rev. Biochem.* 7:339-371.

Izard, J.W. and D. A. Kendall. 1994. Signal peptides: exquisitely designed transport promoters. *Mol. Microbiol.* 13:765-773.

Keegstra, K and K. Cline. 1999. Protein import and routing systems of chloroplasts. *Plant Cell*. 11:557-570.

Kogata, N., K. Nishio, T. Hirohashi, S. Kikuchi, and M. Nakai. 1999. Involvement of a chloroplast homologue of the signal recognition particle receptor protein, FtsY, in protein targeting to thylakoids. *FEBS Letters* 329:329-333.

Kouranov, A. and D.J. Schnell. 1996. Protein translocation at the envelope and thylakoid membranes of chloroplasts. *J. Biol. Chem.* 271:31009-31012.

Kuhn, A., D. Kiefer, C. Kohne, H.-Y. Zhu, W. R. Tschantz and R. E. Dalbey. 1994. Evidence for a loop-like insertion mechanism of pro-Omp A into the inner membrane of *Escherichia coli. Eur. J. Biochem.* 226:891-897.

Lyko, F., B. Martoglio, B. Jungnickel, T.A. Rapoport and B. Dobberstein. 1995. Signal sequence processing in rough microsomes. *J. Biol. Chem.* 270:19873-19878.

Ma, X. and K. Cline. 2000. Precursors bind to specific sites on thylakoid membranes prior to transport on the Delta pH protein translocation system. *J. Biol. Chem.* 275:10016-10022.

Manting, E.H. and A.J.M. Driessen. 2000. *Escherichia coli* translocase: the unravelling of a molecular machine. *Mol. Microbiol.* 37:226-238.

Mikhaleva, N.I., C-L Santini, G. Giordano, M.A. Nesmeyanova, L-F. Wu. 1999. Requirement for phospholipids of the translocation of the trimethylamine *N*-oxide reductase through the Tat pathway in *Escherichia coli*. *FEBS Lett.* 463:331-335.

Moks, T., L. Abrahmsén, B. Nilsson, U. Hellman, J. Sjöquist, and M. Uhlén. 1986. Staphylococcal protein A consists of five IgG-binding domains. *Eur. J. Biochem.* 156:637-643.

Monne, M. I. Nilsson, M. Johansson, N. Elmhed, and G. von Heijne. 1998. Positively and negatively charged residues have different effects on the position in the membrane of a model transmembrane helix. *J. Mol. Biol.* 284:1177-1183.

Moore, M. S. Harrison, E.C. Peterson, and R. Henry. 2000. Chloroplast Oxa1p homolog Albino3 is reguired for post-translational integration of the light harvesting chlorophyll-binding protein into thylakoid membranes. *J. Biol. Chem.* 275:1529-1532.

Mori, H. and K. Cline. 1998. A signal peptide that directs non-Sec transport in bacteria also directs efficient and exclusive transport on the thylakoid Delta pH pathway. *J. Biol. Chem.* 273:11405-11408.

Mori, H., E.J. Summer, X. Ma, and K. Cline. 1999. Component specificity for the thylakoid Sec and Delta pH-dependent protein transport pathways. *J. Cell Biol.* 146: 45-55.

Mothes, W., S. Prehn, and T.A. Rapoport. 1994. Systematic probing of the environment of a translocating secretory protein during translocation through the ER membrane. *EMBO J.* 13:3973-3982.

Mould, R.M. and C. Robinson. 1991. A proton gradient is required for the transport of two lumenal oxygen-evolving proteins across the thylakoid membrane. *J. Biol. Chem.* 266:12189-12193.

Musser, S.M. and S.M. Theg. 2000(a). Characterization of early steps of OE17 precursor transport by the thylakoid ΔpH/Tat machinery. *Eur. J. Biochem.* 267:2588-2598.

Musser, S.M. and S.M. Theg. 2000(b). Proton transfer limits protein translocation rate by the thylakoid ΔpH/Tat machinery. *Biochemistry.* 39:8228-8233.

Neff, D. and N. A. Dencher. 1999. Purification of multisubunit membrane protein complexes: isolation of chloroplast F_oF_1-ATP Synthase, CF_O and CF_1 by blue native electrophoresis. *Biochem. Biophys. Res. Comm.* 259:569-575.

Oliver, D.B., R.J. Cabelli, K.M. Dolan, and G.P. Jarosik. 1990. Azide-resistant mutants of *Escherichia coli* alter the SecA-protein, an azide-sensitive component of the protein export machinery. *Proc. Nat. Acad. Sci. USA.* 87:8227-8231.

Emanuelsson, O., H. Nielsen, and G. von Heijne. 1999. ChloroP, a neural network-based method for predicting chloroplast transit peptides and their cleavage sites. *Protein Sci*. 8: 978-984.

Pool, M.R., E. López-Huetas, and A. Baker. 1998. Characterization of intermediates in the process of plant peroxisomal protein import. *EMBO J.* 17:6854-6862.

Pugsley, A.P. 1993. The complete general secretory pathway in Gram-negtive bacteria. *Microbiol. Rev.* 57:50-108.

Reed, J.E., K. Cline, L.C. Stephens, K.O. Bacot, and P.V. Viitanen. 1990. Early events in the import/assembly pathway of an integral thylakoid protein. *Eur. J. Biochem.* 194:33-34.

Robinson, C., D. Cai, A. Hulford, I.W. Brock, D. Michl, L. Hazell, I. Schmidt, R.G. Herrmann, and R.B. Klösgen. 1994. The presequence of a chimeric construct dictates which of two mechanisms are utilized for translocation across the thylakoid membrane: eveidence for the existence of two distinct translocation systems. *EMBO J.* 13:279-285.

Sambrook, J., E.F. Fritsch, and T. Maniatis. 1989. *Molecular Cloning: A Laboratory Manual*, 2nd Ed., Cold Spring Harbor Laboratory Press, Cold Spring Harbor, NY

Sargent, F., E.G. Bogsch, N.R. Stanley, M. Wexler, C. Robinson, B.C. Berks, and T. Palmer. 1998. Overlapping functions of components of a bacterial Sec-independent protein export pathway. *EMBO J.* 17:3640-3650.

Sargent, F., N. R. Stanley, B.C. Berks, and T. Palmer. 1999. Sec-independent protein translocation in *Escherichia coli*. *J. Biol. Chem.* 274:36073-36082.

Schagger, H. and G. von Jagow. 1991. Blue native electrophoresis for isolation of membrane protein complexes in enzymatically active form. *Anal. Biochem.* 199:223-231.

Schatz, G. 1996. The protein import system of mitochondria. *J. Biol. Chem.* 271:31763-31766.

Schatz, G. and B. Dobberstein. 1996. Common principles of protein translocation across membranes. *Science.* 271:1519-1526.

Schülke, N., N. B. V. Sepuri, and D. Pain.1997. In vivo zippering of inner and outer mitochondrial membranes by a stable translocation intermediate. *Proc. Natl. Acad. Sci. USA.* 94:7314-7319.

Schnell, D.J. and G. Blobel. 1993. Identification of intermediates in the pathway of protein import into chloroplasts and their localization to envelope contact sites. *J. Cell Biol.* 120:103-115.

Settles, A.M. and R. Martienssen. 1998. Old and new pathways of protein export in chloroplasts and bacteria. *Trends in Cell Biol.* 8:494-501.

Settles, A.M., A. Yonetani, A. Baron, D.R. Bush, K. Cline, and R. Martienssen. 1997. Sec-independent protein translocation by the maize Hcf106 protein. *Science*. 278:1467-1470.

Shaw, A.S., J.P.M. Rottier, and J.K. Rose. 1988. Evidence for the loop model of signal-sequence insertion into the endoplasmic reticulum. *Proc. Natl. Acad. Sci. USA.* 85:7592-7596.

Stahl, S. and M. Uhlen. 1997. Bacterial surface display: trends and progress. *Trends Biotech.* 15:185-192.

Stanley, N. R., K. Findlay, B.C. Berks, and T. Palmer. 2001. *Escherichia coli* strains blocked in Tat-dependent protein export exhibit pleiotropic defects in the cell envelope. *J. Bacteriol.* 183:139-144.

Summer, E.J., H. Mori, A.M. Settles, and K. Cline. 2000. The thylakoid ΔpH-dependent pathway machinery facilitates RR-independent N-tail protein integration. *J. Biol. Chem.* 275: 23483-23490.

Teter, S.A. and S.M. Theg. 1998. Energy-transducing thylakoid membranes remain highly impermeable to ions during protein translocation. *Proc. Natl. Acad. Sci. USA* 95:1590-1594.

Thomas, J.D., R.A. Daniel, J. Errington, and C. Robinson. 2001. Export of active green fluorescent protein to the periplasm by the twin-arginine translocase (Tat) pathway in *Escherichia coli. Mol. Microbiol.* 39:47-53.

Thompson, S.J., S.J. Kim, and C. Robinson. 1998. Sec-independent insertion of thylakoid membrane proteins. *J. Biol. Chem.* 273:18979-18963.

van Voorst, F. and B. De Kruijff. 2000. Role of lipids in the translocation of proteins across membranes. *Biochem. J.* 347:601-612.

Voelker, R. and A. Barkan. 1995. Two nuclear mutations disrupt distinct pathways for targeting proteins to the chloroplast thylakoid. *EMBO J.* 14:3905-3914.

Walker, M.B., L.M. Roy, E. Coleman, R. Voelker, and A. Barkan. 1999. The maize *tha4* gene functions in Sec-independent protein transport in chloroplasts and is related to *hcf106*, *tatA*, and *tatB. J. Cell Biol.* 147:267-275.

Weiner, J.H., P.T. Biolous, G.M. Shaw, S.P. Lubitz, L. Frost, G.H. Thomas, J.A. Cole, and R.J.Turner. 1998. A novel and ubiquitious system for membrane targeting and secretion of cofactor-containing proteins. *Cell*. 93:93-101.

Wexler, M., F. Sargent, R.L. Jack, N.R. Stanley, E.G. Bogsch, C. Robinson, B.C. Berks, and T. Palmer. 2000. TatD is a cytoplasmic protein with DNase activity. *J. Biol. Chem.* 275:16717-16722.

Wu, L.-F., B. Ize, A. Chanal, Y. Quentin, and G. Fichant. 2000. Bacterial twin-arginine signal peptide-dependent protein translocation pathway: evolution and mechanism. *J. Mol. Microbiol. Biotechnol.* 2:179-189.

BIOGRAPHICAL SKETCH

Vivian Fincher was born in LaGrange, Georgia, and educated in the public school system. She received her B.S. in Applied Biology from the Georgia Institute of Technology in May 1976. After two years studying microbiology at the University of Georgia, she left graduate school to pursue a career in medical sales. In 1986, she changed career paths again, entering the field of pension planning as an actuarial analyst. Vivian attended Dekalb Community College and Georgia State University part-time between 1984 and 1992 enjoying a variety of interests including, but not limited to, undergraduate business courses and graduate courses in actuarial mathematics. In 1994, she sold her house, quit her job, and moved to Florida to pursue her true love, biological science. She began her research in Dr. Kenneth Cline's lab in the spring of 1995 and received her Ph.D. in May 2001.